Sensor Processing and Path Planning Framework for a Search and Rescue UAV Network

by

Andrew Brown
Jonathan Estabrook
Brian Franklin

A Major Qualifying Project
Submitted to the Faculty
of the
WORCESTER POLYTECHNIC INSTITUTE
in partial fulfillment of the requirements for the
Degree of Bachelors of Science
in
Electrical and Computer Engineering
and
Robotics Engineering
by

May 2012

APPROVED:

Dr. Alexander M. Wyglinski, Advisor

Dr. Taskin Padir, Co-Advisor

MQP-AW1-WND2

Keywords: UAV, Image Processing,
SAR, Navigation, Framework

Abstract

Search and rescue operations are a costly endeavour. The advent of new technologies, such as unmanned aerial vehicles, can decrease the cost of such operations and increase rescue rates by finding the lost individual in a faster manner. However, the issue currently faced is how to develop and deploy such a system comprised of multiple UAVs. This report describes a framework which, through the use of modular components, provides for the autonomous search and detection of a target with the flexibility to change hardware and mission specific components at will. This framework integrates multi-agent path planning, wireless communication and coordination, and on board sensor processing, fusing an FPGA, DSP, and software platform for maximum flexibility with real time performance.

Executive Summary

Each year in the United States, thousands of incidents occur resulting in the need for massive search and rescue efforts to be launched. The brunt of these efforts is undertaken by local law enforcement, the Coast Guard, and the National Park Service supplemented by volunteers.

Budget cuts are the omnipresent reality of today's economy. Search operations are not immune to this truth. With an average cost of $3.7 million dollars per year for park services alone, they are a costly service to ensure public safety. Several states, including New Hampshire, have begun charging lost individuals for the cost of their rescue. While not a new concept, many beaches make their visitors pay for beach stickers that fund lifeguards, these measures have led to individuals refusing much needed help.

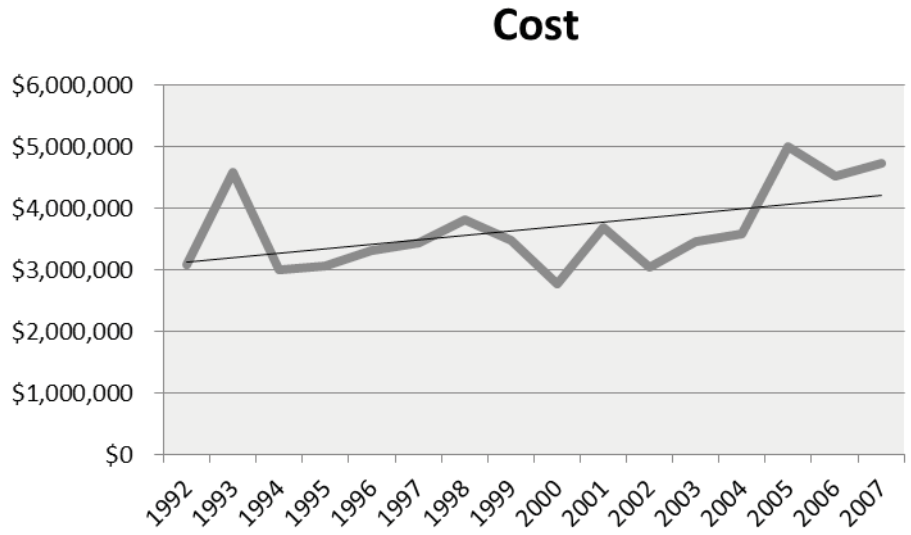

Figure 0.1: Increasing cost of SAR operations.

To reduce the cost of Search and Rescue (SAR), we proposed using multiple, coordinated, autonomous, unmanned aerial vehicles. An implementation, as we propose it, would reduce the number of people required to perform a search per unit area and thus the total cost of SAR operations over time. Our proposal, collectively called Project WiND, is to create autonomous areal vehicles, utilizing downward facing sensors, and wireless communications to perform a search with minimal human interaction.

As the team working on the software framework, our development was two part. We developed a framework to accommodate modular image processing, path planning, navigation, and communication programs. This involved understanding the needs of SAR operators, platform developers, and the communications team, however it also required planning for all scenarios. This pushed our framework to accommodate a design in which all sensor processing occurred on the UAV and away from any base-station or mother-ship. In addition to the framework, we also developed a set of modules which use our framework. These demo modules serve to demonstrate functionality and to guide future developers who will program for our framework.

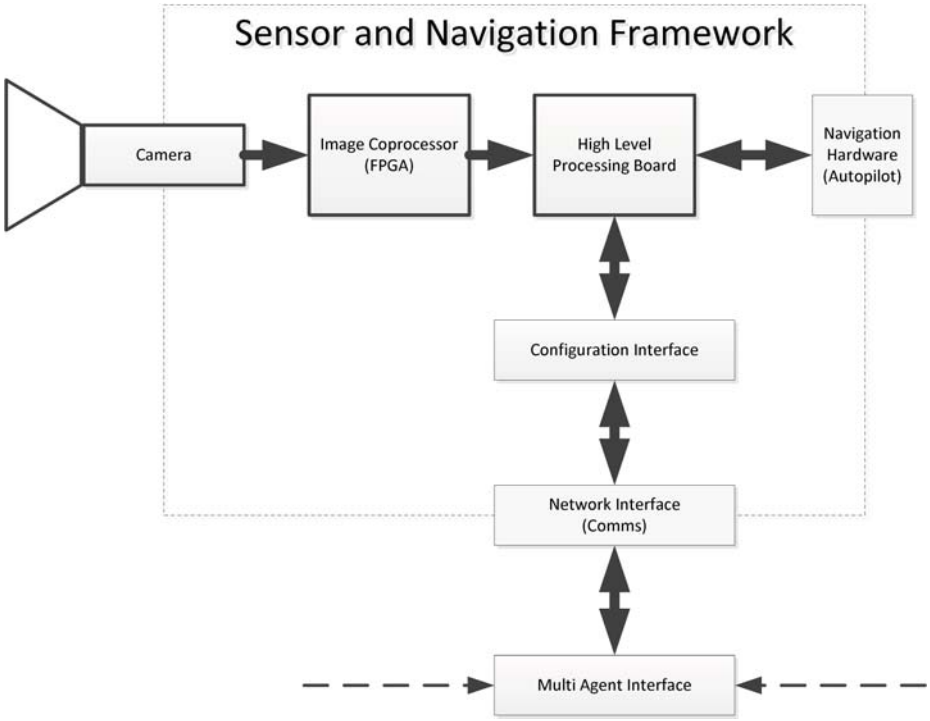

Figure 0.2: WiND framework architecture showing connection between image processing module, high level processor, and other communications and flight components.

We proved the overall concept of a specialized framework for search and rescue. We successfully integrated purpose built modules into this framework and showed general functionality. We installed this framework onto an ARM platform and integrated that with the hardware platform.

We made significant headway in developing a search and rescue specific unmanned aerial vehicle framework. This framework is open for developers to add functionality in the areas of communications, image processing, and navigation. We hope that a future team can finalize the framework and release it as a field-ready development platform.

Contents

List of Figures

List of Tables

Chapter 1

Introduction

1.1 Search and Rescue as a Public Service

Each year in the United States, thousands of incidents occur resulting in the need for massive search and rescue efforts to be launched. The brunt of these efforts is undertaken by local law enforcement, the Coast Guard, and the National Park Service supplemented by volunteers. Budget cuts are the omnipresent reality of today's economy. Search operations are not immune to this truth. With an average cost of $3.7 million dollars per year for park services alone, they are a costly service to ensure public safety [10]. Several states, including New Hampshire, have begun charging lost individuals for the cost of their rescue [11]. While not a new concept, many beaches make their visitors pay for beach stickers that fund lifeguards, these measures have led to individuals refusing much needed help [12].

The wilderness of America's parks and outdoors can be a dangerous place not just. Rescuers are subject to the same rugged terrain and conditions as those they seek to rescue. Rescue coordinators must ask how many lives should be risked to save one.

The need for search and rescue is not one that will go away. Extending beyond the concerns of hikers, natural disasters have brought the necessity search and rescue into the heart of civilization. Rescue personal were at the forefront of lifesaving operations after Hurricane Katrina and more recently the earthquake and following nuclear disaster at Fukashima to name two prominent events in the public's eye.

Figure 1.1: Coast Guard Rescue Personnel during Hurricane Katrina [1]

Finding ways to minimize this cost while improving the response to such incidents is paramount. The resources available to rescue personnel have evolved over the years. What was once the work of volunteers on foot with the help of vehicles and animals now involves aircraft and mixed units of vehicles and individuals on foot. UAV's are the most recent technology to enter the realm of search and rescue. Like their fore-bearers however, in order to take advantage of their full potential they must be managed properly.

1.2 Cost of Search and Rescue

In Figure 1.2 it can be seen that the cost of SAR operations since 1992 has seen a steadily increasing trend. UAVs are a possible solution to this problem due to their operating cost (when compared to manned aerial vehicles), reproducibility, and disposability.

Currently, the command and control of multiple UAVs in a coordinated fashion is a resource intensive operation. This translates into an operation that is more expensive to set up, has a higher cost of operation, and is more prone to failure. Current UAV operations require many people to run and require low latency, high-bandwidth links to operate. These factors add to cost. In addition, information gathered by the UAVs has

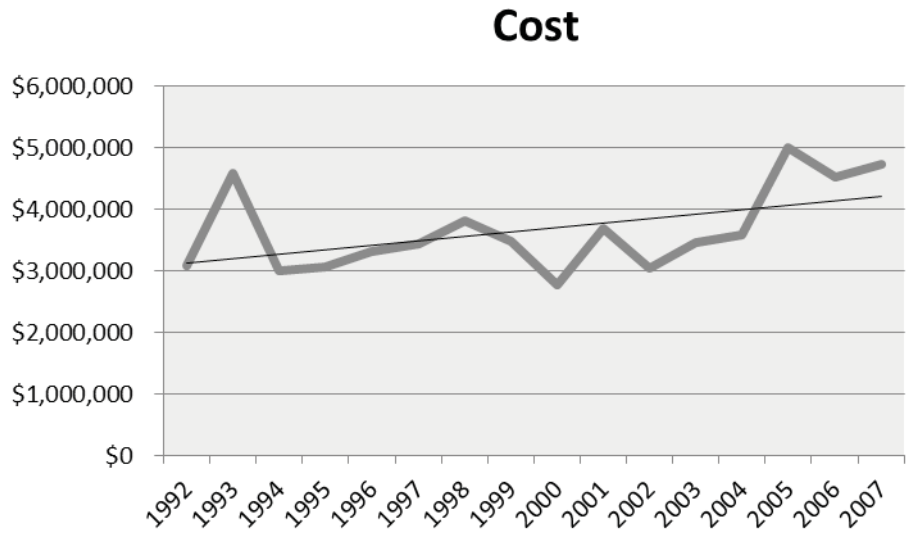

Figure 1.2: Increasing cost of SAR operations since 1992.

no guaranteed means of reaching the correct destination, thus contributing to a potential for communication failure. Data may not reach the correct person at the correct time, or too much data will reach a single person and who is not able to discern the important information.

A major reason the operation of UAVs is so resource intensive is that each UAV requires multiple people to operate. The common setup for a UAV search team, as seen in 1.4, requires at least one pilot per UAV, a handful of coordinators to direct pilots to new objectives and rework flight plans in synchronization with incoming data, and a large number of analyst personnel to interpret the incoming data from each UAV [13].

In a search application, the analysts have to read the incoming data and interpret it in real time and coordinators have to update flight plans based on that data. Adding more UAVs to a search effort will not increase the probability of finding the objective unless the number of support personnel also increases to meet or exceed the minimum interpretation for the incoming data.

The networking of UAVs is a major addition to cost, unreliability, and potential failure. Current UAV technology requires information to be interpreted, in whole, on the ground. This requires each sensor to report information over a radio link in real time. Often, this

Figure 1.3: The MQ-1 Predator Unmanned Aircraft, an Unmanned Aerial Vehicle requiring multiple operators[2]

arrives to a person unfiltered and unmitigated, contributing to information overload and driving the need for analysts to interpret data. Without that full speed, high-bandwidth, uninterrupted link, information is lost.

Conversely, UAVs themselves do not operate without the same link. While control data is significantly less information than the downlink, the UAVs are nevertheless remotely controlled. Current technology addresses this problem of a disconnection by putting the UAV into a blind holding pattern. Modern UAVs have enough logic to circle and while the link is re-established. The most advanced technology can fly the UAV to a pre-programmed location (usually the airfield of origin) and land.

When information is flowing, the data may still not reach the correct person at the correct time. Raw sensor data, such as a live video feed or thermal vision, flight data, weather information, or terrain measurements have no guarantee of detection or communication. A small change or anomaly in an otherwise inactive area my call the analyst to attention and warrant another flyby, but a small flurry of activity may go unnoticed. In the worst case, even the correct detection of an objective may not be prioritized over other interpreted data and get lost in the information overload.

1.3 The UAV Solution to SAR Operations

The relationship between the number of UAVs and the number of people required to support a UAV team is a limiting factor in the use of UAVs for search operations. Even as UAVs increase in ability and decrease in cost, the personnel requirements remain fixed. With the current paradigm, large-scale UAV search teams are not possible. Furthermore, search coordinators cannot fully benefit from the cost, reproducibility, and disposability of UAVs. Without more automated command and self-reliance, UAVs will never overcome this hurtle.

Figure 1.4: Snapshot of the ground control station during a dry run of a Brigham Young University WiSAR UAV. This UAV requires many human operators [3].

A UAV based search team designed to facilitate human operators is a solution to this is deficiency. A system that is capable of coordinating search patterns, filtering gathered

data, and utilizing human input is optimal. By addressing these challenges, a system can be created that utilizes a human operator in the search effort while freeing valuable personnel from the task of coordination.

1.4 A Gap in Current Research

Research into this area has been conducted. It can be divided into three different categories: computer science/AI centric, traditional "search theory," and resource allocation centric methods. Each approach brings a new view to the subject but most if not all ignore the other types of research. Computer science brings endless research into optimization and and coverage problems. "Search theory" brings actual statistics of search operations and probability of detection. Finally, resource allocation, brings with it the coordination of mixed units with mixed capabilities. What is missing at the moment, is research combining the lessons learned from each of the relevant areas. Project WiND aims to close this gap.

1.5 Proposed Approach

The proposed approach to this task is to develop a sensor integration and path planning module capable of handling and filtering data prior to its end destination. This entails moving some of the needed image processing and navigation tasks away from the central control station. The hope is that low-level processing will be used on a drone-by-drone basis to intelligently handle the individual sensor data prior to reporting it back to the mothership and/or base station. In doing so, this project aims to reduce overhead and increase system robustness by partially distributing low-level sensor processing tasks and decision making.

The key conceptual difference from traditional thought is that this framework will treat the autonomous vehicles as "scouts" rather than drones. In low-cost systems, UAVs are typically reliant on a base station for any functionality. Control data is streamed to the drone, and raw sensor data is sent back. By placing some processing on the remote platforms, this gives preliminary decision making capability, but not final decision making capability.

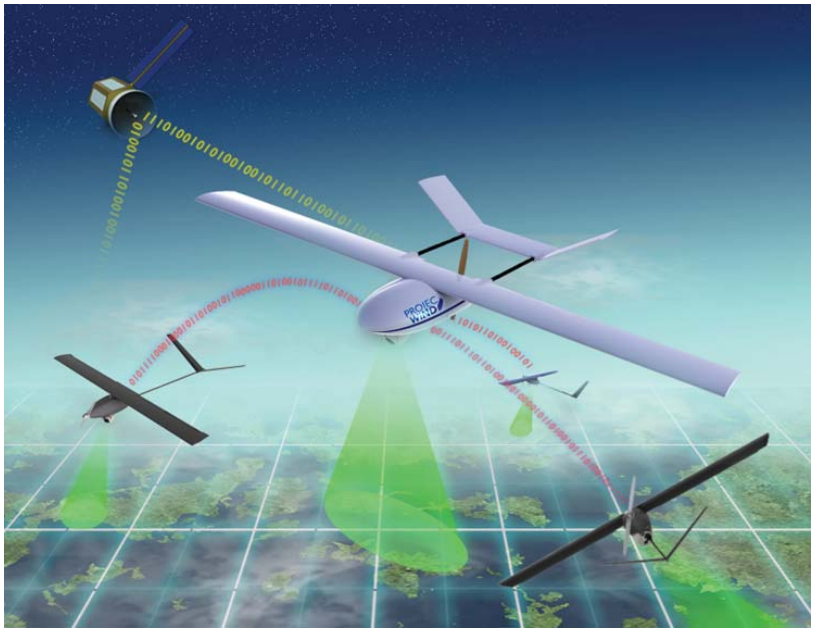

Figure 1.5: Project WiND concept art showing many an Unmanned Aerial Vehicles operating in a coordinated operation. Each utilizes downward looking sensors and wireless communications.

In any system such as this, there will be bottlenecks, whether it be the communications system or the amount of data presented to human operators at the base station. Too much data at either bottleneck presents problems. As such, partially distributed processing will aim to reduce the amount of unneeded data at various bottleneck points.

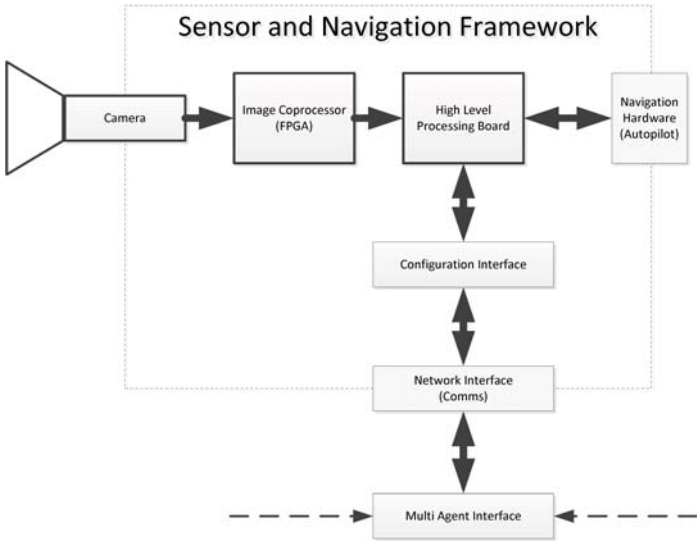

Figure 1.6: WiND framework architecture showing connection between image processing module, high level processor, and other communications and flight components.

In most other scenarios, drones in this context are largely "dumb" in the sense that they operate by complete remote control, in some cases with minimal autonomy, and transmit a raw stream of data back to a processing station. Most of the data processing is done off of the drone itself. In scenarios such as this, the drones may be arguably cheap and expendable, but this presents overhead on the communications link, and potential overhead on the data that is presented to human operators.

Full autonomy, in contrast, is costly, difficult, and potentially dangerous, as it puts final decision making capability in the autonomous system. This comes with a cost overhead as well, as computing power must be put on the vehicle to allow such autonomy, or a low-latency data link must be sustained to maintain control by some form of remote automation system.

In the case of this approach, the project will attempt to provide a platform for apply-

ing a better balance of autonomy and remote control. This module will allow drones to have necessary low-level on-board processing and navigation capability, such that a node can make decisions on the relevance of sensor data prior to transmission over a limited communications pipe, or have the capability to navigate back in the event that it loses communications.

Despite providing more remote autonomy, overarching control will still be done from the base station, but without as much central overhead. By distribution of low-level processing, this project's hypothesis is that data overhead can be reduced and potentially more complex processing methods could be adopted and utilized with greater ease.

Due to the inherent restrictions of fitting complex equipment on an aerial platform, any decisions on what processing is put onto the remote vehicle versus being done at a more powerful command station must be carefully weighed. This framework's processing modules must be relatively light and have low enough power requirements to be sustainable, yet be capable of performing the image processing and navigation tasks required.

By adding remote processing power to the remote platforms, some other advantages become apparent. For a search and rescue task such as this, sensor data transmission need not be real-time, so long as the location and time data is preserved. To this end, this project's approach will be to evaluate and utilize methods of minimizing data reporting during runtime by using initial processing resources on remote platforms to intelligently reduce data throughput needs and effort required on the part of human operators.

1.6 Project Organization and Contributions

This project is one of three cooperative groups at WPI working in a unified effort to produce the flight platforms, software framework, and communications platform needed to execute the SAR operations described using the combined efforts of all groups involved. Shown in Figure 1.7 is the team organization within WPI and with the UNH teams.

The Software team, shown at the top of the WPI portion, will be responsible for the sensor processing and path planning framework development, and as a secondary effort work with the individual teams to accomplish integration of the respective platforms as

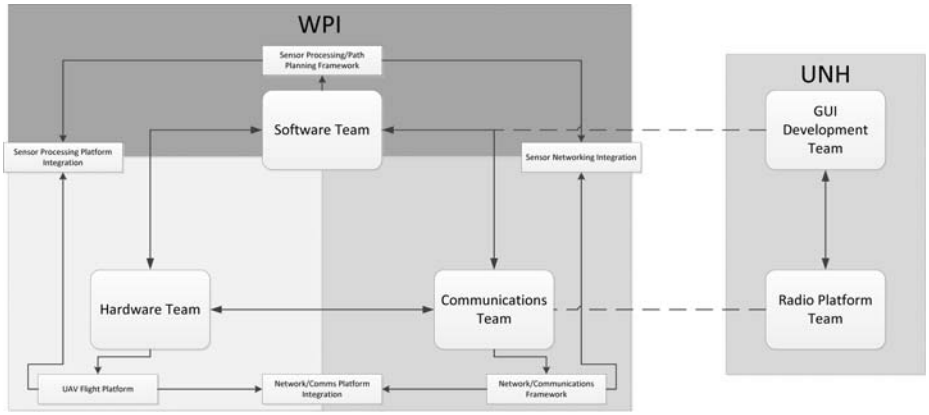

Figure 1.7: Three project components are split between three teams at WPI, and two loosely associated teams at UNH.

they reach completion. Within the software team, tasks were split between development of path planning and project interface components, image processing, and communication methods between the various components of the framework.

1.7 Report Organization

Contained in this report is a description, approach taken, and results gained from this MQP. First, background will be given on the associated topics and relevant similar work explored in the fields associated with UAV path planning, image processing, and SAR operations. Next, the high-level approach proposed by this iteration of the project will be described in depth, followed by a detailed description of the specific planned implementation in the provided timespan. The results at the completion of this project will then be outlined, followed by concluding remarks and suggestions to future teams as to work that could be done to expand or revise this project based on its findings.

Chapter 2

Prior Art

Having established a need for improvements in current Search and Rescue (SAR) tools, it is now necessary to understand the current SAR system and how to improve it with a Unmanned Aerial Vehicle (UAV) framework. This framework will support path planning, navigation, image processing, and extendible modules to interface with communications and other hardware.

This chapter first establishes current search theory and describes some methods for planning optimal search routes for an autonomous aerial platform. Next, this chapter outlines current image processing techniques and how to automate visual detection. Finally, we present recent research related to unmanned aerial vehicles which combine these topics and frameworks for aerial platforms . From this, we fully establish the need for a new UAV framework for SAR applications and the requirements of a framework designed specifically to support the future of SAR.

2.1 Path Planning

2.1.1 Search and Rescue Theory

Modern search theory rose from Allied military research during World War Two aimed at developing optimal search methods to locate enemy naval vessels, specifically submarines [14]. Much of this effort can be traced back to the work of one man, a mathematician named

Bernard Koopman, who used probability to predict and optimize search results. However, it was not until 1973 that Koopman's research was applied directly to land based search and rescue operations by Dennis Kelly [9]. Since then, the field of search theory has grown and is widely adopted today by the like of the United States Coast Guard.

In essence, search theory is about maximizing the probability of success (POS) while minimizing the effort exerted in a search task. It uses probability and information theory to quantize a search operation from movements to locations on the map. Table 2.1, compiled by a Coast Guard review document in 2002, shows the impact on rescue statistics with the introduction of search theory.

Table 2.1: Comparison of SAR before and after the introduction of Search Theory [9]

Period	Average Number of Lives at Risk Per Year	Average Number of Lives Saved Per Year	Average Number of Lives Lost Per Year
Prior to change in search planning methodology (1971 – 1974)	4105	2681 (65%)	1424 (35%)
After change in search planning methodology (1975 – 1978)	4977	3632 (73%)	1345 (27%)
Difference (%)	+ 872 (21.2%)	+ 951 (26.1%)	- 79 (5.5%)

While an official set of terms has not been established, common search methodology is referred to in terms of probability of detection(POD), Probability Of Success(POS), Probability Of Area (POA), effort, sweep width, and coverage [15].

Probability of detection is the likelihood of detecting a target. This factor is solely dependent on how reliable a sensor is used for the detection process, be it eyes or cameras. Often times the probability of detection is represented as a Gaussian distribution about a center point, the sensor's location. As distance from the sensor increases, the probability of detection decreases. Sweep width is the largest distance where a target can reasonably be detected from a sensor. Effort refers to the resources available. Probability of success is simply the likelihood that the target will be found when accounting for all reasonable known variables. It is largely dependent on effort, sweep width and coverage and as such it can be represented as a mathematical equation. In Koopman's original analysis of the

random search case, he found this to be equal to,

$$POS = 1 - e^{-(WL/A)}$$

where "W" is the sweep width, "L" the total length of the random search path, and "A" the total area to be searched [15].

Now that the key search theory concepts are defined and quantified, we now must automate the task. To do this, we first solidify the concepts related to artificial intelligence and path planning.

2.1.2 AI Path Generation

In the field of computer science and the study of Artificial Intelligence (AI) concepts, path planning is typically just an specific application of a graph search algorithm. Path planning algorithms range in complexity from single-agent path planning tasks to multi-agent coordination, and for each of these approaches, the implementation may range from planning a single step ahead to planning out a full and complex movement plan for a navigation task. This section will address how these approaches relate and can build off one another from simplest to most complex.

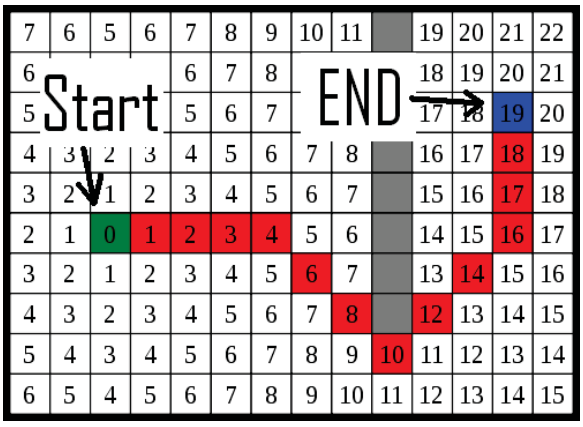

Figure 2.1: Illustration of a path finding algorithm based on difficulty to traverse (cost). The numbers in each grid-square denote difficulty and a path is decided by minimizing the sum of the difficulties in a given path [4].

Greedy Algorithms and Single-Agent Heuristics

In computationally constrained scenarios, particularly in embedded processing applications, fast-running algorithms may at times take precedent over the absolute optimization of the resulting solution. Furthermore, in some path planning problems, optimal path generation can become an infeasibly complicated computational task. In such examples, the path planning task may be a variant of the famous Travelling Salesman problem.

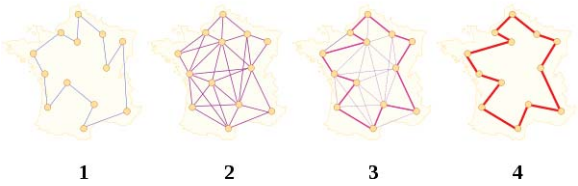

Figure 2.2: Example of travelling salesman algorithm optimizing travel between N points for shortest possible distance. Each iteration of this algorithm reduces the number of possible paths [5].

Table 2.2: Greedy search chooses the next best option, not considering future steps in a search task.

Period	Average Number of Lives at Risk Per Year	Average Number of Lives Saved Per Year	Average Number of Lives Lost Per Year
Prior to change in search planning methodology (1971 – 1974)	4105	2681 (65%)	1424 (35%)
After change in search planning methodology (1975 – 1978)	4977	3632 (73%)	1345 (27%)
Difference (%)	+ 872 (21.2%)	+ 951 (26.1%)	- 79 (5.5%)

Illustrated in 2.2, a greedy search algorithm uses a problem solving heuristic of choosing the locally optimal solution. In other words, the next choice that provides an immediate desired gain will be the one chosen. This is an extremely fast algorithm style to implement, while still providing a result somewhat guided towards the optimal. Furthermore, it can be the basis for more optimal algorithms, making it a good foundation to start with in many

cases.

However, this approach comes with some caveats. For example, in some situations where local optima or barriers may exist, a greedy search algorithm could get stuck at a non-solution or at the wrong solution. This is not desirable for a search task, so for most implementations of this, a modification of a greedy algorithm to address possible failure states will function as a quick and computationally inexpensive algorithm for this task.

Multi-Agent Negotiation

In a multi-agent path-planning scenario, an consequence that must be addressed is collisions and overlap between respective paths. Furthermore, in a dynamic scenario, such as search-and-rescue, additional points of interest may be added at runtime.

In scenarios such as this, weighted bidding is a basic method of intelligently deciding where new tasks can be allocated. In a typical bidding routine, multiple agents are sent a request for bid on a new task. In a time-sensitive scenario, this would also include a time of expiry, in which the agents involved must respond before a fallback choice is assigned.

The bids between agents are calculated by some form of situation and application specific set of parameters. This would give some form of quantized value for the agent to add the new task to its current queue of tasks. Quite simply, whichever agent responds first with the highest bid will be assigned the task.

In particular, in an article published by Oklahoma State University, this precise method is addressed in a multi-robot scenario where communications distance between robots is of concern. In this particular theoretical case, inter-robot distances and distances to new waypoints are used as a measure. This approach, in simulation, shows a robust ability to provide efficient resource distribution using a relatively simple basis for quantizing cost of search [16].

2.2 Image Processing

Path planning and image processing are two very different computational tasks, both with their own challenges and levels of complexity. Path planning, within the field of com-

puter science, is computational problem with solutions that range from trivial to immensely expensive to compute. Image processing, similarly, addresses many potential computational problems, with algorithms that may be trivial in concept, but highly difficult to implement on typical computing hardware. As such, this section will address the relevant background theory of this field.

Image processing is the practice of using signal processing techniques to take an image as an input and produce data pertaining to characteristics of interest in the image. Using such techniques, both hardware and software methods can be implemented to extract important data from visual input [6, 17].

Many techniques exist for implementing image processing. Image processing can be implemented in pure software, often with the aid of a code library such as OpenCV [18]. However, given the nature of image processing, some implementations in pure code are far from optimal.[6] Since an image is represented as a 2-dimensional matrix of pixels, traditional serial processing methods may handle an image one pixel at a time. If quick processing of video data is desired, this may be too inefficient for the convenience of pure code. For example, operating on a standard 640 by 480 pixel image at 15 frames per second requires processing 4.6 million pixels per second. At multiple operations per pixel, this rapidly becomes quite a computationally expensive task.

Newer technologies, such as Graphics Processing Units (GPUs) and Field Programmable Gate Arrays (FPGAs), are designed specifically for processing tasks of this type, rather than generalized processing tasks that CPUs are built to handle. This is often at the cost of some coding conveniences, but allows image processing tasks to be executed in a tremendously more efficient manner. [17] With proper implementation on such hardware, image processing algorithms can be executed on every pixel of an image simultaneously. On FPGAs, this specialization goes one step further, as the digital logic behind the image processing can be implemented in hardware itself.

In the field of Computer Vision, automated image processing has long proven it possible to extract relevant information from images in real-time using a variety of automated filtering techniques[19]. Basic tasks, typically completed by a human can be done by tying image processing into the control framework when the desired visual cues can be described

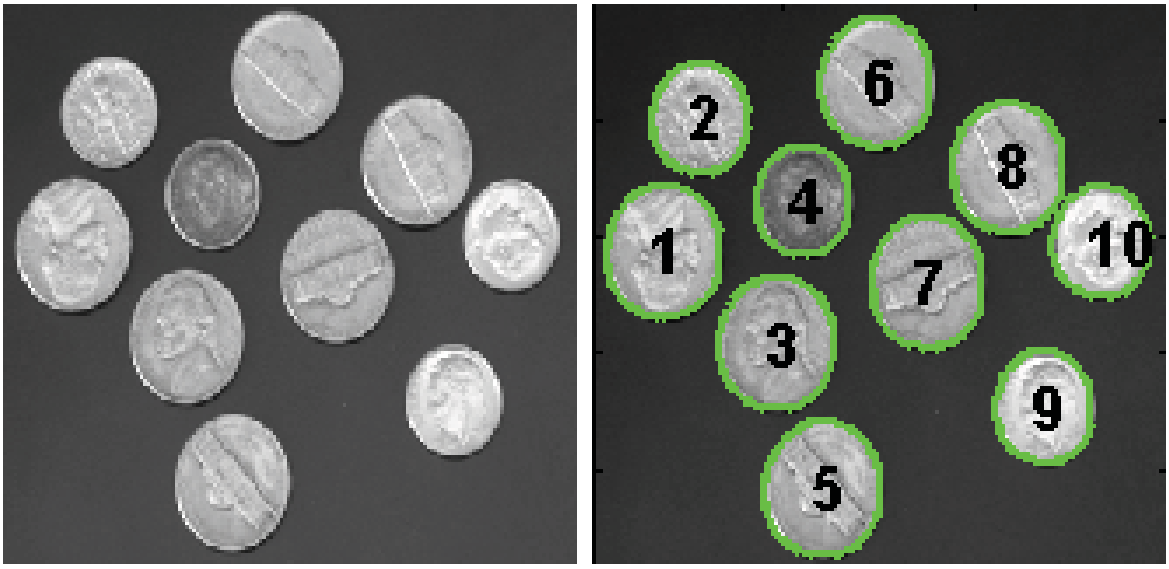

(a) Original Image: Various coins on a surface with varying orientations and arrangement

(b) Processed Image: Individual coins are discerned from the background texture, highlighted, and numbered based on location of center point

Figure 2.3: Example of a blob detection algorithm running in MATLAB

in code [20].

Prior Technique

There are many publications on systems which combine image processing and computer vision with unmanned areal vehicles for feature detection and navigation[21, 22, 23, 24]. However, there is less research focused on developing for systems based on low-power processors such as our target platform [25, 26].

Past projects have taken a hardware approach to image processing using FPGAs to accelerate high-complexity algorithms [27]. Research at Brigham Young University achived a fully on-board stabilization system for a small quad-rotor platform by using parallelized algorithms on an FPGA. To achieve stabilization, they hardware-implemented complex algorithms such as template matching, feature correlation, and distortion correction.

Other research has combined hardware and software for accelerated image processing [28, 29]. In these applications, the combined power of a DSP and FPGA together perform

faster than an FPGA alone. These systems have additional flexibility when system changes can occur in software [29].

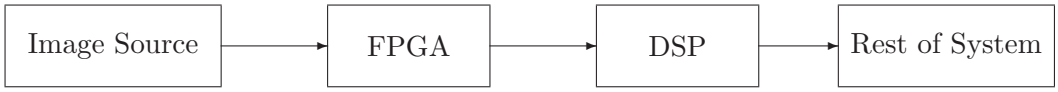

Figure 2.4: An FPGA and DSP Based, modular image processing system

2.3 Prior Integration Projects and Existing Frameworks

Having established a background for search theory and the modern techniques in image processing, we now move forward into current projects that apply these concepts to areal platforms. There are many projects using image processing and UAVs, so we have outlined only a few projects here which most closely coincide the goals of Project WiND.

Research by Brigham Young University (BYU) Computer Science Department describes the development and integration of camera-equipped UAVs into Wilderness Search and Rescue (WiSAR) [13, 30, 31]. Experiments show that the current state of UAV SAR as requiring a minimum of three people per vehicle and describes the modules required for user interfaces to integrate autonomy components with human intelligence [13]. The user interface systems these researchers created are based on extending these teams (an operator, video analyst, and mission manager) plus a ground unit to reasonably direct multiple UAVs [31].

In research related to UAVs and SAR there are two levels of autonomy. The low-level autonomy is responsible for take off and landing, waypoint rally, and gimbaled camera control, as well as containing logic for determining search patterns around waypoints (spiral, lawnmowing, Zamboni) and a pre-defined action for a loss of communication or other safety contingency. An advanced autonomy is responsible for generating a probability distribution, path planning, video mosaicing, and anomaly detection. A probability distribution for the

search area is created by a Bayesian model incorporating human behavior and terrain, as well as a Markov chain Monte Carlo Metropolis-Hasting algorithm to generate distribution changes over time. Path planning is handled by a combination of the Generalized Contour Search and the Intelligent Path Planning algorithms published in the IEEE International Workshop on Safety, Security, and Rescue Robotics and the Journal of Field Robotics respectively [13].

Using quad-rotor style UAVs with downward facing cameras, the researchers at the University of Oxford Computing Library developed navigation algorithms for use with SAR. The algorithms were all based on probabilistic maps and developed to "cope with the uncertainties of real-world deployment." The team used Greedy Heuristics, Potential-based Heuristics, and Partially Observable Markov Decision Process (POMDP) based heuristics. Greedy Heuristics are strategies based on navigating adjacent cells on a probabilistic map, a more advanced variant of this "1-look ahead" was also used. Potential-based Algorithms model goals and obstacles with association and repulsion potentials. POMDP algorithms are a generalization of a Markov Decision Process which optimizes reward against cost of potential actions [32].

The Cooperative Control for UAV Teams project from Massachusetts Institute of Technology Aerospace Controls Laboratory used multiple fix-winged aircraft with GPS feeds combined with a centralized AI to deduce feasible paths around obstacles in the environment while maintaining a path to an objective. The approach uses an extended pedal method named Receding Horizon Task Assignment (RHTA) for real time task assignment and reassignment. Trajectory Optimization is solved using a MILP-based receeding horizon planner RH-MILP. This algorithm gives a "cost-to-go" estimate of each path [33].

In regards to human-UAV interaction, the Phairwell system, developed by BYU, is an augmented virtual reality interface where the operator assigns each UAV in a group a specific task based on input from the video analyst and manager. The Wonder Client for Video Analyst allows the analyst to choose between live video and mosaic views. The video analyst then annotates the video with candidate objectives, these tags are automatically geo-referenced and shown on future video streams. The wonder Client for Mission manager provides the manager with high-level information on what has been searched and how well.

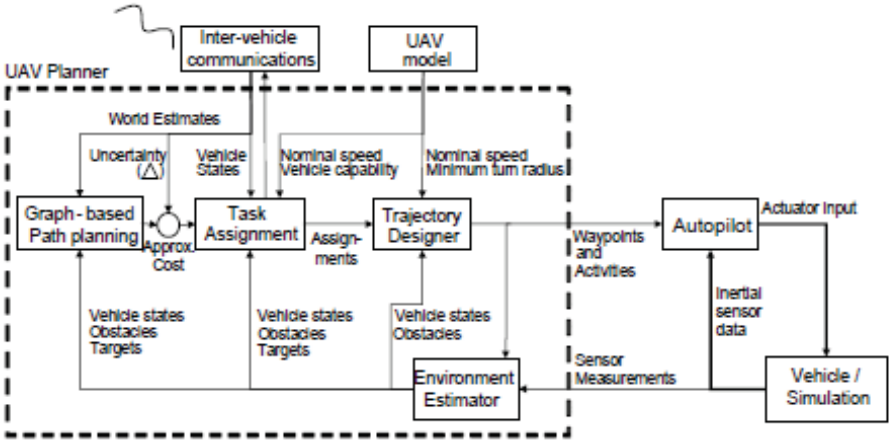

Figure 2.5: MIT UAV architecture showing separation of aircraft control system and path planning system

An additional interface for ground searchers is currently under development [9].

2.4 Chapter Summary

Search and rescue is an area in which a current research base exists. Dating back to World War II, the subject of "search theory," has been applied to save lives. More recently, the advent of unmanned aerial vehicles has paved the way for further research in the area. Topics such as artificial intelligence and image processing are now relevant with "search theory" in the fight to save lives. It is necessary to have a basic knowledge in each of these fields to implement a completely autonomous platform framework for this role.

Chapter 3

Proposed Approach

By adding a level of intelligence above otherwise blind sensor-polling and manual path planning tasks, this system will provide an accessible means of managing and allocating important resources in search and rescue operations, both in personnel and data overhead. The planned architecture will emphasize modularity and portability, especially between its own individual components. This involves the creation of two modules: a path planning module, and an image processing module. Within the UAV fleet, the these modules should be capable of integrating with both the central ground station and the individual drones to simplify high-level management of the existing autopilot and other sensor hardware.

For example, the path planning components would provide a means of generating the waypoints needed for a UAV to search a given area, rather than requiring the end user to manually enter a flight plan. For sensor data, this would also need to be able to provide a high degree of control over data reporting capabilities; that is, what sensor data is sent where in the system, and in what format. In the case of image processing, in a search an rescue operation, this system should assist in the detection of persons on the ground from the UAV, rather than blindly streaming all camera data. Instead, it should provide some informative data on the images and control over what image data is sent back or logged. Overall, this system should facilitate resource management, whether it be effort needed from the persons involved, or reduce unneeded use of limited storage or bandwidth.

As such, the ultimate goal will be a framework that can be used to accomplish these

path-planning and image processing tasks, while providing end users and developers the flexibility to expand on and reconfigure the existing system.

3.1 Framework Architecture

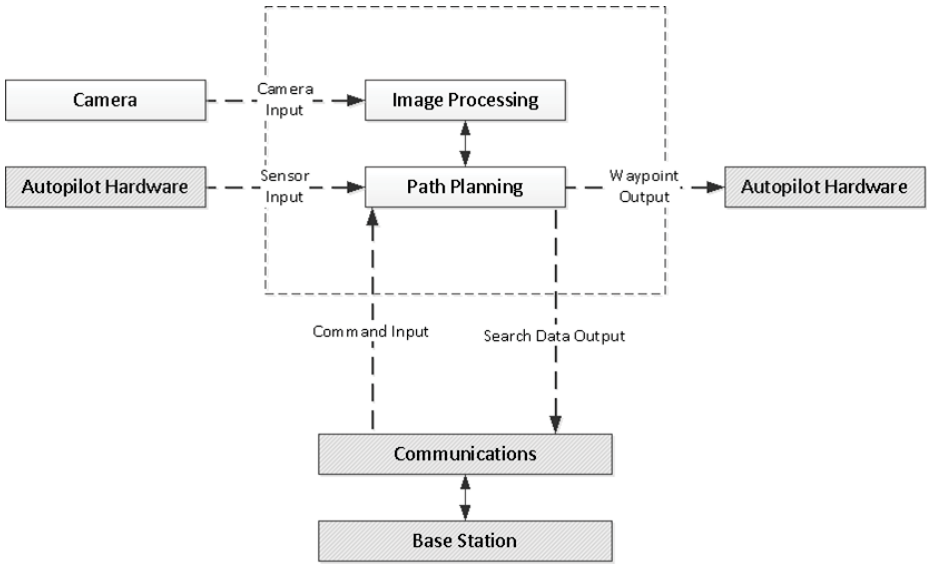

Figure 3.1: The proposed framework architecture, with interchangeable navigation and image processing modules.

Shown in Figure 3.1 is the proposed approach to this framework design. While highly interconnected, the image processing module and path planning module will be interchangeable, and their design should be such that they can be run on a diverse set of platforms and in a variety of configurations.

The path planning module and image processing modules will work alongside one another within each individual UAV to take commands from a ground station, process individual sensor data, and perform individual navigation tasks. This will involve processing image data to reduce the need for transmission of all image data, and generating or modifying flight plans dynamically to manage the on-board autopilot. As a result, this will also function as an accessibility layer of sorts between the ground station, associated network configuration, and whatever platform-specific autopilot and sensor hardware is installed on

each UAV, allowing uniform access, coordination, and management of UAVs even in the presence of differing platform capabilities.

3.2 Path Planning

For a UAV to function autonomously, it needs some method for flying without full direction from a human operator. With an autopilot, this may involve automated flight stabilization, and execution of pre-defined flight routines. Flight plans, however, still may require human intervention to generate, verify, and coordinate between multiple UAVs. A path planning component, in this case, would provide a means of generating flight plans based on higher level requirements given by a human operator, saving them the time and effort they otherwise may spend doing this manually.

For the navigation component, the planned approach is to implement two to three basic algorithms on a platform capable of handling individual path planning tasks, negotiation, and resource allocation between multiple platforms. Since countless algorithms exist for completing these tasks, some of which were outlined previously, it is in the best interests for the scope of this project to lay a basic, functional foundation for this component. This can serve as a proof of concept and easily be expanded on as needed. As such, usability and expandability are major design considerations over depth and sophistication.

As development of an autopilot is a lengthy and highly platform specific task, the navigation module does not operate as an autopilot, nor was it decided to be part of the project to develop an autopilot. Shown in Figure 3.2 is the proposed architecture for this module. The ground control and mobile software components of this platform will perform higher level analysis and operations for navigation. On each UAV, the mobile components will take in telemetry and other flight sensor data, along with commands sent from the ground station. Here, each will serve to generate waypoint paths based on this data, interfacing directly with the platform-specific autopilot, which will manage the actual low-level flight control to follow this planned path.

The ground control portion of this framework will serve as a connecting point between multiple UAVs. Depending on the desired configuration, this may require providing a

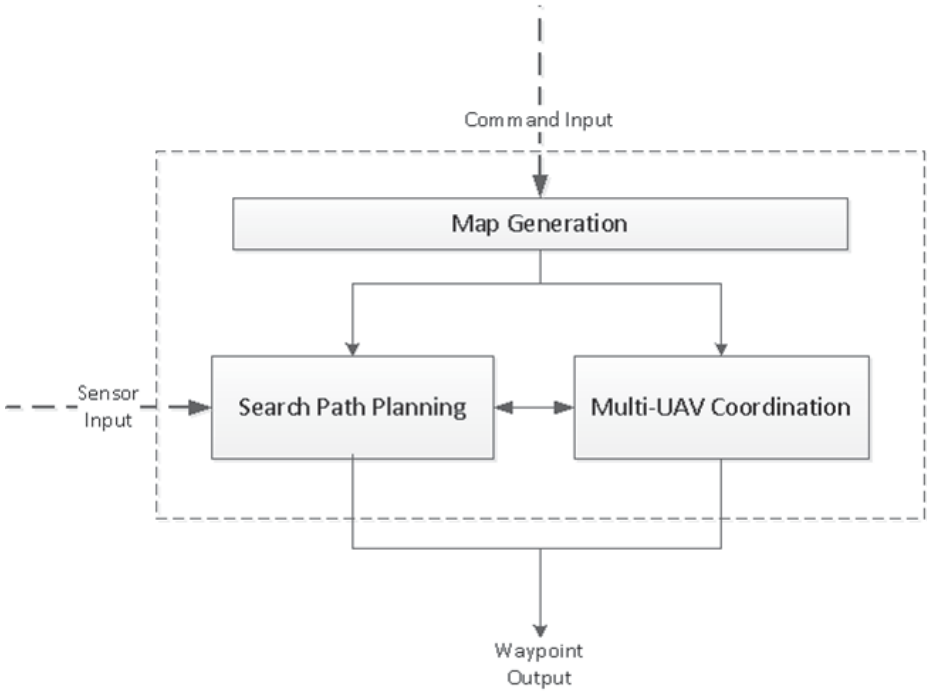

Figure 3.2: Command and sensor inputs provide data for processing and waypoint generation in the path planning module, which will then send planned waypoints to the autopilot hardware.

simple linking point from the system to a user interface for data display and command input, or further processing of accumulated data from all the UAVs in the network. As individual UAV functionality is a stepping stone that must be addressed before multi-UAV coordination can be fully tested, this will first take the form of a simple central interface.

For the autopilot, the hardware team chose a pre-made platform, the Paparazzi, as it is an open-source and relatively well established autopilot platform [34]. It uses the Ivy software bus, a network communications library developed by ENAC research in France, to handle message routing between a ground control software platform and the firmware on the actual mobile autopilot module [35]. From there, it can execute basic flight commands at three levels of autonomy: simple passthrough flight control, stabilized remote controlled flight, and full autonomous flight. The path planning component, in contrast, will link the individual flight module with the overarching framework.

Since this module is capable of taking in flight plans in the form of waypoint lists, execute pre-configured flight routines on command (such as a surveying routine for a given area), and update waypoints at runtime, it will be used to handle the backend navigation tasks. The software module's navigation and path planning task will thus be to generate waypoints and routine commands to then delegate to the autopilot module itself. This way, our module can function to overlay more sophisticated and automated path-generation methods on the pre-existing abilities of the autopilot, and ease the interface between multiple such platforms and the ground station using them.

By providing an accessible and portable module for these path planning tasks, this component will provide an enhancement over the existing usability and resource management capabilities of such autopilot software. The Paparazzi autopilot, like many other hobby oriented options, requires a full ground control suite to be installed for normal use, and customization requires modification of much of the platform-specific code for the autopilot. Furthermore, it does not provide the types of high-level management functions proposed, but rather basic manual path planning, and tuning utilities for the specific autopilot.

In contrast, the proposed path planning module would address this by providing an overarching layer for managing high-level tasks, into which a wide variety of autopilot modules to be interfaced in a uniform manner to a single reconfigurable system. This would

allow users of a variety of platforms to benefit from reduced command and coordination efforts in a search and rescue task, without the development overhead or architecture rigidity of modifying a specific platform's autopilot.

3.3 Image Processing

The proposed image processing component is broken down across two subsystems, a Field Programmable Gate Array (FPGA) co-processor with on-die Digital Signal Processors (DSP), and the software platform, an ARM CPU with on board graphics processing unit (GPU). The choice of using four different types of data processing devices- DSP, FPGA, CPU, GPU - comes from comparisons of different algorithms on different platforms conducted at the University of Tsukuba. The comparison shows that no data processing device has a clear advantage in real time image processing. In the test of two-dimensional filters, the GPU had a much higher throughput for filters using small numbers of pixels but performance decayed rapidly with increasing swatch size [6]. The results also show that the FPGA has higher theoretical throughput in stereo-vision processing and an implementation of the k-means clustering algorithm, however the development overhead to create FPGA modules is much higher than for software, and for these algorithms the CPU had better performance than the GPU [6]. While these comparisons were not performed with the exact hardware or algorithms we used, it was decided that the mixed results showed a need for different implementation options.

3.3.1 FPGA-DSP

FPGAs are advantageous in highly parallelized, high-bandwidth operations [6]. In some situations, the entire image processing subsystem may reside in hardware and the CPU-GPU system may be entirely dedicated to AI and path planning. Current FPGA manufactures such as Xilinx now include "DSP Slices" to improve FPGA utilization and allow for higher operating frequencies [36].

Our implementation includes on-chip buffers and memory for frame-wise operations such as filtering and multi-frame operations such as motion capture. The communication

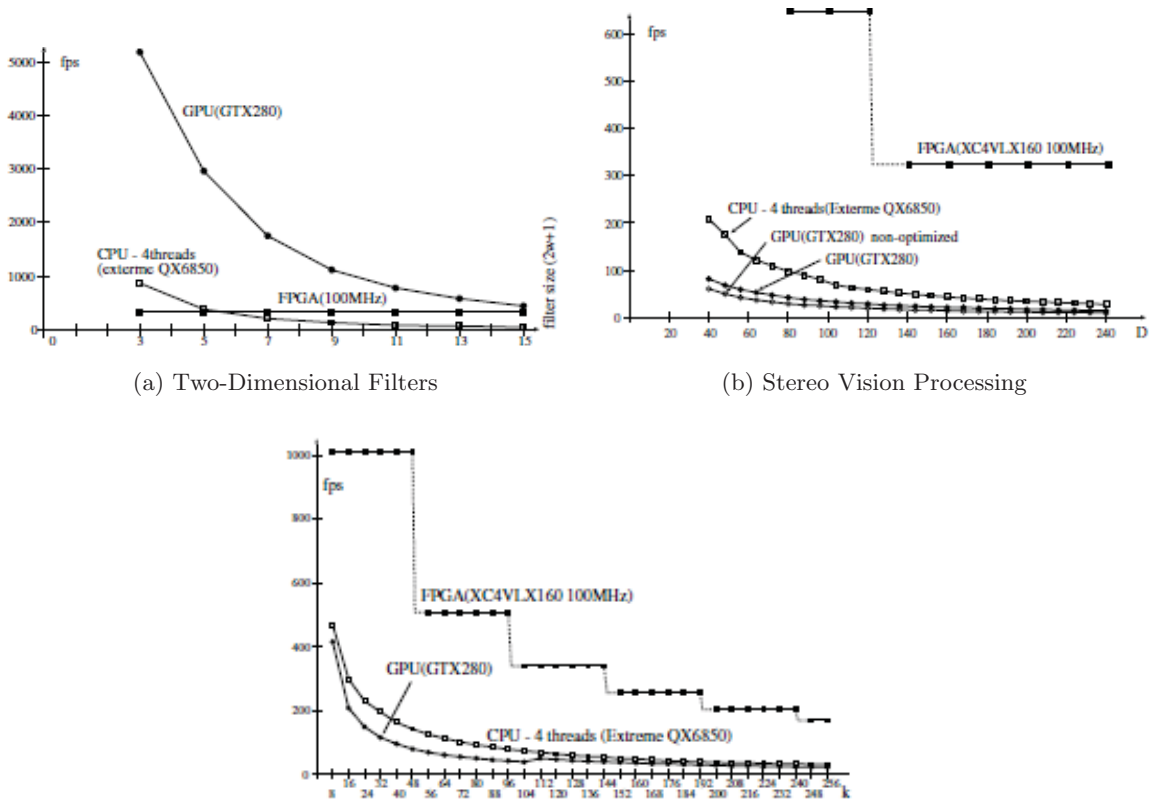

(a) Two-Dimensional Filters

(b) Stereo Vision Processing

(c) K-Means Clustering

Figure 3.3: Comparison of image processing algorithms on FPGA, GPU, CPU [6]

between the CPU-GPU is flexible and can operate at speeds up to 12Mbps.

Unfortunately, the development overhead of describing many image processing algorithms in HDL is much higher than for software. This is partially due to limitations in the current languages and partially due to the proliferation of image processing libraries available for software platforms such as OpenCV and the Matlab Image Processing Toolbox.

3.3.2 CPU-GPU

As part of our focus on developing a flexible and scalable framework for SAR UAVs, we did not limit the developer's ability to process sensor input in hardware or software. The developer can choose not to utilize the FPGA-DSP at all or, more realistically, to to implement part of the image processing subsystem on the FPGA-DSP and the rest in GPU accelerated software. This allows pre-processing or filtering to take place on a platform more suited for the task, and then the highly complex, more sequential mathematical operations to occur in the more flexible environment. This should enable developers to obtain real time performance without sacrificing flexibility.

The example algorithm we developed for this project calculates statistical perimeters on the FPGA-DSP and filters incoming frames to binary images. The CPU-GPU, utilizing the libraries available in OpenCV, would then perform a blob detection and tracks these blobs across multiple frames, eventually deciding if the current location contains a possible person of interest.

3.4 Framework Considerations

In order to make this system appropriately flexible and portable, the approach involved designing the broad foundation of the framework itself, with each module containing enough baseline implemented functionality to show that the overall concept of the system works. That is, the ability of the image processing module and path planning module to perform a demo of their desired tasks.

Furthermore, as a framework, it was important to design the code base in a portable manner. As such, it is expected that the framework will consist of one or more libraries that

can be installed on the platform operating system. This will allow other code to access the library, without the need to recompile the library every time something changes in a project implementing it, or conversely recompiling every project using it when backend library code is changed.

Given the breadth of this task, design choices had to be made to further reflect the time and resource restraints associated with this project. To avoid "feature creep" preventing useful progress, not all components are expected to be utilized to their fullest depth in a single iteration of the project, but necessary functionality will be identified, researched, and groundwork laid to provide the means of implementing the breadth of features desired.

3.5 Chapter Summary

Proposed here is a design for a framework that performs path planning and image processing tasks in a UAV network for search and rescue applications. The path planning component will provide enhancement over the default portability, flexibility, and effort required to use existing autopilot modules, while reducing the effort needed on the part of the operator. The image processing module will provide further enhancement over blindly reporting sensor data, granting the ability to apply some initial processing of image data in its pure, uncompressed form and intelligently report metrics on this data, even in the absence of bandwidth normally needed to stream video.

Overall, this system will provide a layer of enhancement over the integration of existing autopilot and image capture modules, letting developers more easily configure the system to a desired architecture and compensate for bottlenecks in data throughput that might otherwise render some systems unusable. More importantly, for the end user, this will allow UAV based search and rescue missions to be deployed with less resources spent in the planning and coordination of the aircraft involved.

Chapter 4

Implementation

The goal of the team was to create a framework specifically tailored to the problem of wilderness search and rescue with varying unmanned platforms. More specifically, the creation of a platform that was capable of:

1. Multi-agent Coordination and Path Planning
2. Sensor Fusion/Sensor Processing
3. Communication between Varying Platforms

In order to move the proposed framework design from theory to practice it was necessary to implement the components on actual hardware. Numerous requirements were applied as the size, weight, and power of the implementation platforms were limited to what could fit inside the chosen airframes. Each component was evaluated based on relevant criteria and trade-offs made based on availability, cost, and performance. The overall requirements used in the decision making process divided into platform and functionality requirements.

The platform requirements were derived from the airframes themselves in addition to the competing needs of the platform and communications team. Early communication with the platform development team led to both power and weight requirements seen below. These constraints were shared with the communications team (i.e. the total weight of the two team's combined components must be less that 10 lb). This meant that any decisions made would have to be verified with the other two teams before proceeding.

1. The total combined weight must be under 10 lb.

2. All components must be able to fit within the chosen airframe

3. The total power draw from all components must be under 120W

The functionality requirements of the component choice were drawn from the project goal, the creation of a SAR framework.

4.1 System Architecture

To meet these design goals, the framework design proposed earlier must be solidified into specific hardware components, functionalities, and requirements.

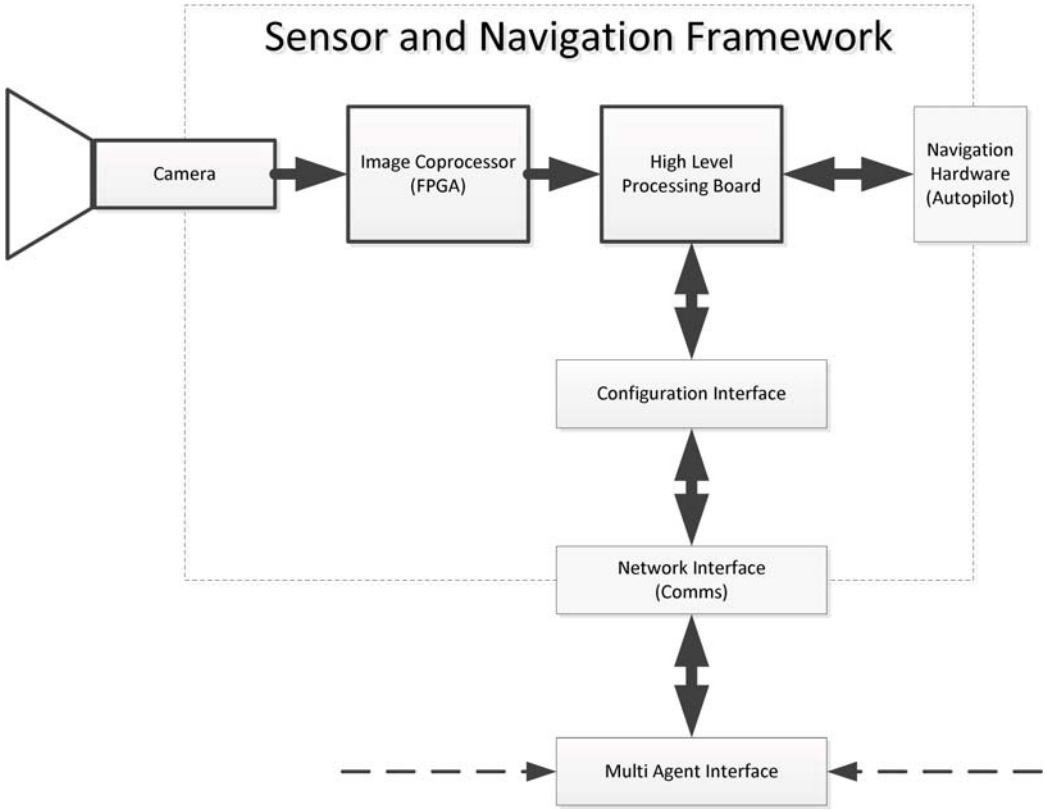

Figure 4.1: Final framework architecture showing connection between image processing module, high level processor, and other communications and flight components.

Shown in Figure 4.1 is the final proposed system architecture. The image processing will primarily be targeted at a discrete coprocessor board, connected directly to the camera and the high level processing board, which will direct path planning, data routing, and general framework configuration tasks. These will link with the communications team's platform for network connectivity, and the hardware team's autopilot and flight sensors for data collection and waypoint control of the individual UAVs.

This will also connect to a ground-station component, which will allow data visualization of messages sent from the UAVs, and command input to the framework itself.

4.2 Navigation Module Development

The hardware needed to have sufficient processing power to run a basic Linux operating system. In doing so, this would remove much of the hardware-specific coding that would need to be done to deal with networking and data acquisition tasks. At the same time, initial hardware considerations included the capability to perform basic image processing tasks, such as video compression or filtering, and be capable of interfacing with the autopilot module that the hardware team would choose for the flight platform.

Early research was weighted between various small form-factor Intel Atom boards, ARM processor boards, and FPGA development boards. Initially this led to choices of development boards with both an ARM processor and an FPGA on the same module. However, availability of such hardware led us to split our module into the purchase of two separate boards. While not necessarily as compact as a single-board option, this allowed for greater flexibility in what was used for each platform.

4.2.1 Hardware Choice

The high-level processing module was chosen from two main categories: mini/pico-ITX Intel-based motherboards, and ARM-based development boards. Initial hardware comparisons were made with low-voltage Intel Core i5 and i7 model ITX boards, however these boards were disproportionately expensive and power inefficient (100 watts being the estimated power needed for a low-voltage i7 board at full processor usage). This shifted focus

towards Intel Atom based boards and ARM development boards.

As can be seen in Table B.1, in comparison with virtually every Intel based board, the ARM development boards had substantially less power demand in proportion to the reported processing power. Atom based systems were typically in the 1 to 1.6 GHz single-core range, while ARM platforms ranged from 700MHz single-core to 1Ghz dual core. These platforms were also typically far less expensive than the Intel based platforms.

Another platform considered early on was the Raspberry Pi. This platform was substantially smaller and less expensive than other ARM platforms in its category, with very comparable hardware. However, accessibility was an issue when looking into acquiring this platform, as it was not released at the time of purchasing, and currently is only available in very limited quantities.

The final choice came down to boards using the TI OMAP ARM processor series. The most prevalent of these platforms are the OMAP 3000 series platforms, which include the multiple variants of the Beagleboard (BeagleBoard, BeagleBoard xM, and recently released BeagleBone). These boards range in processing speed from 700 MHz to 1 GHz on the ARM Cortex-A8 architecture, and include an onboard media acceleration chip and DSP. Many projects of similar nature have used this platform.

Similar to these platforms is the PandaBoard, which uses the newer OMAP 4430 processor, a dual-core 1 GHz ARM Cortex-A9, and is advertised as having enhanced media acceleration from the BeagleBoard platform.

All of these OMAP platforms are capable of running variants of known Linux distributions. Ubuntu, a Debian-based distribution, and Angstrom, a natively compiled Linux distribution for embedded devices, are among the most popular operating systems for these platforms.

The respective similarities between the BeagleBoard variants and the PandaBoard, along with their price range, led to choosing the PandaBoard as the initial high-level processor module. The BeagleBoard was more readily available and a more mature product then the PandaBoard, and has thus been used in many more projects. However, the PandaBoard had the most capable ARM processor, and boasted enhanced HD-capable media acceleration. For these reasons, the PandaBoard was chosen as our initial high-level processing platform.

A BeagleBoard was later purchased in addition as the main processor for a second plane due to supply issues with the PandaBoard. The similarity of the two platforms allowed for a seamless transition at an only minor performance hit.

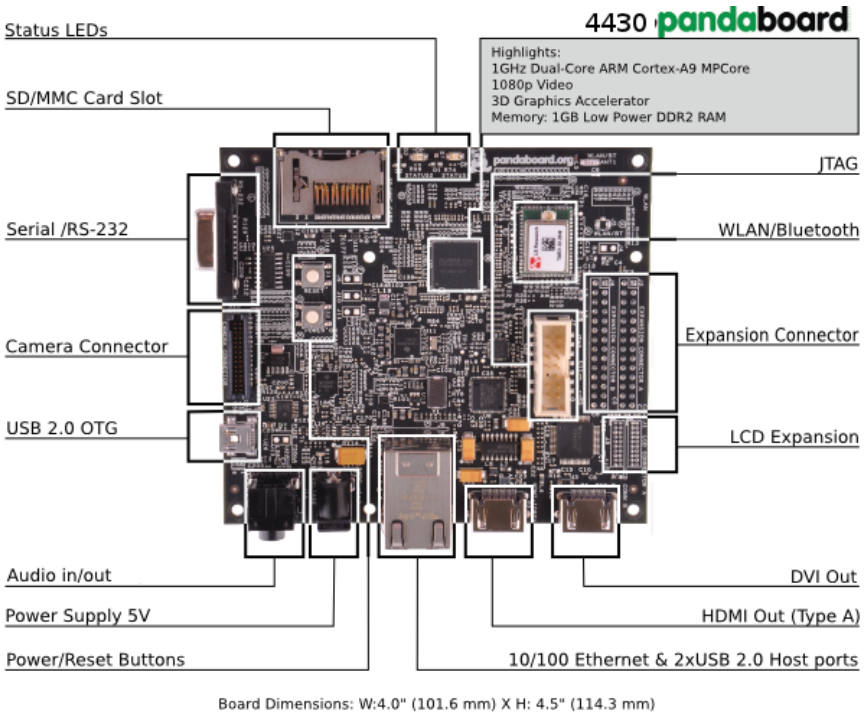

Figure 4.2: High Level Processor Module (PandaBoard)

In terms of weight and power consumption, these OMAP boards are all fully capable of running entirely off of industry standard 5-volt USB power with minimal amperage requirements. Coupled with size and weight, this makes these an ideal target platform for our project.

Our proposed approach to utilize this hardware was to design our code base in a mixed development environment. Utilizing various development tools, our hope is to be able to develop our platform at a higher-level design, then port the code over to our desired target hardware while modifying it to utilize any native peripherals we may wish to use. As an end product, our high-level board should have a usable and expandable base implementation of our software framework and some baseline implementations of our proposed capabilities. It is our goal for the high-level processing platform to provide a usable basis for facilitating

the path-planning and data reporting process of SAR missions.

4.2.2 Path Planning Development

For the path planning module, the map structure needed to be carefully considered before implementation. To provide this functionality in the framework, a robust but manageable map structure needed to be chosen that would provide advantages for both individual UAV path planning, and coordination of search operations between multiple UAVs.

A simple method to initially implement multi-agent coordination is to use a map structure that allows well defined allocation of search areas to a single UAV, such that there is no ambiguity as to which UAV should be in a given area at a given time. Furthermore, compared with a dynamic traffic control approach, this reduces the processing effort necessary on the system for coordination. As such, the individual UAV path planning tasks could be focused on primarily, and basic multi-UAV coordination built off of this functionality.

As mapping tasks necessary in a search and rescue mission would largely comprise tracking sensor data on individual portions of the map, a cell-based map was chosen as it provides a means of classifying and localising an otherwise continuous collection of data points. For this purpose, cell geometry is a simple choice between the only three shapes that uniformly tessellate; triangles, squares, and octagons.

For navigation purposes and programming purposes alike, cell-based grids typically would use a Cartesian coordinate system (x and y coordinates on perpendicular axes) and square cell geometry. This choice is logical when considering the intuitive nature of a Cartesian coordinate system, and the ease by which this data can be represented and addressed in code as a two dimensional array of values. However, from the standpoint of path planning, there are a number of disadvantages to a square cell geometry.

From a computing standpoint, a square-grid was more intuitive, and can be represented in memory more easily. However, in grid-based search algorithms in general, consideration needs to be made for the conditions by which an agent might cross between cells. Across edges between known, adjacent cells, this was not an issue, however corner crossings risk passing into undesired cells. This is especially important in path planning as crossing between cells should be safe for the craft involved, risk of crossing into unwanted cells

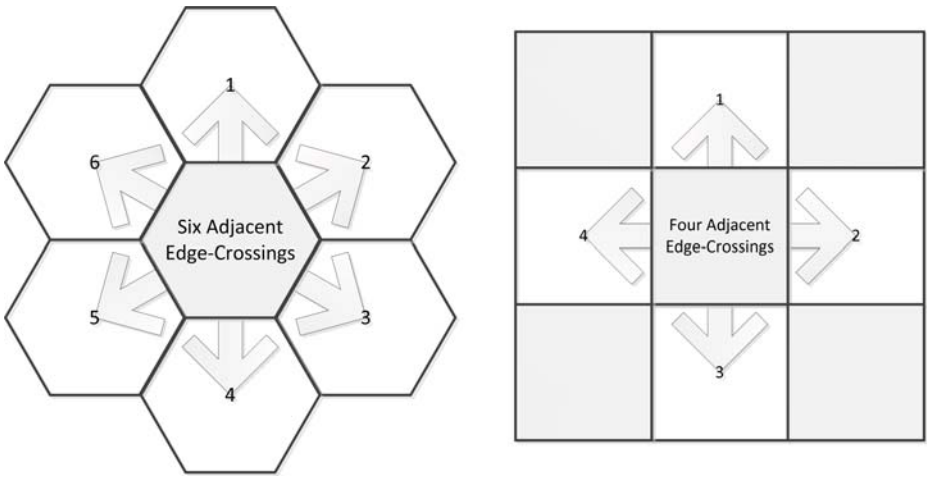

Figure 4.3: Hexagonal cells provide higher edge-crossing options than square grid cells.

should be avoided, thus reducing the options of movement when planning a path. As can be seen in Figure 4.3, hexagonal cells provide substantial navigational benefit in this respect. As opposed to four edge crossings and four corner crossings to adjacent cells in a square grid, the hexagonal geometry provides edge-crossings and no corner crossings on all six adjacent cells, a 50% improvement in safe cell traversal options with no wasted adjacent space.

Addressing the coordinate system in such a search grid is another problem which had to be considered if this was to be implemented. Square grids are simple to describe a coordinate system for, but options for this choice needed to be explored before ruling it out.

The naive approach to solving this problem may involve addressing hexagonal cells in perpendicular rows and columns, in an attempt to emulate a Cartesian coordinate system. However, hexagonal cells do not pack in a perpendicular orientation. As such, this method becomes inefficient as it involves a non-uniform conversion between grid coordinates and actual global coordinates in Cartesian space. The same formula cannot be used to convert all coordinates between systems. However, an elegant solution was devised to address this.

A simple solution to the problem of managing a hexagonal coordinate system is shown in Figure 4.4. Our algorithm, named Clevelandius Stemirinus, works by by skewing a Cartesian plane to accommodate a hexagonal cell geometry, local cell coordinates can again be addressed the same as square cells from a programming standpoint, and conversion between coordinate frames involves a single trigonometric operation.

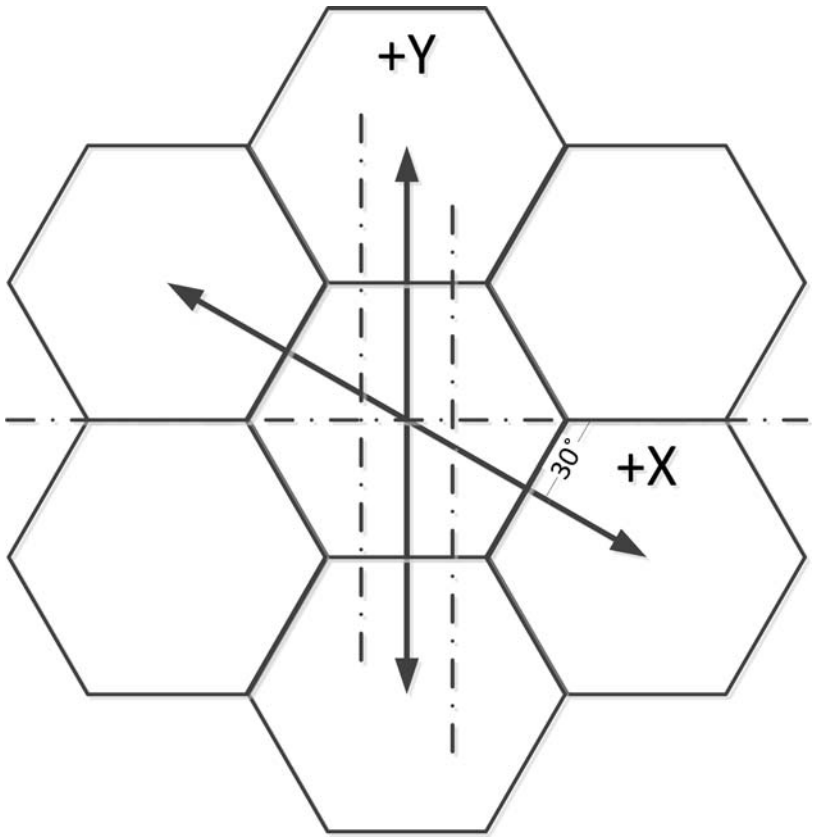

Figure 4.4: A 30-degree-skewed Cartesian coordinate system provides uniform conversion between local and global coordinate references.

At this point in the project, the chosen baseline method for individual-drone navigation needed to allow the platforms to take in a set of allocated waypoints with determined probabilistic weights. If the search plan avoids repeat passes before visiting all assigned waypoints, attempts at path optimization could quickly become computationally untenable due to the mere nature of such a calculation. As cited previously in the Travelling Salesman problem, true optimal navigation between multiple points is an NP-Hard problem, difficult for very powerful computers on even a small number of locations. For this purpose, searching for a nearest high-probability cell was done with the A* algorithm, as described previously and shown in Figure 4.5.

As search coverage is also a consideration, especially in absence of existing search data, a default coverage-emphasized search algorithm needed to be chosen as well. In SAR ap-

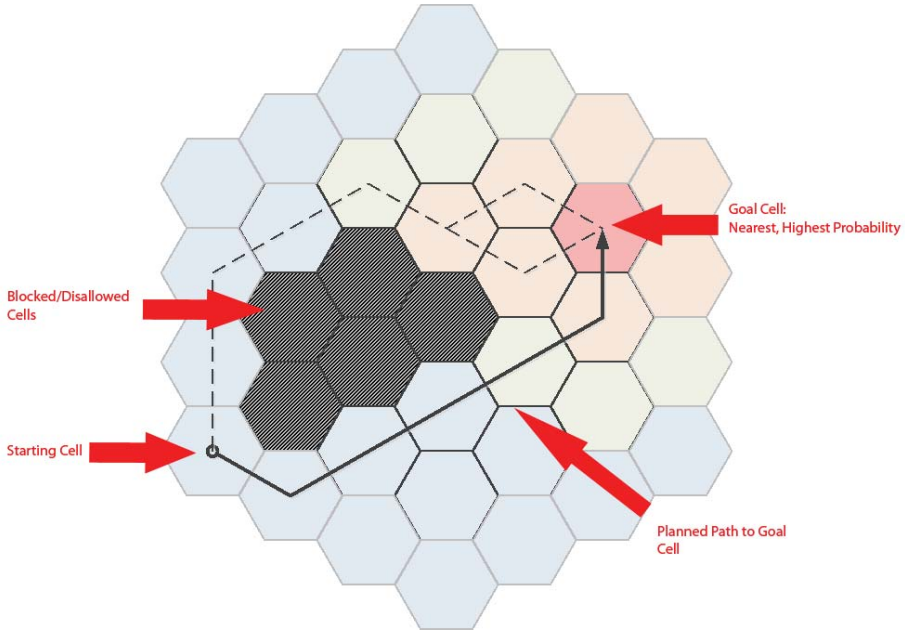

Figure 4.5: Multi-point navigation to the nearest unvisited cell or nearest highest probability cell is performed using the A* algorithm. This provides path planning capability around restricted regions.

plications, or any aerial surveying task, a sweep or spiral is a simple means of covering an area with a high efficiency of coverage. As such, we implemented a generalized algorithm for performing this task.

The overarching approach to using these path planning algorithms needed to provide some means of deciding between path planning approaches and using the available algorithms, instead of explicitly instructing the UAV which method to use. Figure 4.7 shows a method of addressing this problem. By placing the path planning algorithms, whether single-point or multi-point, in a cascaded decision process, this would allow both a uniform command structure for UAV navigation tasks, and easy reconfiguration of path planning behavior as more advanced algorithms are implemented in the future. While not necessarily an overall optimal path planning approach, this will provide a baseline working method of allowing our platform to allocate search points based on parameters beyond mere flight distance.

Once the individual UAV path planning was implemented, the system needed expansion

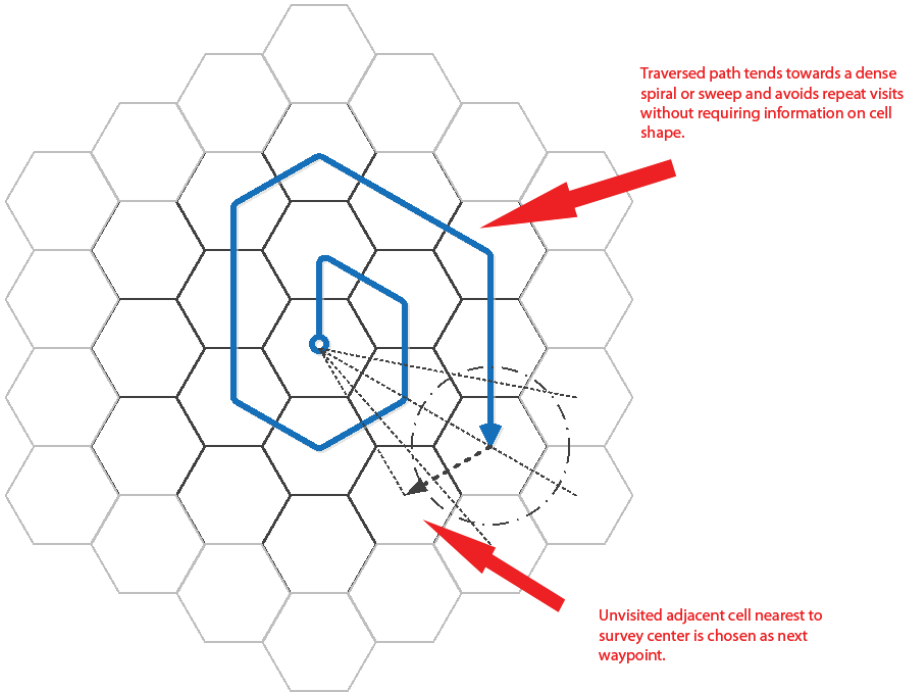

Figure 4.6: A spiral or sweep search can be performed on any uniform grid by choosing the next unvisited cell with a minimum distance to the sweep origin.

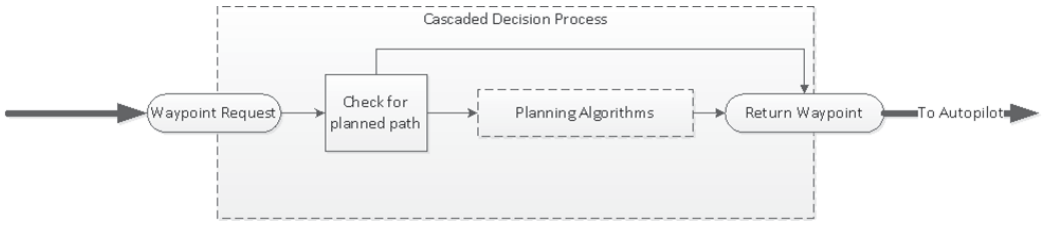

Figure 4.7: Path planning algorithms can be called in a cascaded manner behind a single access point. This allows easy reconfiguration of the decision process.

to perform basic coordination between multiple platforms. In particular, the framework needed to account for a means of handling the addition of new waypoints in a multi-agent environment. To accomplish this, a proposed approach is simple cost bidding.

Using bidding, when a new waypoint is added, whether by detection from one of the drones or manually from the operator interface, its assignment within a drone's search pool can be put up for bid between available drones. Parameters for determining the assigned pool can include the distance from other points in the pool, the fuel consumption of each

craft, and the respective probabilistic weights of the new point of interest versus the existing points in each pool. The result of this calculation comprises the "cost" of this waypoint to each drone. During a bidding procedure, the first drone to respond with the lowest cost within the time of expiry receives the waypoint assignment, at which point it is allocated the necessary search area and its own path planning takes over.

From this baseline, more complex path planning methods can be applied to further expand on the sophistication of this particular aspect of our system.

For the sake of usage in a framework, the navigation code was written to compile to a C/C++ shared object library. This carries the speed advantages of using native code, while being portable by installing as a library to any Linux system.

This was split between a collection of general purpose data structures and geometric functions, search algorithms for operation on the searching grid structures, and a single Agent class interface by which to use this code on a single-plane basis.

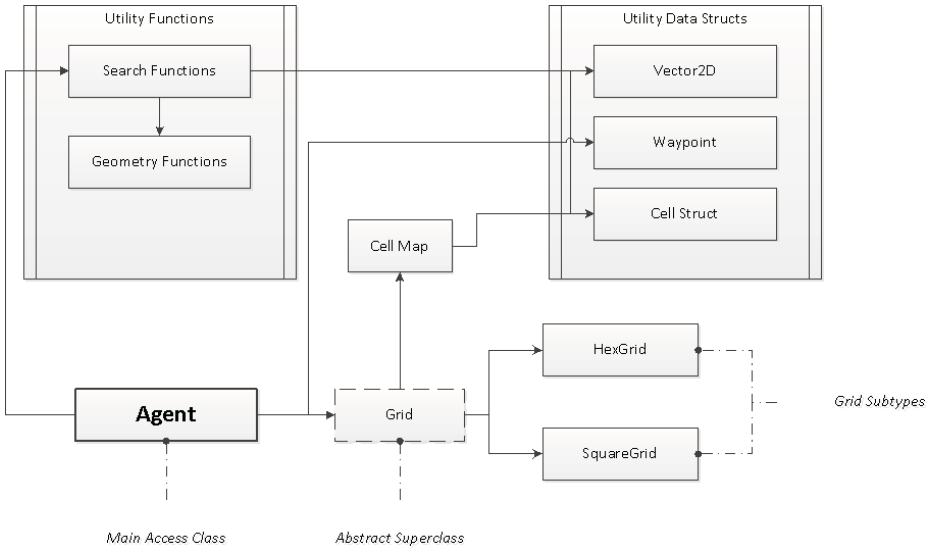

Figure 4.8: Library class structure divides search grid data and utility data types behind a single access class.

In Figure 4.8 the current class structure of the navigation library is outlined. The main access class, Agent, is for the most part the only class that should be linked to an application for usage of the navigation code. This provides access methods for updating agent position,

setting navigation targets, and retrieving resulting waypoints for commands sent to the autopilot hardware. While by design this should be the main access class, for expedience some other classes, like Grid, are linked to some extent for retrieval of specific map data without excessive duplication of code.

Internally, these classes refer to provided function libraries for geometric functions. Currently, the main search algorithm used for multi-point planning is not a true "greedy" search, as originally intended, but rather became a modification of the A* algorithm. This is known to provide much better path planning results without the issues associated with greedy path planning, namely accounting for local extrema conditions.

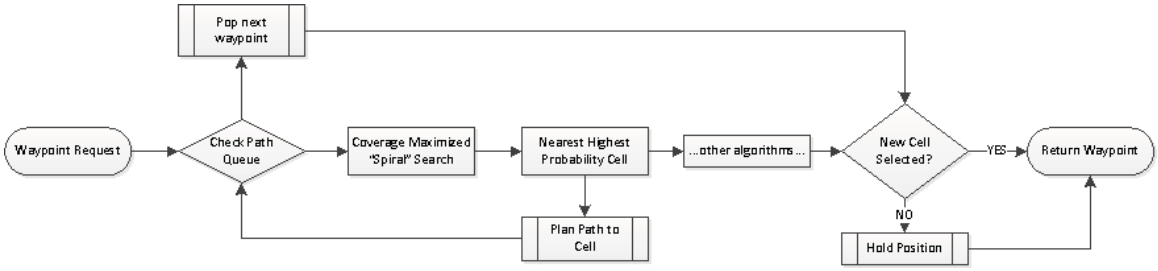

Figure 4.9: Cascaded navigation algorithms provide a robust and progressive decision-making process.

As designed, the navigation algorithms are called from an internal decision cascade behind a single waypoint request. In Figure 4.9, the current cascade structure is shown. The concept behind this structure is to define a multi-algorithm decision process by which each navigation method is utilized. If one fails to generate a new waypoint, the next one is used. This is placed within a single waypoint request method within the Agent class, such that search algorithms used do not have to be chosen at runtime, but rather are abstracted behind an access function. For now, this decision process is well documented but hard coded. Future work could expand on this to allow runtime reconfigurability.

4.2.3 Testing Procedure

To test the success of this approach, the individual UAV navigation system must first be completed before full multi-agent coordination can be tested. Fully evaluating single-UAV

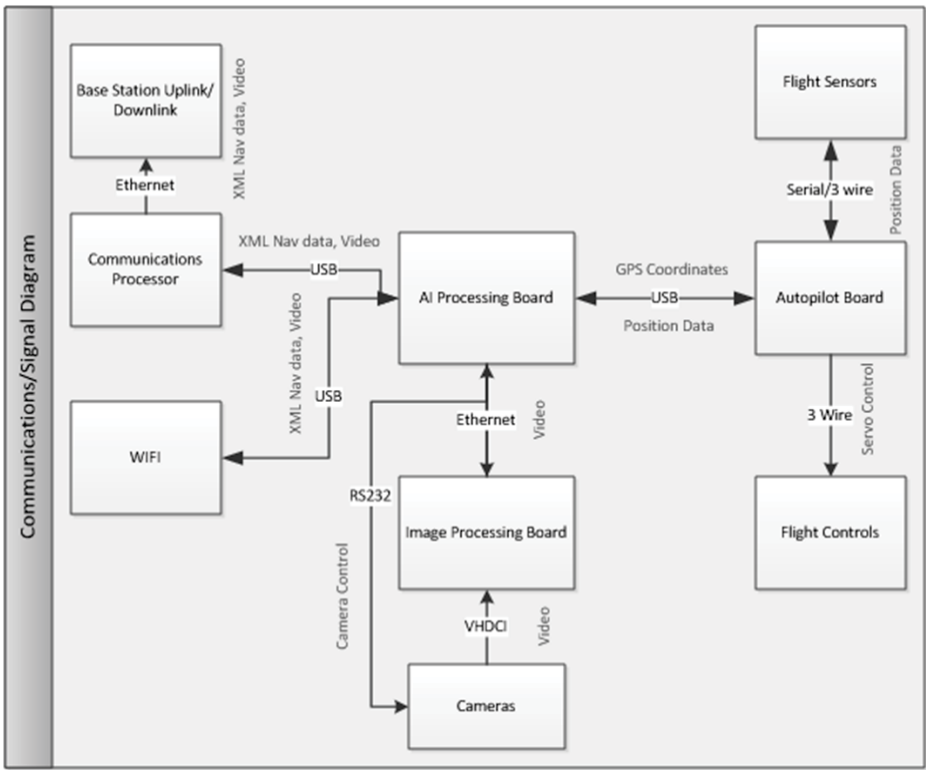

Figure 4.10: Signal Diagram showing the interfaces between different subsystems in the WiND Framework

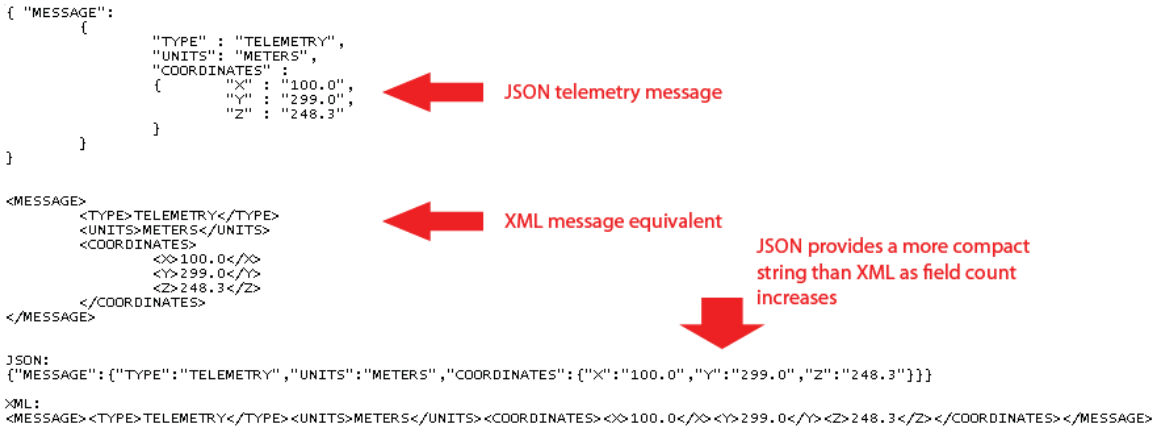

Figure 4.11: JSON provides a more compact representation of data than XML.

navigation on the actual platforms is dependent on the progress of the hardware team, so in absence of this, available methods of simulation were used to observe completion of navigation tasks and overall behavior of the search algorithms. Once further stages of integration can be completed, simulation with the actual autopilot, and ultimately testing on the final platform can be done.

4.3 Communications Formatting

The communications layer itself is the task of the communications team on this project. However, data formatting options were a consideration that needed to be made in order for this framework to interface with any available communications layer. XML and JSON are two structured data formatting languages commonly used in web applications.

String data is very safe over a network or serial connection, in comparison with arbitrary binary data. However, any arbitrary binary data can be encoded into a string to send over such channels of communication. This framework will be geared towards sending and receiving data in a structured data string format. Figure 4.11 shows a comparison of a simple telemetry message represented in both JSON and XML. As can be seen, JSON is significantly more compact in format, giving it less space overhead to use than XML. As such, JSON was chosen as the data formatting choice.

4.4 Image Processing Development

For the task of image processing, the challenge was choosing a platform that would allow for at/near real-time processing of image data and choosing a camera that would give high quality enough images. While these decisions may seem separate, they are very much intertwined as the interfaces available for each platform vary greatly. From this task several functionality requirements were derived:

1. At/Near realtime image processing at 5 fps.
2. Low CPU overhead on main navigation processor.
3. Filter data to transmit between drones/base station.

4.4.1 Hardware Choice

For the image processing, three types of boards were considered: DSP, FPGA, or ARM processor after graphics cards were ruled out due to high power requirements. From prior research it was known that the FPGA would most likely be the fastest option but would be the most difficult option to implement. The ARM platform using a vision library such as OpenCV would be simplest, but slowest due to its general purpose nature. The digital signal processor would be the middle ground.

Image Processing Board

Several board offerings from Texas Instruments, Analog Devices, Xilinx, and Altera were explored and compared on the criteria of cost, availability, processing power, and I/O. The final comparison list comprised of two Xilinx Spartan-6 boards, two DSP boards, and two OMAP based ARM processors.

As can be seen in Table B.2, the LX9 Spartan-6 development board was found to be the best option for the project. This lightweight FPGA development board powered by a Spartan-6 provided just enough I/O combined with more than enough storage for image processing designs.

Figure 4.12: Spartan-6 LX9 Microboard

This key selection of an FPGA for the main sensor interface highlights the platform independence of the framework helped define the sensor interfaces needed, namely a digital camera interface. Furthermore, with the use of an FPGA, an unparalleled processing speed can theoretically be achieved at the cost of ease-of-implementation. It was hoped that the use of such a device would overcome one of the two main obstacles for realtime image processing, restricted algorithm runtime. Based on this sensor fusion platform, corresponding cameras were chosen.

Camera

Many camera options were considered for use as primary sensors in the project. These cameras ranged from webcams, consumer point-and-shoots, thermal, and high quality industrial cameras. Key factors in choosing the camera involved field-of-view (FOV), focal length, resolution, and lens zoom. The target operating altitude was chosen to be 400 ft . Based on initial tests with image processing algorithms it was decided that the camera should produce a digital image with the size of a person being greater than or equal to 100 px^2 at the target operating altitude. This size requirement could be met by either choosing a camera with a larger resolution, or choosing a camera with greater zoom.

Early in the project development there was hope for obtaining a FLIR thermal camera through known contacts. The TAU 640 camera provided the ideal characteristics for this project. Unfortunately this camera proved elusive with prices ranging in the thousands and had the lowest resolution of all options explored.

Initial research also found the possibility of remote controlling high-end consumer(DSLR) cameras. An opensource software program, "GPhoto," running in linux allows for this capability. As with the thermal cameras, cost proved a major barrier in addition to increased weight, increased size, and decreased flexibility. This type of system would have the additional requirements of running linux and It was for these reasons that this class was similarly ruled out.

Typical webcams have low to high resolution specifications with relatively low zoom capability. For example, the Microsoft LifeCam Cinema has a resolution of 1280x720 pixels with a field of view of 73° [37]. Using simple trigonometry, at 400 ft this results in a person being 24 px^2 as seen in Figure 4.13. In addition to the size of a person in frame being smaller than the cut-off,the problem in using such a high resolution camera is higher data rate and higher bandwidth. As most webcams stacked up similarly, or worse, this prospect was dismissed.

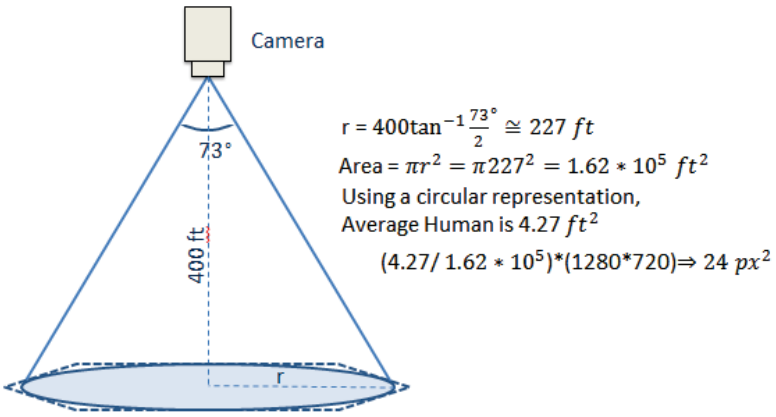

Figure 4.13: Calculation of person size (in pixels) based on altitude and FOV [7]

For interfacing with FPGAs, industrial cameras proved to the most flexible and suited for this task. Offering a wide range of digital and analog options and a dizzying array of performance options, this was the ultimate choice for the project. While the ultimate goal was to have a digital video feed directly into the FPGA, an analog version of the Sony "Block Cam," the FCB-IX45C, was chosen do to its cheap price and performance. With a serial controlled 18x optical and 4x digital zoom the camera could operate in the full

operational range <400 ft while meeting the 100 px^2 requirement. However, due to its analog nature, a video decoder board was also purchased to convert the video output into something suitable for the FPGA.

Figure 4.14: Sony Block Camera[8]

4.4.2 Development

As part of implementing a framework which could support image capture and image processing, we set out to develop our own image processing module for this framework which would:

1. Utilize both software and hardware platforms
2. Work with either an infrared and visible light image source

After research into current image processing techniques and gaining and understand for algorithms specific to applications such as ours, we decided that implementing an existing algorithm on an FPGA or DSP would be a large undertaking. Since our project scope called for this module merely for demonstration and testing purposes, we decided to develop our own, simplified, algorithm based on current technique more suited for the task.

Platform Specific Demo Algorithm

Our target platform, containing an FPGA with DSP slices, and an ARM CPU with an on-chip GPU posed a unique challenge. Hardware accelerated image processing is an active research topic and many masters-level theses have been published on the subject. However, current research in hardware accelerated image processing uses only one or two of these types of processors. We could not find a paper in which four unique processor classifications were used together for a single task.

Our approach, to accommodate a theoretical use of all four processors, was to split the algorithm into four separate tasks which could be computed successively and independently. To address item 2, we develop this algorithm to operate on a *heat map*, what we defined as a single channel of information. In the case of an infrared sensor, the heat map would literally be radiated energy. In the case of a visible light sensor, the heat map would be each color channel separately, interpreted as an intensity.

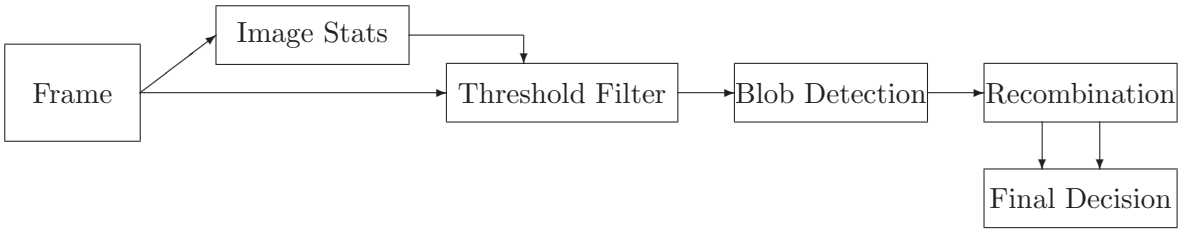

Figure 4.15: A successive and independent, modular image processing algorithm we developed for testing our platform.

These four successive tasks, as seen in Figure 4.15 are:

1. Image Stats - For each channel, compute statistics on the frame. Determine The range of a normal pixel value. Pixels that are outside this range are considered unusual.

2. Threshold Filter - Pass a binary value for each pixel in the image according to membership of the region. For example, pass 1 for unusual pixels, 0 for others.

3. Blob Detection - In the binary image, find clusters of pixels that were identified as unusual. Return only clusters that are approximately the size a person would appear

at the current altitude.

4. Recombination - Compare the separately processed channels if appropriate, perform any additional logic or comparisons to other sensors, and make a final decision on each blob. This step may be used if the algorithm performs any operations on sequential frames.

This algorithm can translate directly into our platform hardware. Computing statistical parameters require large multiplications, divisions, and summations efficiently implemented on a DSP. The threshold filter is a highly paralleled operation suited for an FPGA. Blob detection, while realizable on an FPGA, can be quickly implemented on a GPU using existing code libraries for our platform. Finally, the more generic and interconnected recombination operation is suited for a general purpose CPU.

Simulation Realization

The next step in the development of the image processing demo module was to code the algorithm and test the results. For this, we decided to use Simulink due to its easy to use image processing blockset.

By implementing our algorithm first in simulation, we were able to test how changing different perimeters effected the result. For example, the "Heatmap" block, that determines the threshold of an unusual pixel, could be implemented many different ways. Our final version, shown in 4.17 computed the usual-ness based on the mean and the variance with a few adjustments made via constants. This simple algorithm, when tested on aerial footage of a soccer field, accounted for noisy frames well and could detect our test subjects with fewer than 10 blobs.

The 0-10 blobs this program returned were not all hits. It often returned false positives on shadows, muddy sections, and goal posts. However, since these blobs were all bounded in size, the total data that would be sent over a communications link and reviewed by a human were significantly less than if we streamed back the entire image. More on the performance of this algorithm is in 5.

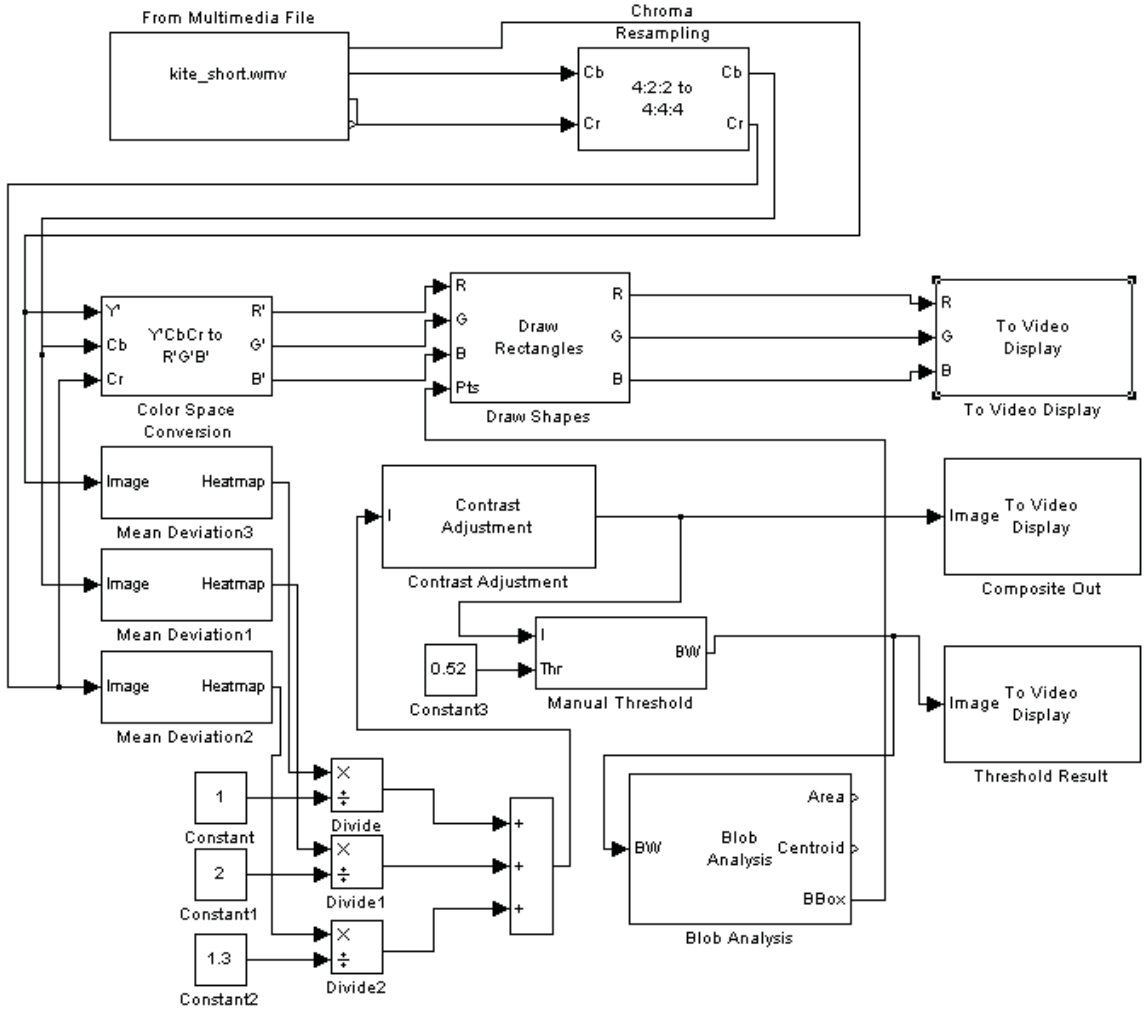

Figure 4.16: Simulink implementation of our custom image processing algorithm showing manual adjustments. This easily adjustable model was used to fine-tune the algorithm.

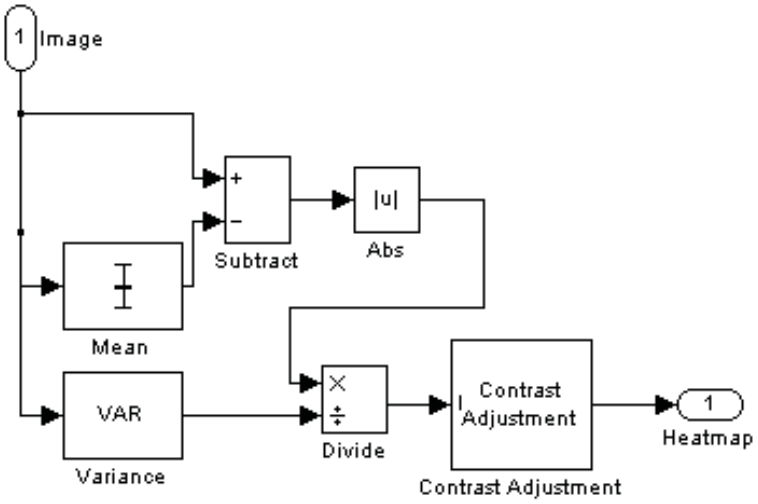

Figure 4.17: Simulink implementation of the "Mean Deviation" block showing the algorithm chosen to define usual versus unusual pixels.

Hardware Realization

While our algorithm can, in theory, be implemented on all parts of our hardware platform, our actual implementation was incomplete. Due mainly to Xilinx licensing, the HDL implementation of this algorithm could no be synthesised, even for testing in an academic setting.

We were however still able to write and test the interfaces for the Camera-FPGA and the FPGA-Pandaboard. The implemented blocks are the Video Decoder, Buffer, Filter, and Communications Subsystem.

The Video Decoder block interfaces with the camera and decoder board, translating the analog NTSC input into 10 bit parallel digital signal. The input to this block is NTSC as defined by the ITU-R BT.656-1 standard. The specific format the video decoder uses 4:2:2 YCbCr as specifiifed by the ITU-R BT.601 standard. This block was written by the team, in Verilog, and uses no external intellectual property.

The Buffer block is a circular buffer capable of holding one channel for a single frame. It is constructed such that multiple buffers can be chained together for use in more complex algorithms. While the buffer is circular, it can be accessed non-linearly for arbitrary pixels.

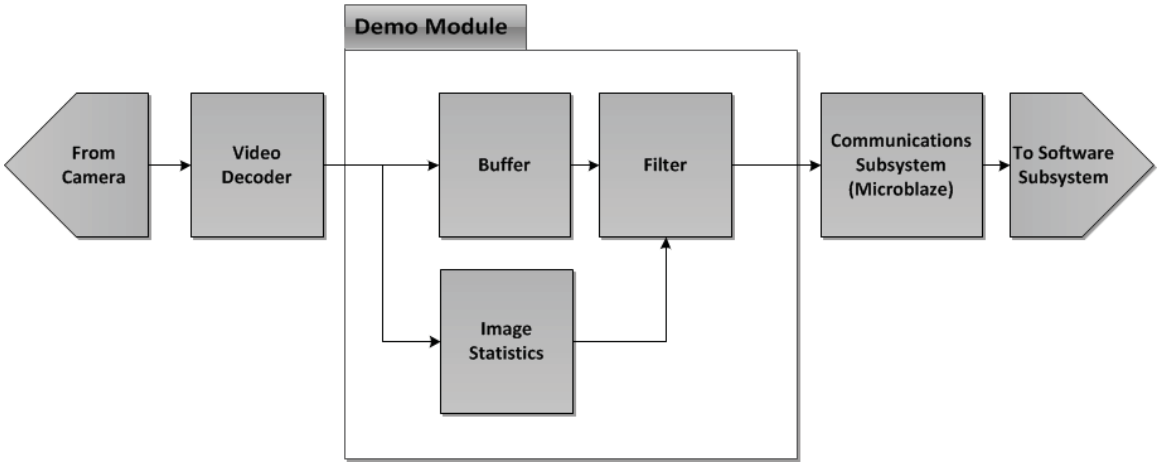

Figure 4.18: Block diagram showing dataflow for the HDL component of the image processing system. The outlined section labeled "Demo Module" shows the application specific blocks.

The location of each pixel in the frame is retained so that algorithms which wish to use specific regions of the frame can operate correctly.

The filter block was originally designed to be a highly parallelized comparison of the image frame against the output of the image statistics block. When the system came together however, we realized that there was a bottleneck between the filter and our implementation of the communications subsystem. In the end, the filter block became a simple, serial, compare function. However more work with the Microblaze processor would remove this bottleneck.

The Communications Subsystem, developed with a Microblaze softcore processor, interfaces the FPGA-DSP chip with the network interface. Using the "Lightweight IP Stack," the softcore processor interfaces with the Pandaboard over a 100Mb ad-hoc LAN.

4.4.3 Testing Procedure

The testing procedure for image processing was divided into two components: algorithm effectiveness and runtime benchmarking.

In order to test algorithm effectiveness, sample image data was required. Unfortunately, due to the limited flights of the actual UAVs through the course of the project, adequate

flight video was not available. An attempt obtain aerial footage via kite and camera setup was attempted but was unsuccessful due to poor video quality and the length of the kite's string prevented flights greater than 150 ft.

Figure 4.19: The team attempted to obtain aerial footage(See Right) via kite(see Left)

Algorithm Effectiveness

To test algorithm effectiveness, it was also determined necessary to test the algorithm on different terrain conditions. For these reasons simulated aerial footage was used in order to test the algorithms under different conditions. Using Adobe Photoshop, test images were created for four different terrains: field, forest, rocky, and snow covered. A person was then added to each, and then the images scaled to correct altitudes of 100 ft, 200 ft, 300 ft, and 400 ft (Figure 4.20). A Matlab script was created to batch test the images using the simulink model and then output hit locations and error results. Since the Image processing algorithm was intended to filter possible results the measures of error were both in reported distance between a "hit" and actual person and whether or not the person was found at all in any of the image "hits."

Runtime Benchmark

In order to be "realtime" an image frame must pass through the entire algorithm from input to output before the next frame arrives. At 5 frames per second this means that the

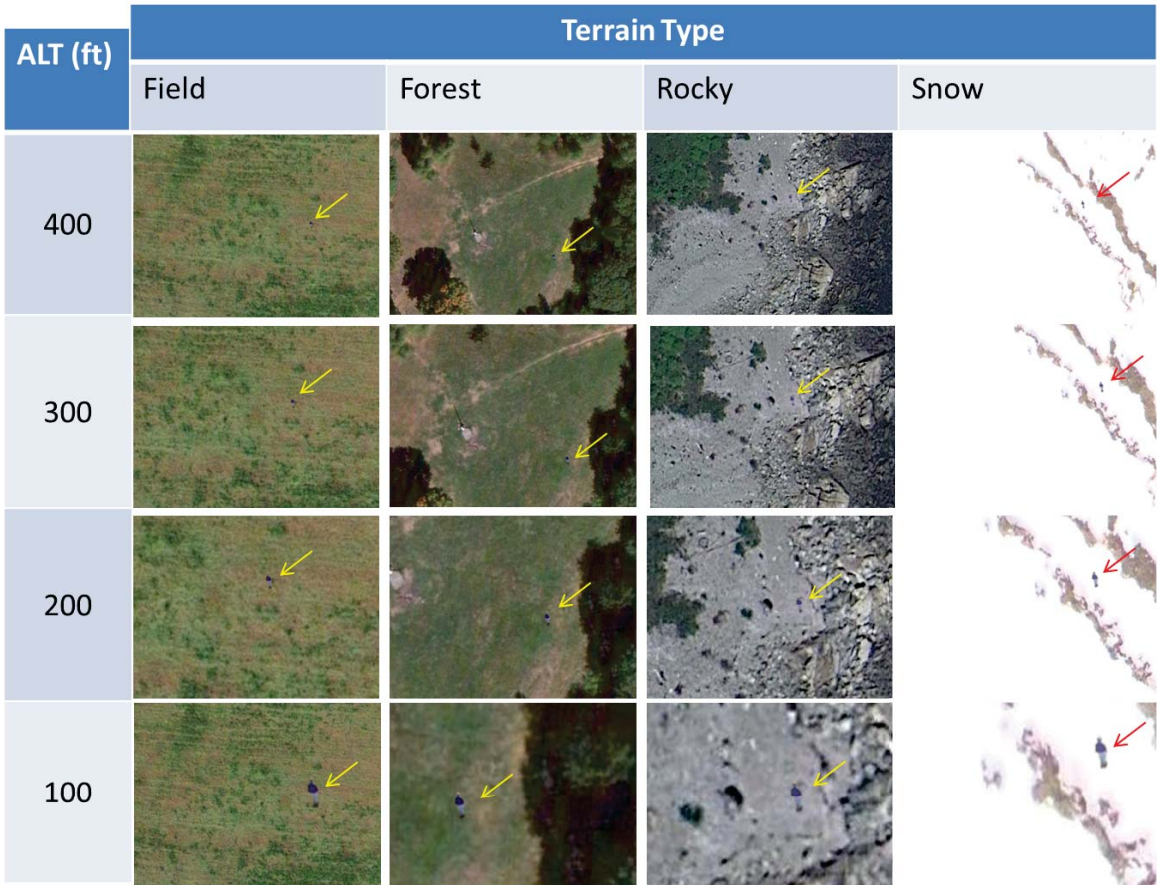

Figure 4.20: The 16 different sample images above represent four altitudes and four different terrains. Arrows show the location of the person in each image

processing of a frame must take place in under 0.20 seconds. To tests the runtime of the algorithm the scheme devised was to simply input a single frame and see how long it would take to appear on the other end.

4.5 Chapter Summary

Over the course of the project the initial framework designed in the approach was implemented in hardware and code. An ARM development board was chosen to perform run the path planning algorithms and handle main communications routing. A Spartan-6 FPGA was chosen to perform the sensor and image processing. Several difficulties arose with driver

issues and proprietary cores but were worked around. With the implementation complete, testing was able to commence.

Chapter 5

Experimental Results

Over the course of this project, many considerations and adjustments in priority had to be made in the completion of components of this framework. Due to time limitations with the hardware team's testing procedures, some software testing procedures were not able to be entirely evaluated. However, as a result of increased efforts towards an effective network application interface, this proved to be a highly useful method for both using and configuring this framework.

5.1 Framework

Network Application Development

Due to deadline conflicts between the UNH development teams and the communications team on this project, some components not originally in the main project architecture were constructed to ease in testing, and, ultimately improve the functionality and usability of the framework on its own. In absence of such components were largely limited to command line printouts from the low level code. To compensate for this, a secondary network interface and user interface were developed for demonstration and testing purposes.

Since both a network interface and a user interface were needed, a web application was deemed the simplest and most versatile approach. In Figure 5.1, the resulting initial implementation of this is shown. This is intended to be a prototype only, as it was originally

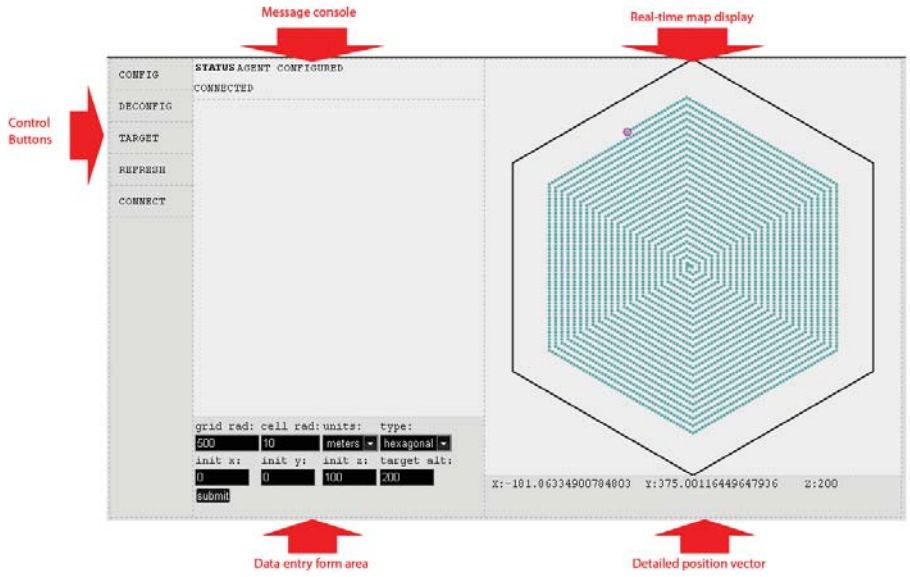

Figure 5.1: The initial network application interface, shown with a simulated flight path, message prompt, and configuration interface.

the task of UNH to develop a user interface, however this component can be used and expanded on quite easily. The interface is written using standard HTML and Javascript, just as a typical webpage.

Developing the framework's interface as a network application carries the benefit of allowing interface with any platform with a capable web browser, with no additional software installation required. To accomplish this, NodeJS was chosen as a pre-existing platform to use. NodeJS is a modification of Google's v8 Javascript engine used in the Chrome web browser, made to run server-side and take package-like modules for expanding functionality.

To use this with the framework libraries, it was found possible to bind native C++ libraries with NodeJS, making the navigation code accessible via a javascript network interface. This made providing a browser-based user interface a far more streamlined task than originally conceived. Furthermore, this allowed application modules to be linked and information flow configured easily outside the existing C/C++ code base, without excessive recompiling.

5.2 Image Processing

The goal of the image processing module was to filter a live video feed to only "person-like" features and limit the amount of data required to send back to the base station. Our implementation returns a maximum of 10 20x20 px images and aims to minimize false-negatives.

5.2.1 Data Reduction

By design, the algorithm greatly reduced the amount of data sent over the communications link. By only sending relevant features in the image as opposed to the entire image, a reduction of 98.2% percent was achieved as given by:

$$Reduction = 1 - \frac{(\#\ of\ features)(area\ of\ feature)}{total\ frame\ area} = 1 - \frac{(10)(20 * 20)}{720 * 480} = .988$$

Figure 5.2: Image processing algorithm run simulated forest setting at 100 ft

For a more illustrative example, consider Figure 5.2. In this sample image, the algorithm has been run on an aerial photograph which clearly contains a person. If we were to send the entire image back with person identified, this would mean a full 740x480 frame with 24 bit color data. Even with compression techniques, this will result in a substantial data-rate

and bandwith demand at even 5 frames-per-second.

However, we are already identifying the key features of the image through our image processing algorithm. We can send only the key features with a sufficient margin to contain the person and greatly reduce data demands on the network. This process can be seen in Figure 5.3.

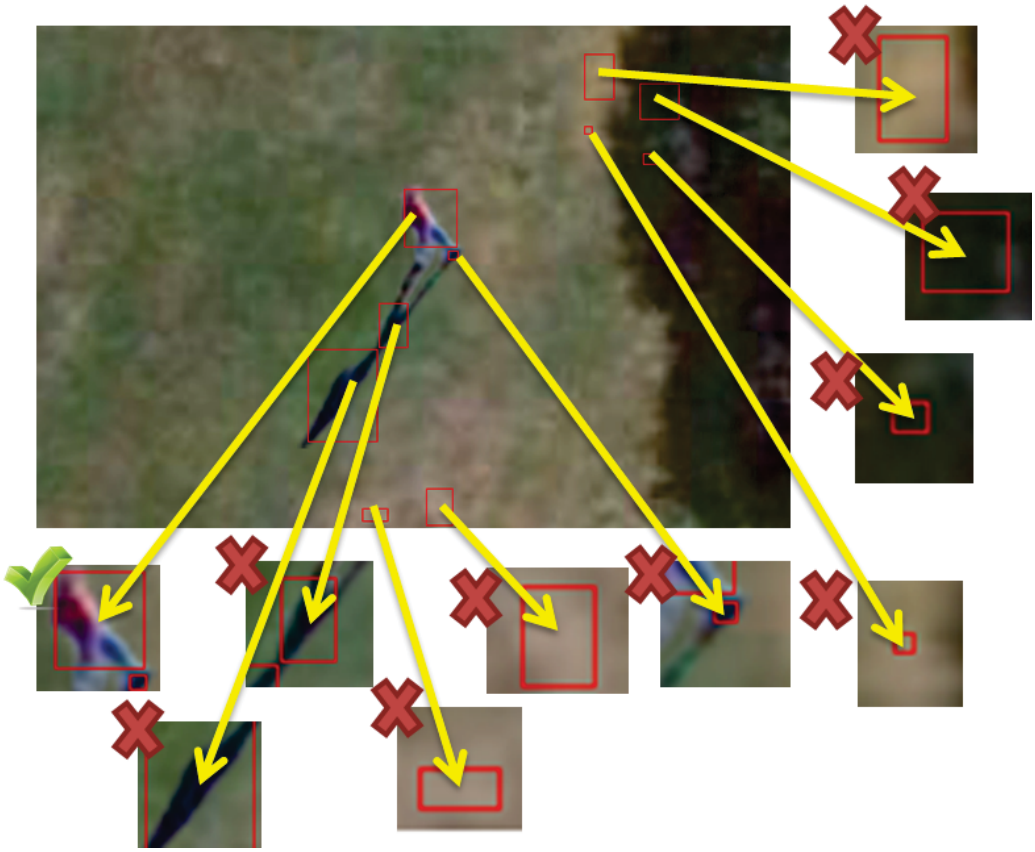

Figure 5.3: The main image is divided into ten smaller images based on objects detected for transmission

5.2.2 Algorithm Effectiveness

The algorithm As you can see from the graph shown in Figure 5.4, over each terrain tested, the algorithm performed best over a flat grassy field and snow. The following pictures in Figure 5.5 shows the successful detection of two people using the image processing

algorithm at each step of the process.

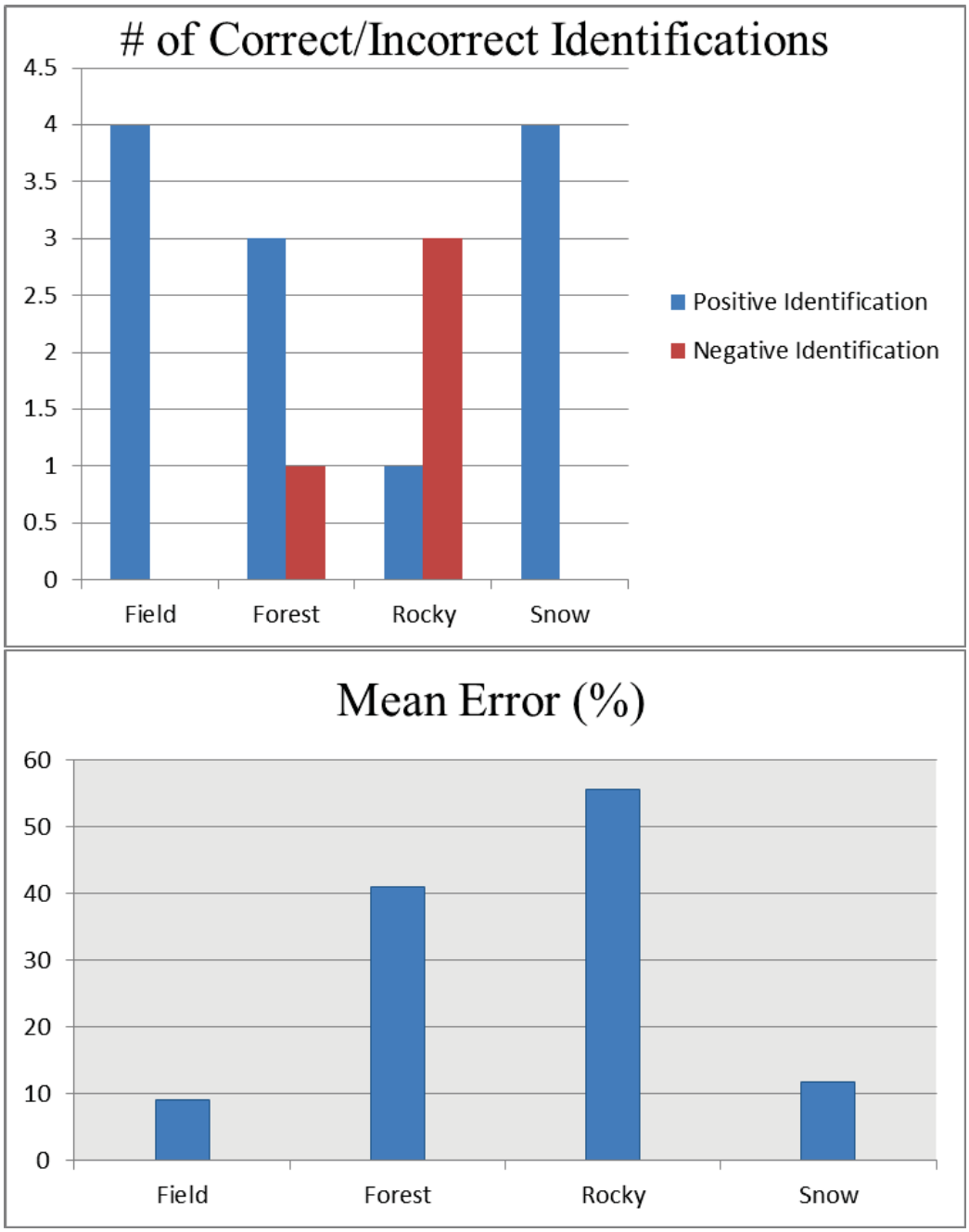

Figure 5.4: Graph showing algorithm effectiveness over different terrains.

In 12 of the 16 test runs, the algorithm was able to positively identify the person as one of the key features in the image. The goal of this algorithm was to filter camera data so

that only "person-like" features would be returned to the user. Because the algorithm was able to do this in the majority of test cases we deem that our implementation was fairly successful. The test results, with bounding boxes highlighted can be found in the Appendix. As can be seen from the data, the algorithm had the most trouble dealing with the "rocky terrain." Logically, this cluttered environment proved to be the least ideal backdrop. When operating under such conditions the base algorithm would benefit from several tweaks such as more filtering and a higher threshold to remove the unwanted noise. Combining data from multiple passes and multiple sensors would also improve performance but were unable to be tested. However, to have much chance of success, the victims would need to head for clearings in the forest to be detected reliably.

These theoretical results show the necessity for adequate camera equipment and justify the decision to purchase a camera with more zoom capabilities. Through further testing on actual aerial footage the "sweet-spot" of zoom could be determined for the algorithm. Armed with this knowledge, accuracy could further be improved as the camera can vary its zoom based on altitude to achieve this.

5.2.3 Hardware Implementation

Unfortunately, the hardware implementation of the image processing algorithm was not fully completed in the span of the project. The FPGA was successfully linked with the video decoder board allowing video input. In addition, a softcore microblaze processor was successfully implemented with custom peripherals to interface with the image processing components and Pandaboard via ethernet and the light weight IP stack. The image processing component itself was not able to be tested due to issues with discussed in Implementation.

5.2.4 Runtime Benchmark

The team was unsuccessful in creating a runtime benchmark due to difficulties with development tools.

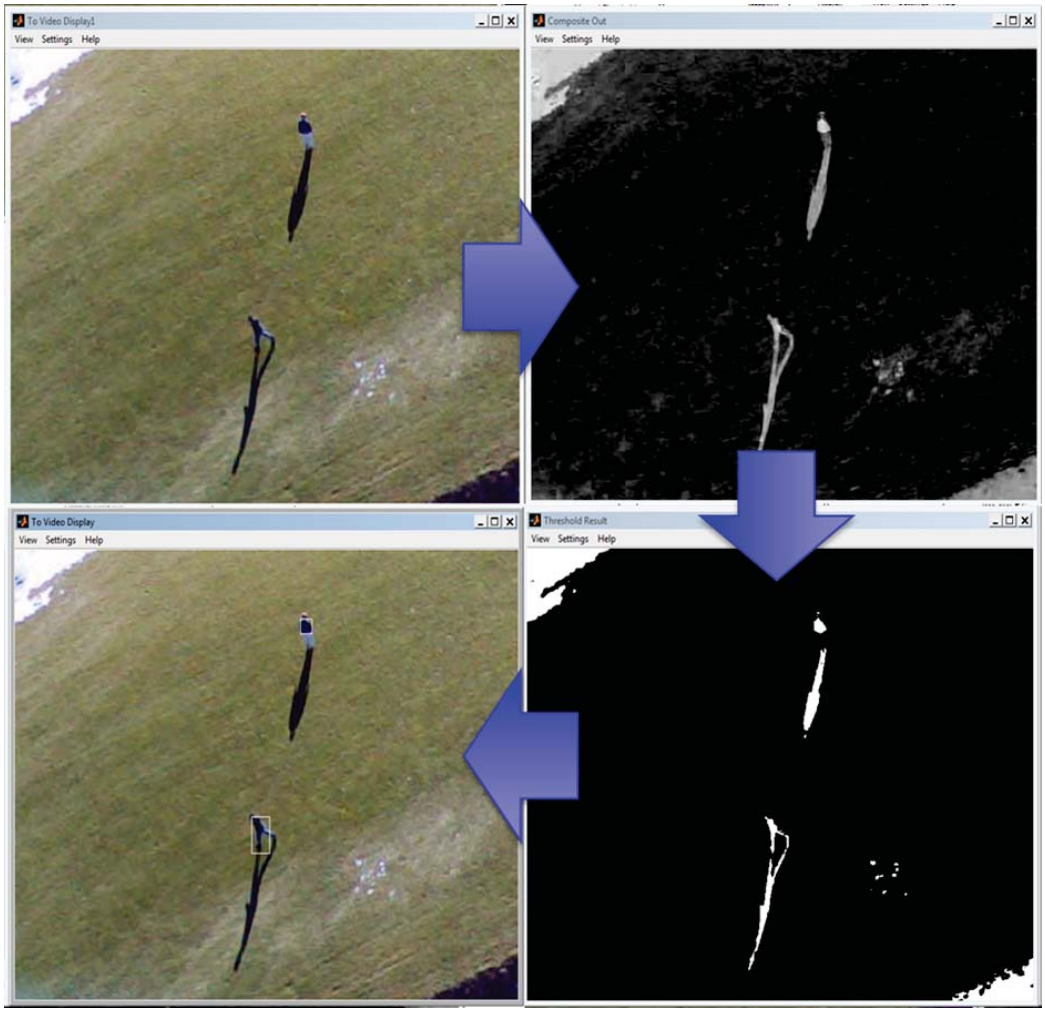

Figure 5.5: Image processing algorithm; from camera in, to heat map generation, binary image filtering, to blob detection.

5.3 Path Planning

In its current state, the Path Planning module consists of a C/C++ shared object library bound with the NodeJS interface. Testing and development on the demonstration interface and prior command line test cases has confirmed the ability to delegate search regions, generate cell maps for the desired search area, and have the path planning agent for an individual drone survey this area.

The binding to NodeJS in the network interface confirms the ability to utilize this frame-

work component from outside software. Secondly, the code has been run on all purchased ARM platforms, as well as AMD and Intel servers, on which it compiles and functions properly. This shows an improvement in contrast with the existing autopilot ground control software, which cannot run on ARM platforms at this time.

Table 5.1: Comparison of path planning resource usage on different platforms during navigation and map generation. For purposes of benchmarking, maps generated had a cell radius of 10m and a grid radius of 50km.

Platform	Processor	% CPU (average)	% CPU (startup)
PandaBoard	Cortex-A9 2x 1GHz	5%	17%
BeagleBoard xM	Cortex-A8 1GHz	7%	26%
BeagleBone	Cortex-A8 750MHz	8%	31%
Workstation	P4 Xeon x2 3.4GHz	4%	7%

In 5.1 a comparison of the CPU utilization of the path planning application, including NodeJS interface, is shown for each ARM platform available and one of the development servers used for this project. For normal operation, this consists of simple surveying of the search grid from randomly selected starting points within 500 meters of origin, so as to introduce conditions in which the default spiral algorithm would fail and other path planning would be utilized without intervention. In all cases, this navigation system will succeed in surveying the entire grid, provided no regions are completely blocked by restricted cells.

Integration efforts with the Hardware team were not entirely possible until quite late in the timeline of this project, due to individual development tasks on part of the software team's module functionality, and the hardware team's testing of the autopilot's functionality on its own. As testing dates for the platforms had to be carefully planned and were often cancelled, many delays in full testing occurred.

Secondly, unforeseen portability issues with portions of the autopilot code itself made full integration of the path planning module not possible in the available time. Namely, despite Paparazzi being open source, large portions of the code modifications found necessary for integration were lacking documentation and a standard structure or interface.Furthermore, despite most of the Paparazzi backend code being in C, the key components that needed porting to the ARM platform for integration were partially written in and linked to both

OCAML and F#, two programming languages that will not run on ARM at this time.

While investigating the documentation on the problem components of the Paparazzi software, a reason for the somewhat fragmented nature of the source code was found. Paparazzi was started by Pascal Brisset, a French researcher and software developer, and most of the ground control code was written by him. Development and documentation efforts were stunted within the community when, in 2010, Pascal died after falling into a crevasse on the north face of the Vigemale Glacier, and his body became trapped within the ice [38],[39].

The development community behind Paparazzi has only recently begun efforts to address these portability issues, so it is possible that this problem does not remain for long. Despite these setbacks, some steps have been taken towards demonstrating integration capability.

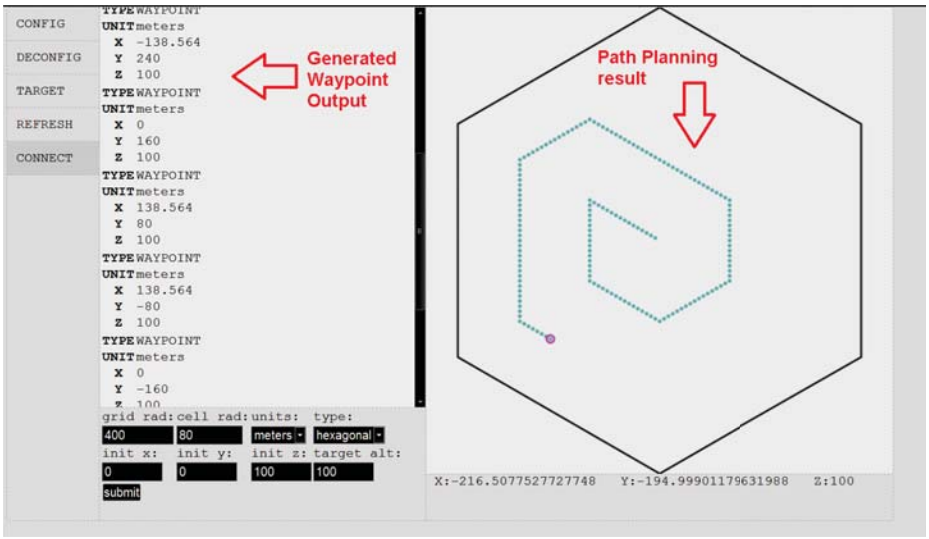

Figure 5.6: The web interface, configured to dump waypoints to the information console for export.

Currently, waypoint outputs from the path planning module can be inserted into the autopilot software, which successfully follows the desired path between search cells. Shown in 5.7 is the Paparazzi autopilot ground control software simulating the hardware team's UAV, successfully following the waypoints generated from the path planning module, shown in 5.6.

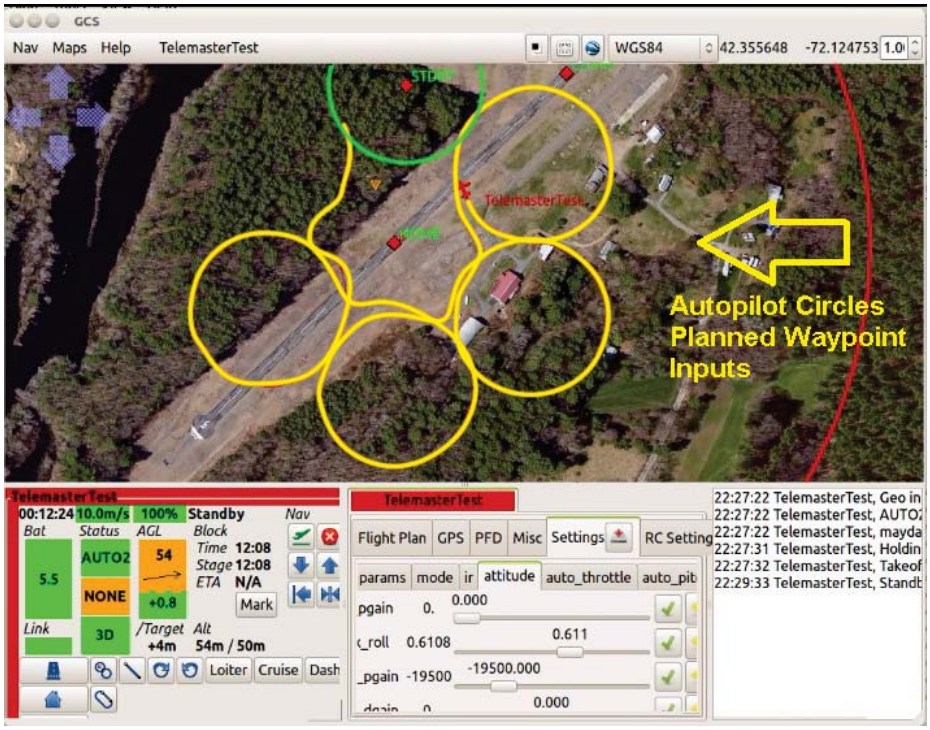

Figure 5.7: The autopilot control software running a hardware-in-the-loop simulation of the waypoint sequence generated from the path planning module.

Please note that, due to the default behavior of the autopilot, waypoints were followed via a circling routine, rather than flying directly through cell centers, as simulated in the path planning interface. This is the default behavior of the Paparazzi autopilot during testing and tuning, and could be changed if necessary once the autopilot is fully operational and has undergone further testing.

5.4 Network Interface Layer

While the communications module itself was not part of this framework, but rather the job of the communications team associated with this project, network communications capability took the assumption that any existing communications layer that the framework would integrate with would either comprise of a serial connection or an ethernet connection that provides an IP address.

In this case, the network capabilities provided by NodeJS allow the framework to easily link with any serial or IP communications layers. Freely available packages exist for serial communications in NodeJS, and methods of utilizing traditional web communications are inherent to the nature of the software.

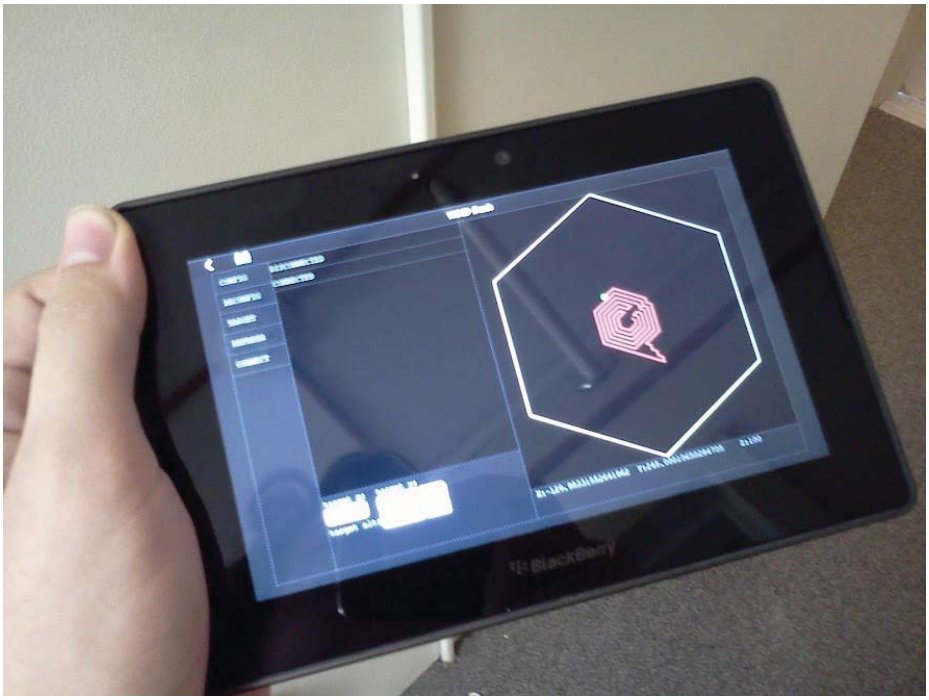

Figure 5.8: The web display allows usage and concurrent data reporting on any mobile or PC platform with a standard web browser.

The web interface, outlined previously, was an initially unplanned result of this project, but proved to be a valuable result of unexpected design needs. In 5.8 the web interface is shown running in the browser of a wifi enabled tablet, still usable without any needed software installation. This interface has been used and configured for testing purposes, and can be used as an example basis for future interface development for this system allows display of messages from the platform, tracking of path planning progress, and remote command entry, all while updating concurrently across any viewing browsers.

5.5 Development Platforms

In order to perform development and testing on the actual hardware, it had to first be setup in a usable development environment. This required installing an configuring a stable Linux distribution with the desired software installations to meet our needs.

For the most part, the only non-standard software we wished to test on this platform was OpenCV. Since image processing is to be implemented on the coprocessor board itself, this is not an absolutely vital functionality, the ability to handle high-level calculations, command processing, and data logging/reporting and path planning are the primary purpose of this board.

5.5.1 Development Environment Setup

The PandaBoard community website has three primarily recommended operating systems for the Pandaboard; Ubuntu, Android, and a minimal validation-only installation, based off of Angstrom.

Initial installation attempts were made with Ubuntu, however performance was slower than expected. Various alternative installations were found, including ARM-optimized builds developed from the Linaro foundation.

Illustrated in Figure 5.9 is an early testing configuration, with a minimal Ubuntu server installation and a light window manager. As can be seen in the diagram, this setup was used for initial package configuration and testing of image capture capabilities. The window manager chosen for this build was OpenBox, shown on both the main display, along with a networked VNC display shown on the laptop monitor. The usage of a networked VNC display confirmed some image capture capabilities, along with providing a relatively smooth image update speed over the network.

Unfortunately, stability issues and graphics incompatibility demanded exploration of alternative distributions. Ubuntu's startup time, even with minimal graphics installed, was unacceptably slow, and attempts to integrate existing proprietary graphics drivers were met with errors, such as system instability and graphics elements not rendering properly.

Alternative Linux installations largely proved to be geared towards Android development

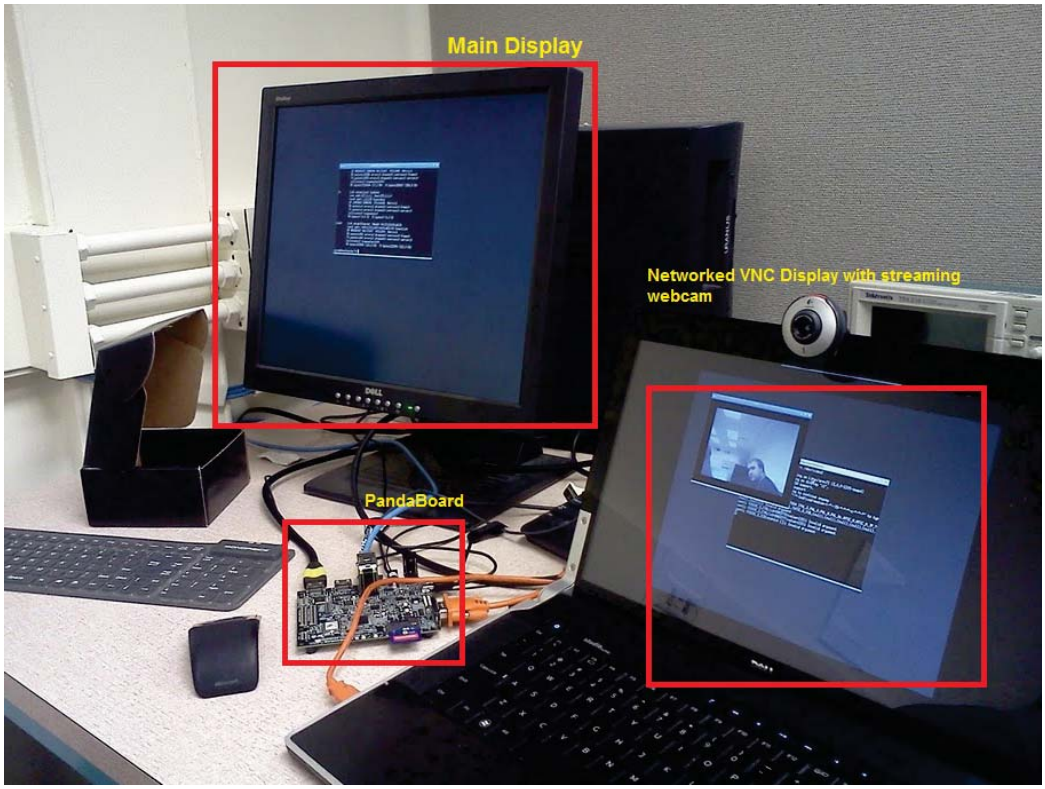

Figure 5.9: Early PandaBoard testing configuration showing image capture capability and networked VNC display.

and utilization of the graphics acceleration for user interface design, rather than. The drivers for these tasks proved to be at a less than usable development state, thus finding a lightweight Linux distribution for other purposes was somewhat difficult.

After further testing, a number of custom Angstrom Linux configurations were installed and tested for basic necessary functionality. While less consistently stable in initial tests, the Angstrom distribution proved significantly faster and less resource intensive than the otherwise recommended Ubuntu builds. Secondly, the online image builder included the option to download a full, custom Linux SDK environment for the chosen system configuration.

To work around the networking issues encountered and allow simplified development and testing, an Ubuntu Virtual Machine was configured to provide a stable, 32-bit cross-compilation environment for the PandaBoard. It was then also configured to provide virtual local network for usage on any development computer's secondary Ethernet port.

The Angstrom SDK was installed on this virtual machine along with other necessary compilation tools. Cross compilation worked for some software components, but results were more consistent and easier to reproduce by compiling natively on the target hardware.

During initial testing efforts on the PandaBoard, attempts were made to utilize the graphics acceleration hardware. Despite the advertised capabilities, usability of this particular feature of the board proved to be poorly supported or documented. The demo programs for this hardware were not able to be successfully compiled, and in the presence of supported drivers for the hardware, some problematic secondary issues arose. Since this was not a primary or vital component of this portion of the hardware, it was decided to not utilize this particular capability.

Later on in development, it was found that a standard element of the ARM Cortex-A series processors could be utilized for acceleration of some image processing or vectorized mathematical tasks. Both the Cortex-A8 and Cortex-A9 contain a Single-Instruction Multiple Data (SIMD) core, called NEON, for performing generalized parallel operations on arrayed datatypes. While not as potentially useful as access to the PandaBoard's graphics core, this particular capability is useful for precisely the types of calculations we would need to do for color filtering or general parallel calculations.

This hardware extension is present in the processors of both the PandaBoard and all BeagleBoard variants, as well as other hardware using the same ARM architecture. This would make our code substantially more portable between platforms, and allow switches to much smaller ARM-based platforms, such as the BeagleBone, with minimal code adaptation.

Initial testing with the NEON core has been done, and both native compilation and cross compilation of NEON-targeted code appears to work. Furthermore, with careful code organization, the GCC compiler can be made to automatically optimize some code to utilize the processor where it otherwise would not. We plan to test implementation of some basic, useful image operations on this, and benchmark them for comparison and future use. As of this point, our code is not utilizing this feature, but it can be applied as appropriate.

With respect to networking issues, it was discovered upon initial tests that the Ethernet controller for the PandaBoard and BeagleBoard lacks a dedicated, unique MAC address. This manifests as a randomly generated MAC address on each activation of the hardware

in some cases, and in all cases results in the generation of an invalid MAC address for usage on the WPI wired network.

This was a major hindrance in our early development process, as most, if not all Linux installations for these platforms required some networking capability to install additional software.

As a temporary fix to this problem, the development VM was configured to act as a passthrough to the second ethernet port on a personal computer. This local network was then bridged through the VM to an actual Internet connection, providing the needed connectivity for packaged updates and other network testing.

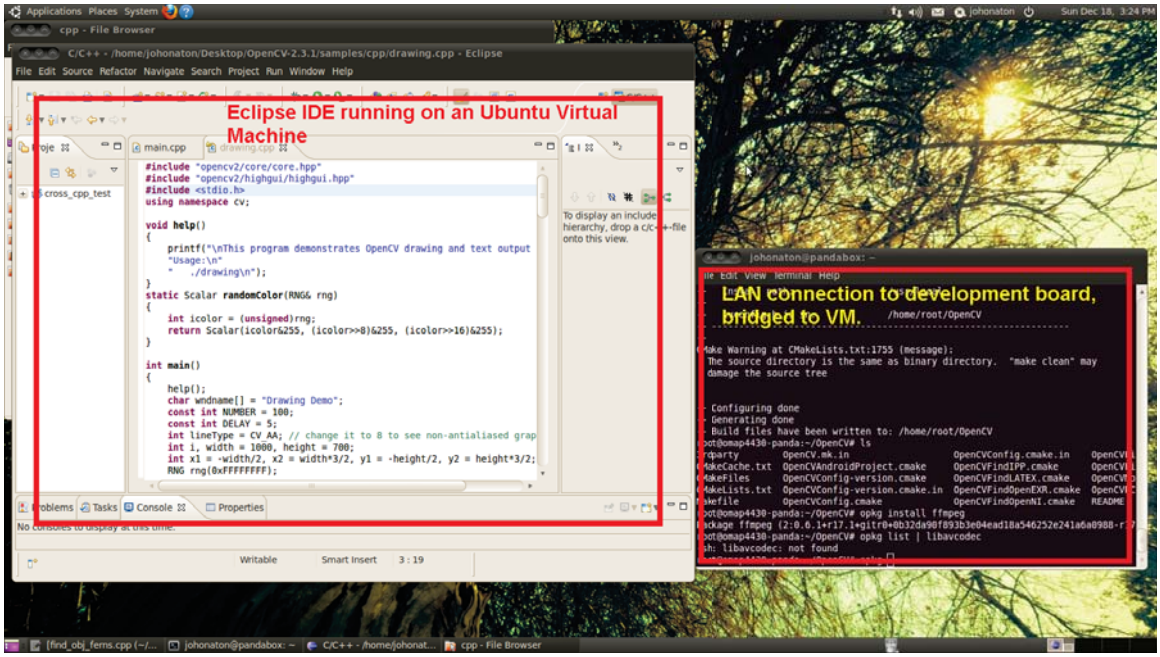

Figure 5.10: VM Development Environment.

This problem was completely resolved, however, with the later addition of our development VM, something which should ease the adoption of any additional platforms. With this development environment, any networking-capable device can now easily be brought up in a local testing network and interfaced with the cross compilation tools we have on the virtual machine.

5.5.2 AI Testing Environment

In order to prototype a user interface for our base station and provide a basis for simulation of our navigation algorithm choices, a testing application and map GUI were constructed within MATLAB to utilize our map and path generation algorithms. The goal of this software was to provide a means of algorithm performance analysis using our gathered SAR statistics and rapid-fire scenario simulations. By calculating probabilistic "time to completion" of our search algorithms, this would both give us a baseline for comparison, and provide a very useful tool for any expansion on our framework.

Due to a bug within MATLAB, however, the GUI portion of this software component was lost before much could be done with it. The entire back-end survived this, however, allowing us to use the grid-generation algorithms developed in MATLAB in the actual software library.

5.6 Chapter Summary

The goal of this project was the creation of a framework for search and rescue operations with unmanned aerial vehicles. In the end, a cross-platform framework with interchangeable modules was successfully created. Demonstration modules for image processing and path-planning were developed. As part of this process an image processing algorithm for detecting people in aerial footage was designed and tested with simulation data. Difficulties with implementation prevented a fully functional hardware design. A path-planning algorithm was created and implemented on an embedded ARM platform which was then tested with a web-based GUI made for the project.

Chapter 6

Conclusion

Designing a framework to support search and rescue UAVs was a unique undertaking that required an immense knowledge of the modular components the team aimed to accommodate as well as a broad understanding of the entire system for integration. An expansive research base, delicate planning, and novel thinking contributed to achieve flexibility and generality of the framework while maintaining SAR specific features.

In the first chapter of this report, a need is presented to reduce the cost of search and rescue operations. To reduce the cost of SAR, the proposed approach was to use multiple, coordinated, autonomous, unmanned aerial vehicles. An implementation, further described, would reduce the number of people required to perform a search per unit area and thus the total cost of SAR operations over time. This greater goal of Project WiND was then divided into three general components, designed and implemented by three WPI teams: the UAV platform, the wireless communications, and the software framework.

As the team working on the software framework, development efforts were two part. The team developed a framework to accommodate modular image processing, path planning, navigation, and communication programs. This involved understanding the needs of SAR operators, platform developers, and the communications team, however it also required planning for all scenarios. This pushed the framework to accommodate a design in which all sensor processing occurred on the UAV and away from any base-station or mother-ship. In addition to the framework, the team also developed a set of modules which use this

framework. These demo modules serve to demonstrate functionality and to guide future developers who will program for and expand on this work.

6.1 Future Work

Originally, this team hoped to leave future work on this project limited to module development, but due to many factors, portions of the framework, such as the hardware image processing, have not been fully tested and remain un-integrated. This is unfortunate, but provides motivation for a future team to focus more on these portions of the existing framework for better usability and create more framework-supplied tools for developers to use. To outline the tasks for future improvement:

- While the team did develop demo modules for image processing and navigation, initial focus was on the framework before integrating into a deployment-ready SAR system. The image processing modules could be significantly improved using more advanced algorithms such as motion-detection, shadow removal, and shape recognition. More of this system can be implemented on the FPGA-DSP, further freeing the software processor for communications and navigation.

- The navigation modules could be improved with more AI designed specifically for multi-agent optimizations and platform specific features. Right now, individual robot navigation is functional, and communications capabilities allow for multi-robot coordination to be implemented and tested when individual platforms are more capable. Additions to this module could include utilizing information such as fuel consumption, effects of weather, and terrain data to improve resource utilization.

- Something this team did not attempt was a more advanced user interface for robot control and information feedback. The existing interface was limited to communicating data on the flight path of a single UAV as part of the testing procedure. It did not have the ability to display information regarding multiple UAVs in coordination or image processing data. A team at the University of New Hampshire is supposedly working on this problem using a Microsoft Surface. However, the current state of

that project is unknown, and advancements in the existing web interface would make this a more valuable framework overall, as well as ease integration if and when the Microsoft Surface is used.

In conclusion, this project demonstrated the overall concept of a specialized framework for search and rescue. The team successfully integrated purpose built modules into this framework and showed general functionality. They then installed this framework onto an ARM platform and integrated that with the hardware platform. However, full integration and testing is unfinished given development status of both the hardware and communications platforms. The modules themselves are limited, and the hardware implementation of image processing was not integrated due to licensing difficulties. The team accommodated for a communications system successfully and implemented a custom interface as an enhancement on the original design, but full testing on the production platforms awaits completion. With dedication, future teams can hopefully improve and finalize this framework and release it as a field-ready development platform.

Appendix A

Glossary

AI	Artificial Intelligence
ARM	Advanced RISC Machines
ATX	Advanced Technology extended
BYU	Brigham Young University
C++	C Plus Plus (Programming Language)
CPU	Central Processing Unit
DSP	Digital Signal Processor
FLIR	Forward Looking Infrared
FOV	Field of View
FPGA	Field Programmable Gate Array
GCC	GNU Compiler Collection
GNU	GNU's Not Unix
GPS	Global Positioning System
GPU	Graphics Processing Unit
HD	High Definition
HDL	Hardware Description Language
HTML	Hypertext Markup Language
IEEE	Institute of Electrical and Electronics Engineer
IP	Image Processing
IP	Internet Protocol
ITU	International Telecommunication Union
ITX	ITX (Variant of ATX)
LAN	Local Area network
MAC	Media Access Control address

MILP	Mixed-Integer Linear Programming
MIT	Massachusetts Institute of Technology
OpenCV	Open Source Computer Vision
POA	Probability of Area
POD	Probability of Detection
POMDP	Partially Observable Markov Decision Process
POS	Probability of Success
RH-MILP	Receding Horizon Mixed-Integer Linear Programming
RHTA	Receding Horizon Task Assignment
SAR	Search and Rescue
SIMD	Single-Instruction Multiple Data
UAV	Unmanned Areal Vehicle
UNH	University of New Hampshire
USB	Universal Serial Bus
VHDL	VHSIC hardware description language
VM	Virtual Machine
VNC	Virtual Network Computing
WiSAR	Wilderness Search and Rescue
WPI	Worcester Polytechnic Institute

Appendix B

Hardware Specifications

SONY BLOCK CAMERA SPECIFICATIONS [8]

HIGHLIGHTS:

18x optical zoom / 4x digital zoom

High speed serial communication (max. 38.4 kbps)

Character generator/Privacy Zones

New Spot AE function

Minimum illumination of 1.0 lux

Programmable custom preset function

SPECIFICATIONS:

Image Sensor: 1/4 type Super HAD CCD

Number of Effective Pixels: Approx. 380,000 pixels (NTSC), 440,000 (PAL)

Lens: 18x Zoom f=4.1 (wide) to 73.8 mm (tele) F1.4 to F3.0

Digital Zoom: 4 x (72x with optical zoom)

Angle of View (H): Approx. 48 degree (Wide end), Approx. 2.7 degree (Tele end)

Min. Object Distance: 10 mm (Wide end), 800 mm (Tele end)

Sync. System: Internal

Minimum Illumination: Less than 1.0 lux typical (50 IRE)

S/N Ratio: More than 50 dB

Electronic Shutter: 1/60 sec. to 1/10,000 sec.

16 steps

Focusing System: Auto (Sensitivity: H, L), One-Push AF, Manual, Infinity

Interval AF, Zoom Trigger AF

White Balance: Auto, ATW, Indoor, Outdoor, One Push WB, Manual WB

Display: Title, Clock

Gain: Auto/Manual (-3 to 28 dB, 2 dB steps)

Aperture Control: 16 steps

Back Light Compensation: ON/OFF

Switch: Zoom tele, Zoom wide

Preset: 6 positions (saved in EEPROM)

Camera Control Interface: VISCA Protocol_TTL/RS-232C signal level_

Baud rate = 9.6 Kbps, 19.2 Kbps, 38.4 Kbps, 1 or 2 Stop bit selectable

Video Output: VBS: 1.0 Vp-p (sync negative)/ Y/C Out

Storage Temperature: -20C to +60C

Operating Temperature: 0C to 50C

Power Consumption: 1.5 W (inactive motors), 2.0 W (active motors) / DC 6 to 12 V

Dimensions (W x H x D): 48.2 x 56.6 x 92.3 mm (1-15/16 x 2-1/4 x 3-3/4 inches)

Mass: Approx. 170 g (6 oz)

Table B.1: AI Hardware Choice Specification Comparison

Item	Pandaboard	Beagleboard-XM	Beaglebone	Raspberry Pi	Mini-ITX i7	Mini-ITX Atom	Pico-ITX Atom
Cost($)	174	149	89	30	¿400.00	74.99	469
Processing	1.2 GHz Dual-Core ARM Cortex A9	1 GHz ARM Cortex A8	700 MHz ARM Cortex A8	700 MHz ARM	2 - 3.5 GHz Intel i7	1.8 GHz Intel Atom	1.6 GHz Intel Atom
Power(mW)	250	250	250	3500	¿100000	52000	30000
I/O	RS232, SD, Mini-USB, DVI, HDMI, Ethernet, Audio, 2x USB	RS232, SD, Mini-USB, DVI, Ethernet, Audio, 4x USB	RS232, Ethernet, 1xUSB, GPIO	RS232, 2xUSB, Ethernet, RCA, GPIO	6xUSB, DVI, Audio, Ethernet, VGA, PS2	4xUSB, Audio, Ethernet, VGA,PS2	4xUSB, Audio, Ethernet, VGA, PS2
Size(in)	4.5x4	3.25x3.25	3.4x2.1	3.3x2.1	6.7x6.7	6.7x6.7	3.9x2.8
Other	Graphics Acceleration Core	NEON Acceleration, Camera port	-		-	-	
Linux?	yes	yes	yes	yes	yes	yes	yes
Source	[40]	[41]	[41]	[42]	[43]	[44]	[45]

Table B.2: Image Processing Hardware Choice Specification Comparison

Item	Atlys	LX9 Microboard	BF506F EZ-KIT	C5535 eZdsp	Pandaboard	Beagleboard-XM
Cost ($)	199	89	199	99	174	149
Processing	N/A (Spartan-6 FPGA)	N/A (Spartan-6 FPGA)	400 MHz DSP	100 MHz DSP	1.2 GHz Dual-Core ARM Cortex A9	1 GHz ARM Cortex A8
Power(mW)	25000	250	250	250	250	250
I/O	Audio, HDMI, Ethernet, USB, GPIO	Ethernet, USB, GPIO	RS232, Audio, GPIO	GPIO, Audio	RS232, SD ,Mini-USB, DVI, HDMI, Ethernet, Audio, 2x USB	RS232, SD, Mini-USB, DVI, Ethernet, Audio, 4x USB
Size(in)	5x5	5x1.5	6x6	3.9x2.8	4.5x4	3.25x3.25
Other	-	-	-	-	Graphics Acceleration Core	NEON Acceleration, Camera port
Linux?	yes	yes	yes	yes	yes	yes
Source	[46]	[47]	[48]	[49]	[40]	[41]

Appendix C

AI Path Planning Code

```
#ifndef __AGENT_H
#define __AGENT_H
/**
 * File:  Agent.hpp
 * Author:  Jonathan Estabrook
 * Description:
 *
 *  Main access class for interfacing with navigation, control, and data
 *  acquisition functions. Effectively this is where you tell the robot
 *  what to do. Most high-level organizational changes in the library
 *  should happen here.
 *
 *  NOTE ON COORDINATES:
 *  For purposes of differentiation "Global" refers to scaled cartesian
     coordinates *relative*
 *  to the search grid origin, in the appropriate units, not true "Global"
     in a Lat/Lon sense.
 *  "Local" refers to integer-unit coordinates for usage within the
 *  search grid. One local unit is scaled by the cell scaling factor for
     global units.
 *
 *  Conversions between Lat/Lon and Global are assumed to happen elsewhere
     before input.
 * */
```

```
#include "Grid.hpp"
#include "WiND_utils.hpp"
#include <list>
#include <string>

namespace WiND{
  class Agent{
  private:
    Grid* world;    //the navigation grid this agent is in
    Cell* cell;   //pointer to the current cell struct

    Waypoint pos;   //the current Waypoint, relative to 0,0,0
    float target_z;   //the target altitude, waypoints will return this z-
        value

    // a two-argument callback function pointer, should it be needed

    void (*callback)(const char*,const char*);

    // list of planned waypoints
    std::list<Cell*> path;
  public:
    /**
    * Constructor, set the desired minimum grid radius, cell size, and units
    **/
    Agent(float _grid_rad, float _cell_rad, std::string _units, std::string
         _grid_type);

    /**
    * Deconstructor
    **/
    ~Agent(){
      delete world;
    }

    /**
    * Returns a pointer to the current grid
```

```
56      **/
        Grid* getWorld();

        /**
        * Returns a pointer to current cell, if valid
61      **/
        Cell* getCurrentCell();

        /**
        * Returns the current position in global (cartesian) coordinates
66      **/
        Waypoint getPosition();

        /**
        * Sets the position by global cartesian coordinates,
71      * relative to origin in applicable units
        **/
        bool setPosition(float _x, float _y, float _z);

        /**
76      *  Plans a path to a position within the search grid,
        *  specified in
        **/
        bool setTargetPoint(float _x, float _y);

81      /**
        *  Set the target agent altitude (independent of x,y)
        **/
        bool setTargetAltitude(float _z);

86      /**
        * Set the event callback function, if applicable
        **/
        bool setCallback(void (*func)(const char*,const char*));

91      /**
        * Get the next waypoint using internal decision process
```

```
        **/
        Waypoint getNextWaypoint();
      };
96  }

    #endif /* __AGENT_H */

    /**
 2   * File:  Agent.cpp
     * Author:  Jonathan Estabrook
     * Description:
     *
     *  Main access class for interfacing with navigation, control, and data
 7   *  acquisition functions. Effectively this is where you tell the robot
     *  what to do. Most high-level organizational changes in the library
     *  should happen here.
     *
     *  NOTE ON COORDINATES:
12   *  For purposes of differentiation "Global" refers to scaled cartesian
         coordinates *relative*
     *  to the search grid origin, in the appropriate units, not true "Global"
         in a Lat/Lon sense.
     *  "Local" refers to integer-unit coordinates for usage within the
     *  search grid. One local unit is scaled by the cell scaling factor for
         global units.
     *
17   *  Conversions between Lat/Lon and Global are assumed to happen elsewhere
         before input.
     * */
    #include "Agent.hpp"

    #include "HexGrid.hpp" //we're using this locally, Agent.h doesn't need it
22

    #include "WiND_search.hpp"

    #include <list>
    #include <set>
```

```
27 #include <algorithm>
   #include <iostream> //TODO
   #include <exception>
   namespace WiND
   {
32   Agent::Agent(float _grid_rad, float _cell_rad, std::string  _units, std::
        string _grid_type){
       if(_grid_type == "hexagon")
       {
         this->world = new HexGrid();
       } else {
37       throw;
       }
       this->world->init(_grid_rad,_cell_rad,_units);
       this->cell = NULL; //indicates uninitialized position
       this->callback = NULL; //uninitialized callback
42   }

     /**
      * Returns pointer to Grid
      */
47   Grid* Agent::getWorld(){
       return this->world;
     }


52   Cell* Agent::getCurrentCell(){
       return this->cell;
     }

     Waypoint Agent::getPosition(){
57     return this->pos;
     }

     /**
      * Set position in global cartesian units, relative to 0,0,0
62    * if the position isn't in-world, return false
```

```
 */
bool Agent::setPosition(float x, float y, float z){
  //update current waypoint
  this->pos.x = x; this->pos.y = y; this->pos.z = z;
  if(callback)callback("UPDATE","position updated");

  Vector2D gCoords = {x,y};
  //find current cell coordinates
  std::pair<int,int> lCoords = this->world->global_2_local(gCoords);
  //get current cell
  this->cell = this->world->getCell(lCoords.first,lCoords.second);
  //if it is a valid cell, set the visited flag
  if(this->cell){ this->cell->visited = true; return true;}
  else return false;
}

bool Agent::setTargetPoint(float _x, float _y){
  //first check if this is a valid point
  Vector2D v = {_x,_y};
  std::pair<int,int> lCoords = this->world->global_2_local(v);
  Cell* c = this->world->getCell(lCoords.first,lCoords.second);
  if(!c) return false;
  else if(c == this->cell) return true;
  else
  {
    this->path = planPath(this->cell,c,this->world);
  }
}

bool Agent::setTargetAltitude(float _z)
{
  this->target_z = _z;
  return true;
}

bool Agent::setCallback(void (*func)(const char*, const char*))
{
```

```
    this->callback = func;
    return (func != NULL);
}

/*************************************************************
* Interface method for single-cell search algorithms
**/
Waypoint Agent::getNextWaypoint(){
// declare pointer to next cell
  Cell* next = NULL;

//first check for pre-planned cells
  if(!(this->path.empty()))
  {
    next = path.front();
    path.pop_front();
    if(callback)callback("STATUS","popping path waypoint!");
  }

// algorithms are chained by priority
// these pick the next cell, in two dimensions, altitude is separate
// attempt using center-spiral method
  next = next?next:getNextSpiral(this->cell, this->world);

// if this fails, attempt using A*, starting a planned path
// to the next unvisited cell
  if(!next)
  {
    Cell* target = getNextUnvisited(this->cell, this->world);
    this->path = target?planPath(this->cell,target,this->world):path;
    if(!(this->path.empty())){
      next = path.front();
      path.pop_front();
    }
  }

// Final sanity check, in the case that we are in a blocked region
```

```
137   // this will return the nearest allowed cell
        next = next?next:getNearestAllowed(this->cell,this->world);


      //* FALLBACK BEHAVIOR, KEEP AT END
142   // the last method called occurs if next waypoint is still null
      // if all algorithms fail, hold position at current cell
        next = next?next:this->cell; //hold position

        int x,y;
147     x = next->x; y = next->y;

        Vector2D gc = this->world->local_2_global(std::make_pair(x,y));

        Waypoint w;
152     w.x = gc.x; w.y = gc.y;
        //altitude is controlled independently
        w.z = this->target_z;  //set from current target altitude
        return w; //return waypoint
      }
157 }
```

```
    #ifndef __GRID_H
    #define __GRID_H
  3
    /**
     * File:  Grid.hpp
     * Author:  Jonathan Estabrook
     * Description:
  8  *
     *  Abstract Superclass for search grids
     *  For now, HexGrid is the only subclass for using a hexagonal grid.
     *  As-is, implementing a square grid with appropriate function changes
         should work seamlessly.
     *  Should other grid types be desired, inherit from this class.
 13  *
     *  EFFICIENCY IMPROVEMENTS TODO:
```

```
 * Right now, cells are created on initialization, at a fixed grid size. This uses a bit of
 * CPU on initialization. This could be improved by having them created on-demand.
 *
 * OTHER TODO:
 * Add some simpler region blocking methods. Right now, this is done by disallowing cells directly.
 * The geometry functions library would be a good thing to use for this.
 * */


#include <map>
#include <list>
#include <utility>
#include <string>
#include <iostream> //TODO: debug

#include "WiND_utils.hpp"

//map-type macro to make things quicker
//integer pairs are used as a map key
#define MAP_TYPE std::map<std::pair<int,int>,Cell>

namespace WiND{
  /**
  * Simple "cell" data struct
  **/
  struct Cell{
    //local grid coordinates (signed integer pair key)
    int x;
    int y;

    float probability;
    bool allowed;
    bool visited;
```

```
48      Cell(int _x,int _y):x(_x),y(_y),visited(false),allowed(true),probability
            (0.5){}
        Cell(){}
        Cell& operator=(Cell& rhs)
        {
          this->probability = rhs.probability;
53        this->allowed = rhs.allowed;
          this->visited = rhs.visited;
          this->x = rhs.x;
          this->y = rhs.y;
          return *this;
58      }
      };


      class Grid{
63    protected:
      MAP_TYPE cellmap;     //map of coordinates to cell structs
      int layers;     //cell layers from center
      float scale;      //scaling factor between local and global units
      std::string units;    //unit label for global coordinates, fairly
          arbitrary
68    std::list<Vector2D> bounds; //list of boundary corners in global
          coordinates

      /**
      *  Generates a grid the given number of cell layers from origin
      */
73    virtual void generate(int _layers)=0;
      public:
      Grid(){}
      /**
      *  Main constructor, should be the one used, initializes the grid
78    */
      virtual void init(float _grid_rad, float _cell_rad, std::string _units) =
          0;
```

```
/**
*  Retrieves a cell pointer by local coordinates
*  shouldn't need to be overloaded, as the map is independent of grid
    shape
*/
Cell* getCell(int _x, int _y){
  MAP_TYPE::iterator it;
  //first check if the cell is in the grid
  //bool in_grid = cell_in_grid(std::make_pair(_x,_y));
  /*if(!in_grid){
    std::cout << "cell not in grid" << std::endl;
    return NULL;
  }
  //then search for cell in map*/
  it = this->cellmap.find(std::make_pair(_x,_y));
  //if it's in the grid, but not the map, make the cell
  /*if(it==cellmap.end())
  {
    Cell c(_x,_y);
    cellmap[std::make_pair(_x,_y)] = c;
    it = this->cellmap.find(std::make_pair(_x,_y));
  }*/
  return (it!=cellmap.end())?(&it->second):NULL;
}

/**
*  Retrieves a list of pointers to neighboring cells
*/
virtual std::list<Cell*> getNeighbors(Cell* c) = 0;

/**
*  Gets the number of cell layers out from origin
*  i.e. the maximum local coordinate magnitude
*/
int getSize(){return layers;}

/**
```

```
     * Returns the boundary corners of the grid
     */
    std::list<Vector2D> getBounds(){return bounds;}

    /**
    * Returns the unit string
    */
    std::string getUnits(){return units;}

    /**
    * converts local coordinates to global cartesian
    * Global coordinates are represented as a custom Vector2D class
    * Local coordinates are a simple integer pair, for easy map lookup
    */
    virtual Vector2D local_2_global(std::pair<int,int> _lCoords) = 0;

    /**
    * converts global coordinates to local
    */
    virtual std::pair<int,int> global_2_local(Vector2D _gCoords) = 0;

    /**
    * Returns the local cell distance between cells
    */
    virtual int local_distance(Cell* a, Cell* b) = 0;

    /**
     * Returns the global cartesian distance between cell centers
     */
    float global_distance(Cell* a, Cell* b)
    {
      int xa,ya,xb,yb;
      xa = a->x; ya = a->y; xb = b->x; yb = b->y;

      Vector2D ca,cb;
      ca = this->local_2_global(std::make_pair(xa,ya));
      cb = this->local_2_global(std::make_pair(xb,yb));
```

```
    return vectorDistance(ca,cb);
  }

  /**
158  * Based on bounds list, determines if the point is in a cell in the grid
       .
   */
  bool point_in_grid(Vector2D _pt)
  {
    //determine nearest center point
163  Vector2D nearest_center = this->local_2_global(this->global_2_local(_pt)
       );
    //if it is in-bounds and its cell is in-bounds, then return true
    return (point_in_polygon(_pt,this->bounds) && point_in_polygon(
       nearest_center,this->bounds));
  }

168 /**
   * Determines if a cell-center is in the grid bounds
   */
  bool cell_in_grid(std::pair<int,int> _cell)
  {
173  Vector2D gCoords = this->local_2_global(_cell);
    return point_in_polygon(gCoords,this->bounds);

  }
  };
178

}

#endif /* __GRID_H */

#ifndef __HEXGRID_H
#define __HEXGRID_H
 3 /**
   * File:  HexGrid.hpp
```

```
 * Author:  Jonathan Estabrook
 * Description:
 *
 *  Hexagonal Search Grid, inherits from the Grid superclass.
 *  NOTE: see Grid.hpp!
 * */
#include "Grid.hpp" //parent class header

//trig constants for coordinate conversions
#define COS_30 0.866025404
#define SIN_30 0.5

namespace WiND{
  class HexGrid : public Grid {
  private:
  virtual void generate(int _layers);
  public:
  /**
  *  Default constructor
  */
  HexGrid():Grid(){}

  virtual void init(float _grid_rad, float _cell_rad, std::string _units);
  /**
  *  Retrieves a list of pointers to neighboring cells
  */
  virtual std::list<Cell*> getNeighbors(Cell* c);
  /**
  * converts local coordinates to global cartesian
  * Global coordinates are represented as a custom Vector2D class
  * Local coordinates are a simple integer pair, for easy map lookup
  */
  virtual Vector2D local_2_global(std::pair<int,int> _lCoords);
  /**
  * converts global coordinates to local
  */
  virtual std::pair<int,int> global_2_local(Vector2D _gCoords);
```

```
    /**
43  * Returns the local cell distance between cells
    */
    virtual int local_distance(Cell* a, Cell* b);
    };
  }
48

  #endif /* __HEXGRID_H */
```

```
 1 /**
   * File:  HexGrid.hpp
   * Author:  Jonathan Estabrook
   * Description:
   *
 6 *  Hexagonal Search Grid, inherits from the Grid superclass.
   *  NOTE: see Grid.hpp!
   * */

  #include "HexGrid.hpp"
11 #include <cstdlib>
  #include <cmath>
  //#include <iostream> //debug

  namespace WiND{
16

    void HexGrid::generate(int _layers){
      int i;
      for (i=-_layers;i<=_layers;i++)
      {
21      int l,r,j;
        l = (i<=0)?(-_layers):(-_layers + i);
        r = (i>=0)?( _layers):( _layers + i);
        for(j=l;j<=r;j++)
        {
26        Cell c(i,j);
          cellmap[std::make_pair(i,j)] = c;
        }
```

```
    }
  }

/**
 * grid generation function based on minor grid radius and minor cell
     radius
 */
void HexGrid::init(float _grid_rad, float _cell_rad, std::string _units)
{
  //NOTE: changed to floor to ensure whole-cell layer bounds
  this->layers = std::floor((_grid_rad/COS_30)/((_cell_rad)*2)); //
      calculate cell layers
  this->scale = (_cell_rad)*2; //scaling factor should be twice the minor
      cell radius
  this->units = _units;

  //fill the boundary list
  float R = _grid_rad/COS_30;

//    std::cout << this->layers << " layers, " << this->scale << " scale, "
    << R << " grid_rad" << std::endl;

  Vector2D pt;
  pt.x = 0; pt.y = R;
  this->bounds.push_back(pt);
  pt.x = R*COS_30; pt.y = R*SIN_30;
  this->bounds.push_back(pt);
  pt.y = -pt.y;
  this->bounds.push_back(pt);
  pt.x = 0; pt.y = -R;
  this->bounds.push_back(pt);
  pt.x = -R*COS_30; pt.y = -R*SIN_30;
  this->bounds.push_back(pt);
  pt.y = -pt.y;
  this->bounds.push_back(pt);
```

```
61      //removing this for now, cells should be created on-demand from boundary
            points
        this->generate(layers);
    }

    // virtual
66  std::list<Cell*> HexGrid::getNeighbors(Cell* c)
    {
        std::list<Cell*> cells;
        //calculate neighbor coordinates
        //first the upper neighbor, go clockwise from here
71      int x,y; x = c->x; y = c->y;
        Cell* neighbor;
        // N  (0,+)
        neighbor = getCell(x  ,y+1);
        if(neighbor) cells.push_back(neighbor);
76      // NE (+,+)
        neighbor = getCell(x+1,y+1);
        if(neighbor) cells.push_back(neighbor);
        // SE (+,0)
        neighbor = getCell(x+1,y  );
81      if(neighbor) cells.push_back(neighbor);
        // S  (0,-)
        neighbor = getCell(x  ,y-1);
        if(neighbor) cells.push_back(neighbor);
        // SW (-,-)
86      neighbor = getCell(x-1,y-1);
        if(neighbor) cells.push_back(neighbor);
        // NW (-,0)
        neighbor = getCell(x-1,y  );
        if(neighbor) cells.push_back(neighbor);
91
        return cells;
    }

    /**
96  *  converts local coordinates to global cartesian
```

```
*  Global coordinates are represented as a custom Vector2D class
*  Local coordinates are a simple integer pair, for easy map lookup
*/
Vector2D HexGrid::local_2_global(std::pair<int,int> _lCoords)
{
  int lx = _lCoords.first;
  int ly = _lCoords.second;
  Vector2D gCoords;
  gCoords.x = ((float)lx*COS_30)*this->scale;
  gCoords.y = ((float)ly - (float)lx*SIN_30)*this->scale;
  return gCoords;
}
/**
*  converts global coordinates to local
*/
std::pair<int,int> HexGrid::global_2_local(Vector2D _gCoords)
{
  float gx = _gCoords.x;
  float gy = _gCoords.y;
  int lx = floor(gx/(COS_30*this->scale) + 0.5);
  int ly = floor(gy/scale+lx*SIN_30 + 0.5);
  return std::make_pair(lx,ly);
}

/**
 * Returns the local cell distance between cells
*/
int HexGrid::local_distance(Cell* a, Cell* b)
{
  int x1,y1,x2,y2;
  x1 = a->x; y1 = a->y; x2 = b->x; y2 = b->y;

    int A = std::abs(x2 - x1);
  int B = std::abs(y2 - y1);
  int C = std::abs(a - b);
  return (C>(A>B?A:B))?C:(A>B?A:B); //max of 3 for hexagonal coordinates
}
```

```
}

#ifndef __SEARCHALGS_H
#define __SEARCHALGS_H
/**
 * File:  WiND_search.hpp
 * Author:  Jonathan Estabrook
 * Description:
 *
 *  Function Library for search methods.
 * */

#include "Grid.hpp"
#include "WiND_utils.hpp"

#include <set>
#include <list>

namespace WiND
{
  /**
   * computes next cell for a spiral about origin (0,0)
   **/
  Cell* getNextSpiral(Cell* _current, Grid* _grid);

  std::list<Cell*> planPath(Cell* _current, Cell* _target, Grid* _grid);

  /**
   * Returns the nearest unvisited cell,
   * breaks ties by returning the one with the highest probability.
   **/
  Cell* getNextUnvisited(Cell* _current, Grid* _grid);

  /**
   * Returns the nearest allowed cell, regardless of being visited or
      probability
   **/
```

```
    Cell* getNearestAllowed(Cell* _current, Grid* _grid);
36
    /**
     * Determines if a cell is in a specified triangle
     **/
    bool isCellInTriangle(Vector2D a, Vector2D b, Vector2D c, Cell* _cell,
        Grid* _grid);
41
    /**
     *  Returns a list of cells in a specified triangle
     **/
    std::set<Cell*> getCellsInTriangle( Vector2D a, Vector2D b, Vector2D c,
        Grid* _grid);
46 }
#endif /* SEARCHALGS_H */

/**
 * File:  WiND_search.cpp
 3 * Author:  Jonathan Estabrook
 * Description:
 *
 *  Function Library for search methods.
 * */
 8 #include "WiND_search.hpp"
#include "WiND_utils.hpp"

#include <algorithm>
#include <list>
13 #include <set>
#include <map>

namespace WiND {

18   /**
     *  Data struct for path planning, currently specialized for A* search
     */
    struct SearchNode{
```

```
  Cell* cell;
  SearchNode* parent;
  unsigned int G; //cost to this cell
  unsigned int H; //estimated cost(straight line)

  SearchNode(Cell* _c, SearchNode* _p, unsigned int _G, unsigned int _H)
  :cell(_c),parent(_p),G(_G),H(_H){}
};

/*
* Spiral/sweep navigation, should work on square grids too when
    implemented
*/
Cell* getNextSpiral(Cell* _current, Grid* _grid)
{
  std::list<Cell*> neighbors = _grid->getNeighbors(_current);
  std::list<Cell*>::iterator it;

  Cell* next = NULL; //initialize to null for failure check

  float odist,min;
  min = -1;

  Cell* origin = _grid->getCell(0,0);

  for(it = neighbors.begin(); it!= neighbors.end(); it++)
  {
    if( !(*it)->visited && (*it)->allowed ){
      odist = _grid->global_distance(origin,*it);
      if(odist <= min || (min < 0)){next=*it; min=odist;}
    }
  }

  return next;
}
```

```
58  /**
     * Cell-list path planning
     */
    std::list<Cell*> planPath(Cell* _current, Cell* _target, Grid* _grid)
    {
63    std::list<SearchNode> store; //store nodes in memory so we can have
          valid pointers
      std::list<Cell*>::iterator cit;
      std::list<Cell*> path;    //return path
      std::map< Cell*, SearchNode* >::iterator it;
      std::map< Cell*, SearchNode* > open; //open map
68    std::map< Cell*, SearchNode* > closed; //closed map

      SearchNode start(_current,NULL,0.0,_grid->global_distance(_current,
          _target));
      store.push_back(start); //store node
      open[_current] = &(store.back()); //place start cell in open list
73
      SearchNode* current_node = &(store.back());
                  // get the first cell, starting at origin for now
                  // TODO: make this a bit more efficient
      while(!open.empty() && (current_node->cell != _target)){
78      //drop current node from open set, place in closed set
        closed[current_node->cell] = current_node;
        open.erase(current_node->cell);
        std::list<Cell*> neighbors = _grid->getNeighbors(current_node->cell);
        //process neighbors
83      for(cit = neighbors.begin(); cit != neighbors.end(); cit++)
        {
          bool inClosed = (closed.find(*cit) != closed.end());
          bool isAllowed = (*cit)->allowed;
          bool inOpen = (open.find(*cit) != open.end());
88
          if(!inClosed && !inOpen && isAllowed){ //if not visited and allowed
            SearchNode node(
              *cit,
              current_node,
```

```
93              current_node->G + _grid->local_distance(current_node->cell,*cit)
                    ,
                _grid->local_distance(*cit,_target));
              store.push_back(node);
              open[*cit] = &(store.back()); //place in open set
            } else if(inOpen){//check if path is more optimal
98            SearchNode* node = open[*cit];
              unsigned int G = current_node->G + _grid->local_distance(
                  current_node->cell,*cit);
              unsigned int cG = node->G;
              if(G < cG){ //if the path is more optimal
                node->parent = current_node; //update parent
103             node->G = G; //update G-score (H should be same in this case)
              }
            }
          }
          //find the lowest cost node in the open list
108       float F = -1;
          for(it = open.begin(); it != open.end(); it++)
          {
            SearchNode* node = it->second;
            float cF = node->G + node->H;
113         if(F == -1 || cF < F){
              current_node = node; //set next node
              F = cF;       //update cost
            }
          }
118     }
        if(current_node->cell == _target){
          SearchNode* traceback = current_node;
          while(traceback->parent){ //while the next parent is not null
            path.push_front(traceback->cell); //add cell to path
123         traceback = traceback->parent; //visit parent
          }
        }

        return path;
```

```
128   }

      /**
       * Returns the nearest unvisited cell
       */
133
      Cell* getNextUnvisited(Cell* _current, Grid* _grid)
      {
        std::list<Cell*> neighbors;
        std::list<Cell*> fringe;
138     std::set<Cell*> explored;
        std::list<Cell*>::iterator it;

        Cell* next = NULL;

143     fringe.push_back(_current);
        while(!fringe.empty())
        {
          if(fringe.front()->visited)
          {
148         neighbors = _grid->getNeighbors(fringe.front());
            //explored.insert(fringe.front());
            fringe.pop_front();
            for(it = neighbors.begin(); it != neighbors.end(); it++)
            {
153           if(explored.find(*it) == explored.end() && (*it)->allowed)
              {
                fringe.push_back(*it);
                explored.insert(*it);
              }
158         }
          }
          else
          {
            float max = 0;
163         for(it = fringe.begin(); it != fringe.end(); it++)
            {
```

```
            float P = (*it)->probability;
            if(P > max)
            {
168           next = *it;
              max = P;
            }
          }
          break;
173     }
      }
      return next;
    }

178

    /**
     * Returns the nearest allowed cell
     * Useful for handling unexpected blocked conditions
     */
183
    Cell* getNearestAllowed(Cell* _current, Grid* _grid)
    {
      std::list<Cell*> neighbors;
      std::list<Cell*> fringe;
188   std::set<Cell*> explored;
      std::list<Cell*>::iterator it;

      Cell* next = NULL; //pointer to the next cell, initialized to null

193   fringe.push_back(_current);
      while(!fringe.empty()) //while fringe isn't empty and no next cell is
          assigned
      {
        if(!(fringe.front()->allowed)) //if the cell isn't open, expand out
        {
198       neighbors = _grid->getNeighbors(fringe.front());
          fringe.pop_front();
          for(it = neighbors.begin(); it != neighbors.end(); it++)
```

```
        {
          if(explored.find(*it) == explored.end()) //if unexplored
203       {
            fringe.push_back(*it);
            explored.insert(*it);
          }
        }
208   }
      else //if the fringe front is allowed, we've found at least one open
          cell
      {
        float min = -1;
        for(it = fringe.begin(); it != fringe.end(); it++)
213     {
          float D = _grid->global_distance(*it,_current);
          if(min == -1 || D < min)
          {
            next = *it;
218         min = D;
          }
        }
        break;
      }
223 }
    return next;
}

bool isCellInTriangle(Vector2D a, Vector2D b, Vector2D c, Cell* _cell,
    Grid* _grid)
228 {
    int x,y; x = _cell->x; y = _cell->y;
    //round the points to nearest cell center coordinates
    Vector2D A = _grid->local_2_global(_grid->global_2_local(a));
    Vector2D B = _grid->local_2_global(_grid->global_2_local(b));
233 Vector2D C = _grid->local_2_global(_grid->global_2_local(c));

    Vector2D pt = _grid->local_2_global(std::make_pair(x,y));
```

```
    return isInTriangle(A,B,C,pt); //call to geometry function
    //return isInTriangle(a,b,c,pt);
}

std::set<Cell*> getCellsInTriangle(Vector2D a, Vector2D b, Vector2D c,
    Grid* _grid)
{
  std::set<Cell*> cells;
  std::list<Cell*> neighbors;
  std::set<Cell*> explored;
  std::list<Cell*> fringe;
  std::list<Cell*>::iterator it;
  // get the first cell, starting at origin for now
  // TODO: this could probably be made a bit more efficient
  Cell* cell = _grid->getCell(0,0);
  fringe.push_back(cell);
  explored.insert(cell);
  while(!fringe.empty())
  {

    neighbors = _grid->getNeighbors(fringe.front());
    //explored.insert(fringe.front());
    //check if current cell is in triangle
    if(isCellInTriangle(a,b,c,fringe.front(),_grid))
    {
      cells.insert(fringe.front());
    }
    //pop from fringe
    fringe.pop_front();
    //add neighbors
    for(it = neighbors.begin(); it != neighbors.end(); it++)
    {
      if(explored.find(*it)== explored.end())
      {
        fringe.push_back(*it);
        explored.insert(*it);
      }
```

```
        }
273     }
        return cells;
      }

    }

    #ifndef __WIND_GEOMETRY_H
    #define __WIND_GEOMETRY_H
  3 /**
     * File:  WiND_utils.hpp
     * Author:  Jonathan Estabrook
     * Description:
     *
  8  *  Basic utility functions and useful data type library.
     *  Geometric functions and such should go here for usage in other places.
     * */
    #include <list>
    namespace WiND
 13 {
      /**
      * Waypoint Data Struct,
      * Relative to 0,0,0 cartesian on grid
      */
 18   struct  Waypoint{
        float x;
        float y;
        float z;
      };
 23
      struct  Vector2D{
        /** The coordinates
        ********************/
        float x;
 28     float y;
        /** Operators
        ********************/
```

```
    Vector2D add(const Vector2D &v)
    {Vector2D p = {x+v.x,y+v.y}; return p;}

    Vector2D sub(const Vector2D &v)
    {Vector2D p = {x-v.x,y-v.y}; return p;}

    float dot(const Vector2D &v)
    {return (x*v.x+y*v.y);}

    //don't need cross product for now
  };

  /****GEOMETRY FUNCTIONS****/
  bool isInTriangle(Vector2D a, Vector2D b, Vector2D c, Vector2D target);

  float vectorDistance(Vector2D a, Vector2D b);

  bool point_in_polygon(Vector2D _pt, std::list<Vector2D> _polygon);
}
#endif

/**
* File: WiND_geometry.cpp
* Author: Jonathan Estabrook
* Description: basic geometric functions
*/

#include "WiND_utils.hpp"
#include <cmath>

namespace WiND
{
  /**
  * Returns if target is in triangle defined by a,b,c
  */
  bool isInTriangle(Vector2D a, Vector2D b, Vector2D c, Vector2D target){
    // Compute edges
```

```
    Vector2D v0 = c.sub(a);
    Vector2D v1 = b.sub(a);
    Vector2D v2 = target.sub(a);

    // Compute dot products
    float dot00 = v0.dot(v0);
    float dot01 = v0.dot(v1);
    float dot02 = v0.dot(v2);
    float dot11 = v1.dot(v1);
    float dot12 = v1.dot(v2);

    // Compute barycentric coordinates
    float invDenom = 1/(dot00 * dot11 - dot01 * dot01);
    float u = (dot11 * dot02 - dot01 * dot12) * invDenom;
    float v = (dot00 * dot12 - dot01 * dot02) * invDenom;

    // Check if point is in triangle
    return (u >= 0) && (v >= 0) && (u + v < 1);
}
/**
 *  Returns vector distance between points
 */
float vectorDistance(Vector2D a, Vector2D b)
{
   return std::sqrt((b.x-a.x)*(b.x-a.x)+(b.y-a.y)*(b.y-a.y));
}

bool point_in_polygon(Vector2D _pt, std::list<Vector2D> _polygon)
{
  std::list<Vector2D>::iterator it,last;
  it = _polygon.begin(); last = it; it++;
  bool oddCrosses = false;
  for(; it != _polygon.end(); it++)
  {
    float ix,jx,iy,jy;
    ix = (*it).x; iy = (*it).y; jx = (*last).x; jy = (*last).y;
    if((  (jy < _pt.y && iy >= _pt.y) ||
```

```
          (iy < _pt.y && jy >= _pt.y)) &&
55        (ix <= _pt.x && jx <= _pt.x))
        {
          if(ix + (_pt.y-iy)/(jy-iy)*(jx-ix)< _pt.x)
          {
            oddCrosses = !oddCrosses;
60        }
          last = it;
        }
      }
      return oddCrosses;
65
    }

}

/**
2 * File: test.cpp
* Simple demo file for hexagonal grid navigation
*/
#include <iostream> //for debug
#include <list>
7 #include <utility>
#include "Grid.hpp"
#include "Agent.hpp"
#include "WiND_search.hpp"
#include "WiND_utils.hpp"
12
/**
* Usage specific, prints grid to prompt
*/
void print_grid(WiND::Agent& a)
17 {
  int size = a.getWorld()->getSize();
  for(int i=size; i >= -size; i--)
  {
    std::string p;
```

```
22      if(i<0){
      p.assign(-i,' ');
      std::cout << p;
        }
        for(int j=-size; j <= size; j++)
27      {
      WiND::Cell* s = a.getWorld()->getCell(j,i);

      if(s){
        if(s == a.getCurrentCell()) std::cout << "X ";
32      else if(s->visited) std::cout << "o ";
        else if(!s->allowed) std::cout << "- ";
        else std::cout << ". ";
      }
      else std::cout << " ";
37      }
        std::cout << std::endl;
       }
    }

42  void callback_test(const char* _event, const char*  _arg)
    {
      std::cout << "CALLBACK: " << _event << ":" <<  _arg << std::endl;
    }

47  /**
    * Main function
    */
    int main()
    {
52
      WiND::Agent agent(50.0,3.0,"meters","hexagon"); //should make a roughly
          12-layer grid
      agent.setPosition(-10.0,3.0,100.0);
      //agent.setPosition(5,5,100);
      agent.setTargetAltitude(300);
57    //agent.setTargetPoint(30,30);
```

```
    agent.setCallback(callback_test);

    WiND::Vector2D a = {0,0};
    WiND::Vector2D b = {-25,-0.1};
62  WiND::Vector2D c = {0,25};



    WiND::Grid* grid = agent.getWorld();
67  std::set<WiND::Cell*> triangle = WiND::getCellsInTriangle(a,b,c,grid);
    std::set<WiND::Cell*>::iterator it;
    for(it = triangle.begin(); it != triangle.end(); it++){(*it)->allowed =
        false;}

    std::cout << "Testing Agent Navigation, non-center starting position" <<
        std::endl;
72  std::cin.ignore();
    print_grid(agent);

    WiND::Waypoint next;
    WiND::Waypoint pos;
77
    while(true)
    {
    next = agent.getNextWaypoint();
    pos = agent.getPosition();
82  WiND::Vector2D gCoords = {pos.x,pos.y};
    std::pair<int,int> hpos = agent.getWorld()->global_2_local(gCoords);
    if(next.x == pos.x && next.y == pos.y) break;
    std::cout << pos.x << "," << pos.y << "," << pos.z << std::endl;
    std::cout << hpos.first << "," << hpos.second << std::endl;
87  print_grid(agent); //print current state
    agent.setPosition(next.x, next.y, next.z); //update position
    usleep(200000);
    }
    print_grid(agent);
92  std::cout << "done..." << std::endl;
```

```
}
```

Appendix D

Framework Outline

```
module.exports = require('./lib/WiND');

/**
 *  File: WiND.cc
 *  Author: Jonathan Estabrook
 *  Description:
 *
 *  This file is the binding between the libWiND library and its NodeJS
    module.
 *  Bindings between C/C++ and Javascript happen here.
 *
 *  For any methods/function bindings, add a wrapper method within the
    WiND_node
 *  class here. Other utility methods can be added directly here too, and
    bound to
 *  the Javascript module.
 **/

#include <v8.h>
#include <node.h>
#include <string>
#include <sstream>
#include <list>
```

```
// the WiND library
#include <WiND/Agent.hpp>

using namespace v8;
using namespace node;

//some useful macros for repetitive v8 conversion tasks
// see http://github.com/pquerna/node-extension-examples
#define REQ_STR_ARG(I, VAR)             \
  if(args.Length() <= I || !args[I]->IsString())        \
    return ThrowException(Exception::TypeError(     \
      String::New("Argument " #I " must be a string")));  \
  Local<String> VAR = Local<String>::Cast(args[I])

#define REQ_FUN_ARG(I, VAR)             \
  if(args.Length() <= I || !args[I]->IsFunction())      \
    return ThrowException(Exception::TypeError(     \
      String::New("Argument " #I " must be a function")));  \
  Local<Function> VAR = Local<Function>::Cast(args[I])

#define REQ_FLO_ARG(I, VAR)             \
  if(args.Length() <= I || !args[I]->IsNumber())        \
    return ThrowException(Exception::TypeError(     \
      String::New("Argument " #I " must be a number")));  \
  Local<Number> VAR = Local<Number>::Cast(args[I])

#define TO_STRING(V8STR,ASCIISTR,VAR)           \
  String::AsciiValue ASCIISTR(V8STR);         \
  const char* VAR = *ASCIISTR

#define TO_V8STRING(STR,VAR)              \
  Local<String> VAR = String::New(STR)

#define CHECK_POINTER(PTR,ERRMSG)           \
  if(!PTR) return ThrowException(Exception::ReferenceError(String::New(
      ERRMSG)))
```

```
57 namespace WiND_node{
     class Agent : ObjectWrap
     {
     private:
       WiND::Agent* m_agent; //pointer to wrapped WiND::Agent
62   public:
       static Persistent<FunctionTemplate> s_ct;
       static void Init(Handle<Object> target)
       {
         HandleScope scope;
67       Local<FunctionTemplate> t = FunctionTemplate::New(New);

         s_ct = Persistent<FunctionTemplate>::New(t);
         s_ct->InstanceTemplate()->SetInternalFieldCount(1);
         s_ct->SetClassName(String::NewSymbol("Agent"));
72
         //to bind c++ methods to the javascript follow this template:
         //NODE_SET_PROTOTYPE_METHOD(s_ct, "js_name", cpp_name);
         NODE_SET_PROTOTYPE_METHOD(s_ct, "configure", Configure);
         NODE_SET_PROTOTYPE_METHOD(s_ct, "deconfigure", Deconfigure);
77       NODE_SET_PROTOTYPE_METHOD(s_ct, "get_position", GetPosition);
         NODE_SET_PROTOTYPE_METHOD(s_ct, "set_position", SetPosition);
         NODE_SET_PROTOTYPE_METHOD(s_ct, "get_next_waypoint", GetNextWaypoint);
         NODE_SET_PROTOTYPE_METHOD(s_ct, "get_grid_bounds", GetGridBounds);
         NODE_SET_PROTOTYPE_METHOD(s_ct, "set_target_point", SetTargetPoint);
82       NODE_SET_PROTOTYPE_METHOD(s_ct, "set_target_altitude",
             SetTargetAltitude);

         target->Set(String::NewSymbol("Agent"),s_ct->GetFunction());
       }

87     Agent():m_agent(NULL){} //constructor
       ~Agent()
       {
         delete this->m_agent;
```

```
    this->m_agent = NULL;
92  }

    // v8 method for constructing from Javascript
    static Handle<Value> New(const Arguments& args)
    {
97    HandleScope scope;
      Agent* hw = new Agent();  //create a WiND_node::Agent object
      hw->Wrap(args.This());    //store refernece inside args.This();
      return args.This();   //return reference from args.This();
    }
102
    // configure wrapper method, sends initialization request to Agent
    static Handle<Value> Configure(const Arguments& args)
    {
      HandleScope scope;
107   Agent* a = ObjectWrap::Unwrap<Agent>(args.This());
      if(a->m_agent) return ThrowException(Exception::ReferenceError(
        String::New("Agent already initialized, use deconfigure first")));
      REQ_FLO_ARG(0,_min_grid_rad);
      REQ_FLO_ARG(1,_min_cell_rad);
112   REQ_STR_ARG(2,_units);
      REQ_STR_ARG(3,_grid_type);

      float mgr = _min_grid_rad->Value();
      float mcr = _min_cell_rad->Value();
117   TO_STRING(_units,unitval,u);
      TO_STRING(_grid_type,gtval,gt);

      a->m_agent = new WiND::Agent(mgr,mcr,u,gt);
      return scope.Close(Null());
122   }

    // deconfigure method, simply deletes the agent for a hard-reset
    // could be made a bit better in the future if needed
    static Handle<Value> Deconfigure(const Arguments& args)
127 {
```

```
    HandleScope scope;
    Agent* a = ObjectWrap::Unwrap<Agent>(args.This());
    if(a->m_agent){
      delete a->m_agent;
132   a->m_agent = NULL;
    }
    return scope.Close(Null());
  }

137 static Handle<Value> GetPosition(const Arguments& args)
  {
    HandleScope scope;
    Agent* a = ObjectWrap::Unwrap<Agent>(args.This());
    CHECK_POINTER(a->m_agent,"Agent is not initialized!");
142   WiND::Waypoint wp = a->m_agent->getPosition();
    std::stringstream ss;
    ss << "{\"TYPE\":\"WAYPOINT\"";
    ss << ",\"UNIT\":\"" << a->m_agent->getWorld()->getUnits() << "\"";
    ss << ",\"X\":" << wp.x;
147   ss << ",\"Y\":" << wp.y;
    ss << ",\"Z\":" << wp.z << "}";
    TO_V8STRING(ss.str().c_str(),result);
    return scope.Close(result);
  }
152
  static Handle<Value> SetPosition(const Arguments& args)
  {
    HandleScope scope;
    Agent* a = ObjectWrap::Unwrap<Agent>(args.This());
157   CHECK_POINTER(a->m_agent,"Agent is not initialized!");
    REQ_FLO_ARG(0,_x);
    REQ_FLO_ARG(1,_y);
    REQ_FLO_ARG(2,_z);
    float x = _x->Value();
162   float y = _y->Value();
    float z = _z->Value();
    a->m_agent->setPosition(x,y,z);
```

```
    return scope.Close(Null());
  }

  static Handle<Value> GetNextWaypoint(const Arguments& args)
  {
    HandleScope scope;
    Agent* a = ObjectWrap::Unwrap<Agent>(args.This());
    CHECK_POINTER(a->m_agent,"Agent is not initialized!");
    WiND::Waypoint wp = a->m_agent->getNextWaypoint();
    std::stringstream ss;
    ss << "{\"TYPE\":\"WAYPOINT\"";
    ss << ",\"UNIT\":\"" << a->m_agent->getWorld()->getUnits() << "\"";
    ss << ",\"X\":" << wp.x;
    ss << ",\"Y\":" << wp.y;
    ss << ",\"Z\":" << wp.z << "}";
    TO_V8STRING(ss.str().c_str(),result);
    return scope.Close(result);
  }

  static Handle<Value> GetGridBounds(const Arguments& args)
  {
    HandleScope scope;
    Agent* a = ObjectWrap::Unwrap<Agent>(args.This());
    CHECK_POINTER(a->m_agent,"Agent is not initialized!");
    std::list<WiND::Vector2D> bounds = a->m_agent->getWorld()->getBounds()
        ;
    std::list<WiND::Vector2D>::iterator it;
    std::stringstream ss;
    ss << "[";
    for(it=bounds.begin();it!=bounds.end();it++)
    {
      if(it!=bounds.begin()) ss << ",";
      ss << "{\"x\":" << (*it).x << ",\"y\":" << (*it).y << "}";
    }
    ss << "]";
    TO_V8STRING(ss.str().c_str(),result);
    return scope.Close(result);
```

```
    }

  static Handle<Value> SetTargetPoint(const Arguments& args)
  {
    HandleScope scope;
    Agent* a = ObjectWrap::Unwrap<Agent>(args.This());
    CHECK_POINTER(a->m_agent,"Agent is not initialized!");
    REQ_FLO_ARG(0, _x);
    REQ_FLO_ARG(1, _y);
    float x = _x->Value();
    float y = _y->Value();
    a->m_agent->setTargetPoint(x,y);
    return scope.Close(Null());
  }

  static Handle<Value> SetTargetAltitude(const Arguments& args)
  {
    HandleScope scope;
    Agent* a = ObjectWrap::Unwrap<Agent>(args.This());
    CHECK_POINTER(a->m_agent,"Agent is not initialized!");
    REQ_FLO_ARG(0, _z);
    float z = _z->Value();
    a->m_agent->setTargetAltitude(z);
    return scope.Close(Null());
  }

};

/**********************************************
 *  The code below is needed for bindings to work properly
 *  Bindings to other objects would need to place their Init() methods
 *  within the init function below.
 **/
Persistent<FunctionTemplate> Agent::s_ct;

extern "C" {
  static void init (Handle<Object> target)
```

```
        {
          Agent::Init(target);
        }

242     NODE_MODULE(WiND, init);
      }

    }

    /**
     *  File: WiND.cc
     *  Author: Jonathan Estabrook
 4   *  Description:
     *
     *  This file is the binding between the libWiND library and its NodeJS
        module.
     *  Bindings between C/C++ and Javascript happen here.
     *
 9   *  For any methods/function bindings, add a wrapper method within the
        WiND_node
     *  class here. Other utility methods can be added directly here too, and
        bound to
     *  the Javascript module.
     **/

14  #include <v8.h>
    #include <node.h>
    #include <string>
    #include <sstream>
    #include <list>
19
    // the WiND library
    #include <WiND/Agent.hpp>

    using namespace v8;
24  using namespace node;
```

```
//some useful macros for repetitive v8 conversion tasks
// see http://github.com/pquerna/node-extension-examples
#define REQ_STR_ARG(I, VAR)                \
  if(args.Length() <= I || !args[I]->IsString())        \
    return ThrowException(Exception::TypeError(     \
      String::New("Argument " #I " must be a string")));  \
  Local<String> VAR = Local<String>::Cast(args[I])

#define REQ_FUN_ARG(I, VAR)                \
  if(args.Length() <= I || !args[I]->IsFunction())      \
    return ThrowException(Exception::TypeError(     \
      String::New("Argument " #I " must be a function")));  \
  Local<Function> VAR = Local<Function>::Cast(args[I])

#define REQ_FLO_ARG(I, VAR)                \
  if(args.Length() <= I || !args[I]->IsNumber())        \
    return ThrowException(Exception::TypeError(     \
      String::New("Argument " #I " must be a number")));  \
  Local<Number> VAR = Local<Number>::Cast(args[I])

#define TO_STRING(V8STR,ASCIISTR,VAR)           \
  String::AsciiValue ASCIISTR(V8STR);         \
  const char* VAR = *ASCIISTR

#define TO_V8STRING(STR,VAR)              \
  Local<String> VAR = String::New(STR)

#define CHECK_POINTER(PTR,ERRMSG)           \
  if(!PTR) return ThrowException(Exception::ReferenceError(String::New(
      ERRMSG)))


namespace WiND_node{
  class Agent : ObjectWrap
  {
  private:
    WiND::Agent* m_agent; //pointer to wrapped WiND::Agent
```

```
public:
  static Persistent<FunctionTemplate> s_ct;
  static void Init(Handle<Object> target)
  {
    HandleScope scope;
    Local<FunctionTemplate> t = FunctionTemplate::New(New);

    s_ct = Persistent<FunctionTemplate>::New(t);
    s_ct->InstanceTemplate()->SetInternalFieldCount(1);
    s_ct->SetClassName(String::NewSymbol("Agent"));

    //to bind c++ methods to the javascript follow this template:
    //NODE_SET_PROTOTYPE_METHOD(s_ct, "js_name", cpp_name);
    NODE_SET_PROTOTYPE_METHOD(s_ct, "configure", Configure);
    NODE_SET_PROTOTYPE_METHOD(s_ct, "deconfigure", Deconfigure);
    NODE_SET_PROTOTYPE_METHOD(s_ct, "get_position", GetPosition);
    NODE_SET_PROTOTYPE_METHOD(s_ct, "set_position", SetPosition);
    NODE_SET_PROTOTYPE_METHOD(s_ct, "get_next_waypoint", GetNextWaypoint);
    NODE_SET_PROTOTYPE_METHOD(s_ct, "get_grid_bounds", GetGridBounds);
    NODE_SET_PROTOTYPE_METHOD(s_ct, "set_target_point", SetTargetPoint);
    NODE_SET_PROTOTYPE_METHOD(s_ct, "set_target_altitude",
        SetTargetAltitude);

    target->Set(String::NewSymbol("Agent"),s_ct->GetFunction());
  }

  Agent():m_agent(NULL){} //constructor
  ~Agent()
  {
    delete this->m_agent;
    this->m_agent = NULL;
  }

  // v8 method for constructing from Javascript
  static Handle<Value> New(const Arguments& args)
  {
    HandleScope scope;
```

```
  Agent* hw = new Agent();  //create a WiND_node::Agent object
  hw->Wrap(args.This());    //store refernece inside args.This();
  return args.This();   //return reference from args.This();
}

// configure wrapper method, sends initialization request to Agent
static Handle<Value> Configure(const Arguments& args)
{
  HandleScope scope;
  Agent* a = ObjectWrap::Unwrap<Agent>(args.This());
  if(a->m_agent) return ThrowException(Exception::ReferenceError(
    String::New("Agent already initialized, use deconfigure first")));
  REQ_FLO_ARG(0,_min_grid_rad);
  REQ_FLO_ARG(1,_min_cell_rad);
  REQ_STR_ARG(2,_units);
  REQ_STR_ARG(3,_grid_type);

  float mgr = _min_grid_rad->Value();
  float mcr = _min_cell_rad->Value();
  TO_STRING(_units,unitval,u);
  TO_STRING(_grid_type,gtval,gt);

  a->m_agent = new WiND::Agent(mgr,mcr,u,gt);
  return scope.Close(Null());
}

// deconfigure method, simply deletes the agent for a hard-reset
// could be made a bit better in the future if needed
static Handle<Value> Deconfigure(const Arguments& args)
{
  HandleScope scope;
  Agent* a = ObjectWrap::Unwrap<Agent>(args.This());
  if(a->m_agent){
    delete a->m_agent;
    a->m_agent = NULL;
  }
  return scope.Close(Null());
```

```
}

static Handle<Value> GetPosition(const Arguments& args)
{
  HandleScope scope;
  Agent* a = ObjectWrap::Unwrap<Agent>(args.This());
  CHECK_POINTER(a->m_agent,"Agent is not initialized!");
  WiND::Waypoint wp = a->m_agent->getPosition();
  std::stringstream ss;
  ss << "{\"TYPE\":\"WAYPOINT\"";
  ss << ",\"UNIT\":\"" << a->m_agent->getWorld()->getUnits() << "\"";
  ss << ",\"X\":" << wp.x;
  ss << ",\"Y\":" << wp.y;
  ss << ",\"Z\":" << wp.z << "}";
  TO_V8STRING(ss.str().c_str(),result);
  return scope.Close(result);
}

static Handle<Value> SetPosition(const Arguments& args)
{
  HandleScope scope;
  Agent* a = ObjectWrap::Unwrap<Agent>(args.This());
  CHECK_POINTER(a->m_agent,"Agent is not initialized!");
  REQ_FLO_ARG(0,_x);
  REQ_FLO_ARG(1,_y);
  REQ_FLO_ARG(2,_z);
  float x = _x->Value();
  float y = _y->Value();
  float z = _z->Value();
  a->m_agent->setPosition(x,y,z);
  return scope.Close(Null());
}

static Handle<Value> GetNextWaypoint(const Arguments& args)
{
  HandleScope scope;
  Agent* a = ObjectWrap::Unwrap<Agent>(args.This());
```

```
    CHECK_POINTER(a->m_agent,"Agent is not initialized!");
    WiND::Waypoint wp = a->m_agent->getNextWaypoint();
174 std::stringstream ss;
    ss << "{\"TYPE\":\"WAYPOINT\"";
    ss << ",\"UNIT\":\"" << a->m_agent->getWorld()->getUnits() << "\"";
    ss << ",\"X\":" << wp.x;
    ss << ",\"Y\":" << wp.y;
179 ss << ",\"Z\":" << wp.z << "}";
    TO_V8STRING(ss.str().c_str(),result);
    return scope.Close(result);
  }

184 static Handle<Value> GetGridBounds(const Arguments& args)
  {
    HandleScope scope;
    Agent* a = ObjectWrap::Unwrap<Agent>(args.This());
    CHECK_POINTER(a->m_agent,"Agent is not initialized!");
189 std::list<WiND::Vector2D> bounds = a->m_agent->getWorld()->getBounds()
      ;
    std::list<WiND::Vector2D>::iterator it;
    std::stringstream ss;
    ss << "[";
    for(it=bounds.begin();it!=bounds.end();it++)
194 {
      if(it!=bounds.begin()) ss << ",";
      ss << "{\"x\":" << (*it).x << ",\"y\":" << (*it).y << "}";
    }
    ss << "]";
199 TO_V8STRING(ss.str().c_str(),result);
    return scope.Close(result);
  }

  static Handle<Value> SetTargetPoint(const Arguments& args)
204 {
    HandleScope scope;
    Agent* a = ObjectWrap::Unwrap<Agent>(args.This());
    CHECK_POINTER(a->m_agent,"Agent is not initialized!");
```

```
      REQ_FLO_ARG(0, _x);
      REQ_FLO_ARG(1, _y);
      float x = _x->Value();
      float y = _y->Value();
      a->m_agent->setTargetPoint(x,y);
      return scope.Close(Null());
    }

    static Handle<Value> SetTargetAltitude(const Arguments& args)
    {
      HandleScope scope;
      Agent* a = ObjectWrap::Unwrap<Agent>(args.This());
      CHECK_POINTER(a->m_agent,"Agent is not initialized!");
      REQ_FLO_ARG(0, _z);
      float z = _z->Value();
      a->m_agent->setTargetAltitude(z);
      return scope.Close(Null());
    }

};

/**********************************************
 *  The code below is needed for bindings to work properly
 *  Bindings to other objects would need to place their Init() methods
 *  within the init function below.
 **/
Persistent<FunctionTemplate> Agent::s_ct;

extern "C" {
  static void init (Handle<Object> target)
  {
    Agent::Init(target);
  }

  NODE_MODULE(WiND, init);
}
```

```
}

// A javascript layer to simplify using the binding

var WiND = require('../build/Release/WiND.node');
var Tester = require('./Tester');

module.exports.Agent = WiND.Agent;
module.exports.Tester = Tester;

// a simple means of testing navigation by providing smooth movement
    feedback

var util = require('util');
module.exports = Tester;

function Tester(agent,event_emitter){
  this.start = startStep;
  this.stop = function(){clearInterval(this.handle)};
  this.agent = agent;
  this.events = event_emitter;
};

function get_step(a,b)
{
  var step = {};
  step.X = b.X-a.X; step.Y = b.Y-a.Y; step.Z = b.Z-a.Z;
  var mag = Math.sqrt(step.X*step.X + step.Y*step.Y + step.Z*step.Z);
  step.X /= mag; step.Y /= mag; step.Z /=mag;
  return step;
}

function distance(a,b)
{
  var step = {};
  step.X = b.X-a.X; step.Y = b.Y-a.Y; step.Z = b.Z-a.Z;
  var mag = Math.sqrt(step.X*step.X + step.Y*step.Y + step.Z*step.Z);
  return mag;
```

```
}

function startStep(interval,margin,speed){
  var myself = this; //to fix the reference issue
  clearInterval(this.handle);
  var waypoint = JSON.parse(myself.agent.get_next_waypoint());
  this.handle = setInterval(function(){
    var pos = JSON.parse(myself.agent.get_position());
    console.log(distance(pos,waypoint));
    if(distance(pos,waypoint) < margin)
    {
      waypoint = JSON.parse(myself.agent.get_next_waypoint());
      util.debug("updating waypoint");
    }

    var step = get_step(pos,waypoint);
    pos.X += step.X*(speed*(interval/1000));
    pos.Y += step.Y*(speed*(interval/1000));
    pos.Z += step.Z*(speed*(interval/1000));
    myself.agent.set_position(pos.X, pos.Y, pos.Z);
    myself.events.emit('telemetry',pos);
  },interval);
}

function toNumber(value)
{
  var numVal = parseFloat(value);
  if(isNaN(numVal))
  {
    alert(value + " is not a number"); return;
  }
  return numVal;
};

function display_msg(msg)
{
  if(typeof msg != "object") return display_msg($.parseJSON(msg));
```

```
    var d = "<table class='msg'>";
    $.each(msg, function(field,value){
      d+= "<tr><th><p>"+field+"</p></th><td>"+
      ((typeof value != "object")?(value):(display_msg(value)))+
      "</td></tr>";
    });
    d+="</table>";
    return d;
};

var canvas_scaling = 1;

function draw_shape(layer,stage,pts,stroke)
{
    var shape = new Kinetic.Polygon({
      points: scale_shape(pts,stage),
      stroke: stroke,
      strokeWidth:2
    });
    layer.add(shape);
    layer.draw();
    return shape;
}

function scale_shape(pts,stage)
{
    for(var i = 0; i<pts.length; i++)
    {
      pts[i].x *=  canvas_scaling;
      pts[i].y *= -canvas_scaling;
      pts[i].x += stage.width/2;
      pts[i].y += stage.height/2;
    }
    console.log(pts);
    return pts;
}
```

```
function draw_point(layer,pt)
{
  var circ = new Kinetic.Circle({
    x: pt.x,
    y: pt.y,
    radius: 2,
    fill: "#a55"
  });
  layer.add(circ);
  layer.draw();
  return circ;
}

function scale_point(pt,stage)
{
  pt.x *= canvas_scaling;
  pt.y *= -canvas_scaling;
  pt.x += stage.width/2;
  pt.y += stage.height/2;
}

function calculate_scaling(pts,stage)
{
  var max_pt = pts[0];
  for(var i=0;i<pts.length;i++)
  {
    if(Math.abs(pts[i].x) > Math.abs(max_pt.x) && Math.abs(pts[i].y) > Math.
        abs(max_pt.y))
      max_pt = pts[i];
  }
  max_pt.x = Math.abs(max_pt.x);
  max_pt.y = Math.abs(max_pt.y);
  var s = (max_pt.x>max_pt.y)?(stage.width/(2*max_pt.x)):(stage.width/(2*
      max_pt.y));
  return s;
}
```

```
$(function(){

  var socket = io.connect(document.location.host);

  socket.on('connect', function(){
    $('#feed').prepend("<pre>CONNECTED</pre>");
  });

  socket.on('disconnect',function(){
    $('#feed').prepend("<pre>DISCONNECTED</pre>");
  });

  socket.on('telemetry', function(msg){
    var pt = {};
    pt.x = msg.X;
    pt.y = msg.Y;
    scale_point(pt,stage);
    draw_point(back_layer,pt);
    dot.x = pt.x;
    dot.y = pt.y;
    back_layer.draw();
    front_layer.draw();
    var d = "<pre> X:" + msg.X + "  Y:"+msg.Y+" Z:"+msg.Z+"</pre>";
    $('#telemetry').html(d);
  });

  socket.on('warning', function(msg){
    $('#feed').prepend(display_msg(msg));
  });

  socket.on('error', function(msg){
    $('#feed').prepend(display_msg(msg)).fadeIn();
  });

  socket.on('status', function(msg){
    $('#feed').prepend(display_msg(msg)).fadeIn();
  });
```

```
socket.on('bounds', function(msg){
  console.log(msg);
  var points = JSON.parse(msg);
  console.log(points);
  canvas_scaling = calculate_scaling(points,stage);
  draw_shape(back_layer,stage,points,"#eee");
});


// User Input

$('#input').children().hide();

$('#config').click(function(){
  //socket.emit('configure',JSON.parse($('#prompt').val()));
  $('#input').children().hide();
  $('#config_form').show();
});

$('#refresh').click(function(){
  socket.emit('get_bounds');
});

$('#target').click(function(){
  $('#input').children().hide();
  $('#target_form').show();
});

$('#target_form #submit_pt').click(function(){
  var target = {};
  target.x = toNumber($('#target_form #tar_x').val());
  target.y = toNumber($('#target_form #tar_y').val());
  socket.emit('target_point',target);
});

$('#target_form #submit_alt').click(function(){
```

```
    var target = {};
    target.alt = toNumber($('#target_form #tar_alt').val());
    socket.emit('target_alt',target);
  });
  $('#config_form #submit').click(function(){
    var config = {};
    config.grid_type = $('#config_form #grid_type').val();
    config.units = $('#config_form #units').val();
    config.grid_rad = toNumber($('#config_form #grid_rad').val());
    config.cell_rad = toNumber($('#config_form #cell_rad').val());

    config.init_x = toNumber($('#config_form #init_x').val());
    config.init_y = toNumber($('#config_form #init_y').val());
    config.init_z = toNumber($('#config_form #init_z').val());
    config.target_alt = toNumber($('#config_form #target_alt').val());

    canvas_scaling = stage.width/(2*config.grid_rad);
    //TODO: add a bit more validation
    socket.emit('configure',config);

  });

  $('#connect').click(function(){
    $('#input').children().hide();
    $('#connect_form').show();
  });

  // Map Drawing Stuff
  var stage = new Kinetic.Stage("map",500,500);
  var back_layer = new Kinetic.Layer();
  var front_layer = new Kinetic.Layer();
  var dot = new Kinetic.Circle({
    x: stage.width/2,
    y: stage.width/2,
    stroke: '#0f0',
    strokeWidth: 2,
    radius: 4
```

```
});

front_layer.add(dot);

/*var hexagon = new Kinetic.RegularPolygon({
  x: stage.width/2,
  y: stage.width/2,
  sides: 6,
  radius: stage.width/2,
  stroke: "#eee",
  strokeWidth: 3
});*/

//layer.add(hexagon);
stage.add(back_layer);
stage.add(front_layer);

});
```

```
/*
 * GET home page.
 */

exports.index = function(req, res){
  res.render('index', { title: 'WiND Dash' })
};
```

```
//  h1= title
#controls
  ul
    li
      a#config(href='#') CONFIG
    li
      a#deconfig(href='#') DECONFIG
    li
      a#target(href='#') TARGET
    li
```

```
        a#refresh(href='#') REFRESH
    li
        a#connect(href='#') CONNECT
#main
  #display
    #map
    #telemetry
  #console
    #feed
    #input
      form#target_form
        table
          tr
            td target x:
            td target y:
          tr
            td
              input(id="tar_x",type="text",size="6")
            td
              input(id="tar_y",type="text",size="6")
            td
              input(id="submit_pt",type="submit",value="submit");
          tr
            td target alt:
            td
              input(id="tar_alt",type="text",size="6")
            td
              input(id="submit_alt",type="submit",value="submit");

      form#connect_form
        table
          tr
            td address:
          tr
            td
              input(id="address",type="text")
            td
```

```
          input(id="submit",type="submit",value="connect")
      form#config_form
        table
          tr
52          td grid rad:
            td cell rad:
            td units:
            td type:
          tr
57          td
              input(id="grid_rad",type="text",size="7")
            td
              input(id="cell_rad",type="text",size="6")
            td
62            select(id="units")
                option(value="meters") meters
                option(value="feet") feet
            td
              select(id="grid_type")
67              option(value="hexagon") hexagonal
          tr
            td init x:
            td init y:
            td init z:
72          td target alt:
          tr
            td
              input(id="init_x",type="text",size="5")
            td
77            input(id="init_y",type="text",size="5")
            td
              input(id="init_z",type="text",size="5")
            td
              input(id="target_alt",type="text",size="5")
82        tr
            td
              input(type="submit", value="submit", id="submit")
```

```
!!! 5
html
  head
    title= title
    link(rel='stylesheet', href='/stylesheets/style.css')
    script(type='text/javascript', src='/javascripts/jquery-1.6.3.min.js')
    script(type='text/javascript', src='/javascripts/kinetic-v3.8.1.min.js')
    script(type='text/javascript', src='/socket.io/socket.io.js')
    script(type='text/javascript', src='/javascripts/client.js')

  body
    #wrapper!= body
```

```
/**
 * This is the main express.js application for the WiND configuration
     interface
 */



// link dependencies
var express = require('express')
  , WiND = require('WiND')
  , events = require('events')
  , io = require('socket.io')
  , routes = require('./routes');

var app = module.exports = express.createServer();
var agent = new WiND.Agent();
var eventEmitter = new events.EventEmitter();
var tester = new WiND.Tester(agent,eventEmitter);

// Express.js Configuration

app.configure(function(){
  app.set('views', __dirname + '/views');
  app.set('view engine', 'jade');
  app.use(express.bodyParser());
```

```
    app.use(express.methodOverride());
    app.use(require('stylus').middleware({ src: __dirname + '/public' }));
    app.use(app.router);
    app.use(express.static(__dirname + '/public'));
});

app.configure('development', function(){
    app.use(express.errorHandler({ dumpExceptions: true, showStack: true }));
});

app.configure('production', function(){
    app.use(express.errorHandler());
});

// Define HTTP Routes
app.get('/', routes.index);

app.listen(3000); //listen on port 3000 (change if needed)
console.log("Express server listening on port %d in %s mode", app.address().
    port, app.settings.env);


// begin listening on socket.io
io = io.listen(app);
io.sockets.on('connection',message_handler);


// function for handling socket.io messages (client side requests)
function message_handler(client)
{
    var addr = client.handshake.address;
    console.log("CONNECTION " + client.id + " accepted from " + addr.address);
    client.on('disconnect', function()
    {
        console.log("Connection " + client.id + " terminated.");
    });
```

```
    // configure message received
    client.on('configure', function(config)
    {
63    try{
      agent.configure(config.grid_rad,
          config.cell_rad,
          config.units,
          config.grid_type);
68    agent.set_position(config.init_x,config.init_y,config.init_z);
      agent.set_target_altitude(config.target_alt);
      tester.start(500,3,20);
      client.emit('status',{STATUS :'AGENT CONFIGURED'});
      client.emit('bounds',agent.get_grid_bounds());
73    } catch(err){
      client.emit('error',{ERROR : err.message});
      }
    });

78  // target request message received
    client.on('target_point', function(target)
    {
      try{
      agent.set_target_point(target.x,target.y);
83    } catch(err){
      client.emit('error',{ERROR : err.message});
      }
    });

88  // target altitude request received
    client.on('target_alt', function(target)
    {
      try{
      agent.set_target_altitude(target.alt);
93    } catch(err){
      client.emit('error',{ERROR : err.message});
      }
    });
```

```
  // grid boundary point request, send back a list of points
  client.on('get_bounds',function(){
    try{
    client.emit('bounds',agent.get_grid_bounds());
    } catch(err){
    client.emit('error',{ERROR: err.message});
    }
  });
};

// event emitter links to socket.io for broadcast

// on telemetry events, broadcast telemetry data
eventEmitter.on('telemetry',function(msg){
  io.sockets.emit('telemetry',msg);
});
```

```
#!/bin/sh

#outputs an mjpeg video at 5 fps for given number of frames
gst-launch -e v4l2src num-buffers=$1 ! videorate ! video/x-raw-yuv, width
    =640, height=480, framerate=5/1 ! jpegenc ! avimux ! filesink location=
    $2.avi
```

```
/**
* File: WiND_geometry.cpp
* Author: Jonathan Estabrook
* Description: basic geometric functions
*/

#include "WiND_utils.hpp"
#include <cmath>

namespace WiND
{
  /**
  * Returns if target is in triangle defined by a,b,c
```

```
*/
bool isInTriangle(Vector2D a, Vector2D b, Vector2D c, Vector2D target){
  // Compute edges
  Vector2D v0 = c.sub(a);
  Vector2D v1 = b.sub(a);
  Vector2D v2 = target.sub(a);

  // Compute dot products
  float dot00 = v0.dot(v0);
  float dot01 = v0.dot(v1);
  float dot02 = v0.dot(v2);
  float dot11 = v1.dot(v1);
  float dot12 = v1.dot(v2);

  // Compute barycentric coordinates
  float invDenom = 1/(dot00 * dot11 - dot01 * dot01);
  float u = (dot11 * dot02 - dot01 * dot12) * invDenom;
  float v = (dot00 * dot12 - dot01 * dot02) * invDenom;

  // Check if point is in triangle
  return (u >= 0) && (v >= 0) && (u + v < 1);
}
/**
 *  Returns vector distance between points
 */
float vectorDistance(Vector2D a, Vector2D b)
{
   return std::sqrt((b.x-a.x)*(b.x-a.x)+(b.y-a.y)*(b.y-a.y));
}

bool point_in_polygon(Vector2D _pt, std::list<Vector2D> _polygon)
{
  std::list<Vector2D>::iterator it,last;
  it = _polygon.begin(); last = it; it++;
  bool oddCrosses = false;
  for(; it != _polygon.end(); it++)
  {
```

```
        float ix,jx,iy,jy;
        ix = (*it).x; iy = (*it).y; jx = (*last).x; jy = (*last).y;
        if((  (jy < _pt.y && iy >= _pt.y) ||
          (iy < _pt.y && jy >= _pt.y)) &&
          (ix <= _pt.x && jx <= _pt.x))
        {
          if(ix + (_pt.y-iy)/(jy-iy)*(jx-ix)< _pt.x)
          {
            oddCrosses = !oddCrosses;
          }
          last = it;
        }
      }
      return oddCrosses;

    }

  }

  /**
   * File:  WiND_search.cpp
   * Author:  Jonathan Estabrook
   * Description:
   *
   *  Function Library for search methods.
   * */
  #include "WiND_search.hpp"
  #include "WiND_utils.hpp"

  #include <algorithm>
  #include <list>
  #include <set>
  #include <map>

  namespace WiND {

    /**
```

```
 *  Data struct for path planning, currently specialized for A* search
 */
struct SearchNode{
  Cell* cell;
  SearchNode* parent;
  unsigned int G; //cost to this cell
  unsigned int H; //estimated cost(straight line)

  SearchNode(Cell* _c, SearchNode* _p, unsigned int _G, unsigned int _H)
  :cell(_c),parent(_p),G(_G),H(_H){}
};

/*
* Spiral/sweep navigation, should work on square grids too when
    implemented
*/
Cell* getNextSpiral(Cell* _current, Grid* _grid)
{
  std::list<Cell*> neighbors = _grid->getNeighbors(_current);
  std::list<Cell*>::iterator it;

  Cell* next = NULL; //initialize to null for failure check

  float odist,min;
  min = -1;

  Cell* origin = _grid->getCell(0,0);

  for(it = neighbors.begin(); it!= neighbors.end(); it++)
  {
    if( !(*it)->visited && (*it)->allowed ){
      odist = _grid->global_distance(origin,*it);
      if(odist <= min || (min < 0)){next=*it; min=odist;}
    }
  }

  return next;
```

```
}

/**
 * Cell-list path planning
 */
std::list<Cell*> planPath(Cell* _current, Cell* _target, Grid* _grid)
{
  std::list<SearchNode> store; //store nodes in memory so we can have
      valid pointers
  std::list<Cell*>::iterator cit;
  std::list<Cell*> path;    //return path
  std::map< Cell*, SearchNode* >::iterator it;
  std::map< Cell*, SearchNode* > open; //open map
  std::map< Cell*, SearchNode* > closed; //closed map

  SearchNode start(_current,NULL,0.0,_grid->global_distance(_current,
      _target));
  store.push_back(start); //store node
  open[_current] = &(store.back()); //place start cell in open list

  SearchNode* current_node = &(store.back());
              // get the first cell, starting at origin for now
              // TODO: make this a bit more efficient
  while(!open.empty() && (current_node->cell != _target)){
    //drop current node from open set, place in closed set
    closed[current_node->cell] = current_node;
    open.erase(current_node->cell);
    std::list<Cell*> neighbors = _grid->getNeighbors(current_node->cell);
    //process neighbors
    for(cit = neighbors.begin(); cit != neighbors.end(); cit++)
    {
      bool inClosed = (closed.find(*cit) != closed.end());
      bool isAllowed = (*cit)->allowed;
      bool inOpen = (open.find(*cit) != open.end());

      if(!inClosed && !inOpen && isAllowed){ //if not visited and allowed
```

```
            SearchNode node(
              *cit,
92            current_node,
              current_node->G + _grid->local_distance(current_node->cell,*cit)
                  ,
              _grid->local_distance(*cit,_target));
            store.push_back(node);
            open[*cit] = &(store.back()); //place in open set
97        } else if(inOpen){//check if path is more optimal
            SearchNode* node = open[*cit];
            unsigned int G = current_node->G + _grid->local_distance(
                current_node->cell,*cit);
            unsigned int cG = node->G;
            if(G < cG){ //if the path is more optimal
102           node->parent = current_node; //update parent
              node->G = G; //update G-score (H should be same in this case)
            }
          }
        }
107     //find the lowest cost node in the open list
        float F = -1;
        for(it = open.begin(); it != open.end(); it++)
        {
          SearchNode* node = it->second;
112       float cF = node->G + node->H;
          if(F == -1 || cF < F){
            current_node = node; //set next node
            F = cF;       //update cost
          }
117     }
      }
      if(current_node->cell == _target){
        SearchNode* traceback = current_node;
        while(traceback->parent){ //while the next parent is not null
122       path.push_front(traceback->cell); //add cell to path
          traceback = traceback->parent; //visit parent
        }
```

```
  }

  return path;
}

/**
 * Returns the nearest unvisited cell
 */

Cell* getNextUnvisited(Cell* _current, Grid* _grid)
{
  std::list<Cell*> neighbors;
  std::list<Cell*> fringe;
  std::set<Cell*> explored;
  std::list<Cell*>::iterator it;

  Cell* next = NULL;

  fringe.push_back(_current);
  while(!fringe.empty())
  {
    if(fringe.front()->visited)
    {
      neighbors = _grid->getNeighbors(fringe.front());
      //explored.insert(fringe.front());
      fringe.pop_front();
      for(it = neighbors.begin(); it != neighbors.end(); it++)
      {
        if(explored.find(*it) == explored.end() && (*it)->allowed)
        {
          fringe.push_back(*it);
          explored.insert(*it);
        }
      }
    }
    else
    {
```

```
162         float max = 0;
            for(it = fringe.begin(); it != fringe.end(); it++)
            {
              float P = (*it)->probability;
              if(P > max)
167           {
                next = *it;
                max = P;
              }
            }
172         break;
          }
        }
        return next;
      }
177

      /**
       * Returns the nearest allowed cell
       * Useful for handling unexpected blocked conditions
182    */

      Cell* getNearestAllowed(Cell* _current, Grid* _grid)
      {
        std::list<Cell*> neighbors;
187     std::list<Cell*> fringe;
        std::set<Cell*> explored;
        std::list<Cell*>::iterator it;

        Cell* next = NULL; //pointer to the next cell, initialized to null
192
        fringe.push_back(_current);
        while(!fringe.empty()) //while fringe isn't empty and no next cell is
            assigned
        {
          if(!(fringe.front()->allowed)) //if the cell isn't open, expand out
197       {
```

```
        neighbors = _grid->getNeighbors(fringe.front());
        fringe.pop_front();
        for(it = neighbors.begin(); it != neighbors.end(); it++)
        {
202       if(explored.find(*it) == explored.end()) //if unexplored
          {
            fringe.push_back(*it);
            explored.insert(*it);
          }
207     }
      }
      else //if the fringe front is allowed, we've found at least one open
          cell
      {
        float min = -1;
212     for(it = fringe.begin(); it != fringe.end(); it++)
        {
          float D = _grid->global_distance(*it,_current);
          if(min == -1 || D < min)
          {
217         next = *it;
            min = D;
          }
        }
        break;
222   }
    }
    return next;
  }

227 bool isCellInTriangle(Vector2D a, Vector2D b, Vector2D c, Cell* _cell,
      Grid* _grid)
  {
    int x,y; x = _cell->x; y = _cell->y;
    //round the points to nearest cell center coordinates
    Vector2D A = _grid->local_2_global(_grid->global_2_local(a));
232 Vector2D B = _grid->local_2_global(_grid->global_2_local(b));
```

```
  Vector2D C = _grid->local_2_global(_grid->global_2_local(c));

  Vector2D pt = _grid->local_2_global(std::make_pair(x,y));
  return isInTriangle(A,B,C,pt); //call to geometry function
  //return isInTriangle(a,b,c,pt);
}

std::set<Cell*> getCellsInTriangle(Vector2D a, Vector2D b, Vector2D c,
    Grid* _grid)
{
  std::set<Cell*> cells;
  std::list<Cell*> neighbors;
  std::set<Cell*> explored;
  std::list<Cell*> fringe;
  std::list<Cell*>::iterator it;
  // get the first cell, starting at origin for now
  // TODO: this could probably be made a bit more efficient
  Cell* cell = _grid->getCell(0,0);
  fringe.push_back(cell);
  explored.insert(cell);
  while(!fringe.empty())
  {

    neighbors = _grid->getNeighbors(fringe.front());
    //explored.insert(fringe.front());
    //check if current cell is in triangle
    if(isCellInTriangle(a,b,c,fringe.front(),_grid))
    {
      cells.insert(fringe.front());
    }
    //pop from fringe
    fringe.pop_front();
    //add neighbors
    for(it = neighbors.begin(); it != neighbors.end(); it++)
    {
      if(explored.find(*it)== explored.end())
      {
```

```
            fringe.push_back(*it);
            explored.insert(*it);
          }
272       }
      }
      return cells;
    }

277 }
```

```
/**
* File: test.cpp
3 * Simple demo file for hexagonal grid navigation
*/
#include <iostream> //for debug
#include <list>
#include <utility>
8 #include "Grid.hpp"
#include "Agent.hpp"
#include "WiND_search.hpp"
#include "WiND_utils.hpp"

13 /**
* Usage specific, prints grid to prompt
*/
void print_grid(WiND::Agent& a)
{
18   int size = a.getWorld()->getSize();
    for(int i=size; i >= -size; i--)
    {
      std::string p;
      if(i<0){
23   p.assign(-i,' ');
    std::cout << p;
      }
      for(int j=-size; j <= size; j++)
      {
```

```
28    WiND::Cell* s = a.getWorld()->getCell(j,i);

      if(s){
        if(s == a.getCurrentCell()) std::cout << "X ";
        else if(s->visited) std::cout << "o ";
33      else if(!s->allowed) std::cout << "- ";
        else std::cout << ". ";
      }
      else std::cout << " ";
        }
38      std::cout << std::endl;
       }
    }

    void callback_test(const char* _event, const char*  _arg)
43  {
      std::cout << "CALLBACK: " << _event << ":" <<  _arg << std::endl;
    }

    /**
48  * Main function
    */
    int main()
    {

53    WiND::Agent agent(50.0,3.0,"meters","hexagon"); //should make a roughly
          12-layer grid
      agent.setPosition(-10.0,3.0,100.0);
      //agent.setPosition(5,5,100);
      agent.setTargetAltitude(300);
      //agent.setTargetPoint(30,30);
58    agent.setCallback(callback_test);

      WiND::Vector2D a = {0,0};
      WiND::Vector2D b = {-25,-0.1};
      WiND::Vector2D c = {0,25};
63
```

```
    WiND::Grid* grid = agent.getWorld();
    std::set<WiND::Cell*> triangle = WiND::getCellsInTriangle(a,b,c,grid);
68  std::set<WiND::Cell*>::iterator it;
    for(it = triangle.begin(); it != triangle.end(); it++){(*it)->allowed =
        false;}

    std::cout << "Testing Agent Navigation, non-center starting position" <<
        std::endl;
    std::cin.ignore();
73  print_grid(agent);

    WiND::Waypoint next;
    WiND::Waypoint pos;

78  while(true)
    {
    next = agent.getNextWaypoint();
    pos = agent.getPosition();
    WiND::Vector2D gCoords = {pos.x,pos.y};
83  std::pair<int,int> hpos = agent.getWorld()->global_2_local(gCoords);
    if(next.x == pos.x && next.y == pos.y) break;
    std::cout << pos.x << "," << pos.y << "," << pos.z << std::endl;
    std::cout << hpos.first << "," << hpos.second << std::endl;
    print_grid(agent); //print current state
88  agent.setPosition(next.x, next.y, next.z); //update position
    usleep(200000);
    }
    print_grid(agent);
    std::cout << "done..." << std::endl;
93 }
```

```
/**
 2  * File:  HexGrid.hpp
    * Author:  Jonathan Estabrook
    * Description:
```

```
 *
 *  Hexagonal Search Grid, inherits from the Grid superclass.
 *  NOTE: see Grid.hpp!
 * */

#include "HexGrid.hpp"
#include <cstdlib>
#include <cmath>
//#include <iostream> //debug

namespace WiND{

  void HexGrid::generate(int _layers){
    int i;
    for (i=-_layers;i<=_layers;i++)
    {
      int l,r,j;
      l = (i<=0)?(-_layers):(-_layers + i);
      r = (i>=0)?( _layers):( _layers + i);
      for(j=l;j<=r;j++)
      {
        Cell c(i,j);
        cellmap[std::make_pair(i,j)] = c;
      }
    }
  }

  /**
   * grid generation function based on minor grid radius and minor cell
       radius
   */
  void HexGrid::init(float _grid_rad, float _cell_rad, std::string _units)
  {
    //NOTE: changed to floor to ensure whole-cell layer bounds
    this->layers = std::floor((_grid_rad/COS_30)/((_cell_rad)*2)); //
        calculate cell layers
```

```
        this->scale = (_cell_rad)*2; //scaling factor should be twice the minor
            cell radius
        this->units = _units;

42      //fill the boundary list
        float R = _grid_rad/COS_30;

    //    std::cout << this->layers << " layers, " << this->scale << " scale, "
        << R << " grid_rad" << std::endl;

47      Vector2D pt;
        pt.x = 0; pt.y = R;
        this->bounds.push_back(pt);
        pt.x = R*COS_30; pt.y = R*SIN_30;
        this->bounds.push_back(pt);
52      pt.y = -pt.y;
        this->bounds.push_back(pt);
        pt.x = 0; pt.y = -R;
        this->bounds.push_back(pt);
        pt.x = -R*COS_30; pt.y = -R*SIN_30;
57      this->bounds.push_back(pt);
        pt.y = -pt.y;
        this->bounds.push_back(pt);

        //removing this for now, cells should be created on-demand from boundary
            points
62      this->generate(layers);
      }

      // virtual
      std::list<Cell*> HexGrid::getNeighbors(Cell* c)
67    {
        std::list<Cell*> cells;
        //calculate neighbor coordinates
        //first the upper neighbor, go clockwise from here
        int x,y; x = c->x; y = c->y;
72      Cell* neighbor;
```

```
    // N  (0,+)
    neighbor = getCell(x  ,y+1);
    if(neighbor) cells.push_back(neighbor);
    // NE (+,+)
    neighbor = getCell(x+1,y+1);
    if(neighbor) cells.push_back(neighbor);
    // SE (+,0)
    neighbor = getCell(x+1,y  );
    if(neighbor) cells.push_back(neighbor);
    // S  (0,-)
    neighbor = getCell(x  ,y-1);
    if(neighbor) cells.push_back(neighbor);
    // SW (-,-)
    neighbor = getCell(x-1,y-1);
    if(neighbor) cells.push_back(neighbor);
    // NW (-,0)
    neighbor = getCell(x-1,y  );
    if(neighbor) cells.push_back(neighbor);

    return cells;
}

/**
*  converts local coordinates to global cartesian
*  Global coordinates are represented as a custom Vector2D class
*  Local coordinates are a simple integer pair, for easy map lookup
*/
Vector2D HexGrid::local_2_global(std::pair<int,int> _lCoords)
{
    int lx = _lCoords.first;
    int ly = _lCoords.second;
    Vector2D gCoords;
    gCoords.x = ((float)lx*COS_30)*this->scale;
    gCoords.y = ((float)ly - (float)lx*SIN_30)*this->scale;
    return gCoords;
}
/**
```

```
     *  converts global coordinates to local
     */
112  std::pair<int,int> HexGrid::global_2_local(Vector2D _gCoords)
     {
       float gx = _gCoords.x;
       float gy = _gCoords.y;
       int lx = floor(gx/(COS_30*this->scale) + 0.5);
117    int ly = floor(gy/scale+lx*SIN_30 + 0.5);
       return std::make_pair(lx,ly);
     }

     /**
122   * Returns the local cell distance between cells
     */
     int HexGrid::local_distance(Cell* a, Cell* b)
     {
       int x1,y1,x2,y2;
127    x1 = a->x; y1 = a->y; x2 = b->x; y2 = b->y;

         int A = std::abs(x2 - x1);
       int B = std::abs(y2 - y1);
       int C = std::abs(a - b);
132    return (C>(A>B?A:B))?C:(A>B?A:B); //max of 3 for hexagonal coordinates
     }
   }
```

```
 1 /**
    * File:  Agent.cpp
    * Author:  Jonathan Estabrook
    * Description:
    *
 6  *  Main access class for interfacing with navigation, control, and data
    *  acquisition functions. Effectively this is where you tell the robot
    *  what to do. Most high-level organizational changes in the library
    *  should happen here.
    *
11  *  NOTE ON COORDINATES:
```

```
 * For purposes of differentiation "Global" refers to scaled cartesian
    coordinates *relative*
 * to the search grid origin, in the appropriate units, not true "Global"
    in a Lat/Lon sense.
 * "Local" refers to integer-unit coordinates for usage within the
 * search grid. One local unit is scaled by the cell scaling factor for
    global units.
 *
 * Conversions between Lat/Lon and Global are assumed to happen elsewhere
    before input.
 * */
#include "Agent.hpp"

#include "HexGrid.hpp" //we're using this locally, Agent.h doesn't need it

#include "WiND_search.hpp"

#include <list>
#include <set>
#include <algorithm>
#include <iostream> //TODO
#include <exception>
namespace WiND
{
  Agent::Agent(float _grid_rad, float _cell_rad, std::string  _units, std::
     string _grid_type){
    if(_grid_type == "hexagon")
    {
      this->world = new HexGrid();
    } else {
      throw;
    }
    this->world->init(_grid_rad,_cell_rad,_units);
    this->cell = NULL; //indicates uninitialized position
    this->callback = NULL; //uninitialized callback
  }
```

```
/**
 * Returns pointer to Grid
 */
Grid* Agent::getWorld(){
  return this->world;
}


Cell* Agent::getCurrentCell(){
  return this->cell;
}

Waypoint Agent::getPosition(){
  return this->pos;
}

/**
 * Set position in global cartesian units, relative to 0,0,0
 * if the position isn't in-world, return false
 */
bool Agent::setPosition(float x, float y, float z){
  //update current waypoint
  this->pos.x = x; this->pos.y = y; this->pos.z = z;
  if(callback)callback("UPDATE","position updated");

  Vector2D gCoords = {x,y};
  //find current cell coordinates
  std::pair<int,int> lCoords = this->world->global_2_local(gCoords);
  //get current cell
  this->cell = this->world->getCell(lCoords.first,lCoords.second);
  //if it is a valid cell, set the visited flag
  if(this->cell){ this->cell->visited = true; return true;}
  else return false;
}

bool Agent::setTargetPoint(float _x, float _y){
  //first check if this is a valid point
```

```
81      Vector2D v = {_x,_y};
        std::pair<int,int> lCoords = this->world->global_2_local(v);
        Cell* c = this->world->getCell(lCoords.first,lCoords.second);
        if(!c) return false;
        else if(c == this->cell) return true;
86      else
        {
          this->path = planPath(this->cell,c,this->world);
        }
      }
91
      bool Agent::setTargetAltitude(float _z)
      {
        this->target_z = _z;
        return true;
96    }

      bool Agent::setCallback(void (*func)(const char*, const char*))
      {
        this->callback = func;
101     return (func != NULL);
      }

      /*****************************************************************
      * Interface method for single-cell search algorithms
106   **/
      Waypoint Agent::getNextWaypoint(){
      // declare pointer to next cell
        Cell* next = NULL;

111   //first check for pre-planned cells
        if(!(this->path.empty()))
        {
          next = path.front();
          path.pop_front();
116       if(callback)callback("STATUS","popping path waypoint!");
        }
```

```
    // algorithms are chained by priority
    // these pick the next cell, in two dimensions, altitude is separate
121 // attempt using center-spiral method
      next = next?next:getNextSpiral(this->cell, this->world);

    // if this fails, attempt using A*, starting a planned path
    // to the next unvisited cell
126   if(!next)
      {
        Cell* target = getNextUnvisited(this->cell, this->world);
        this->path = target?planPath(this->cell,target,this->world):path;
        if(!(this->path.empty())){
131       next = path.front();
          path.pop_front();
        }
      }

136 // Final sanity check, in the case that we are in a blocked region
    // this will return the nearest allowed cell
      next = next?next:getNearestAllowed(this->cell,this->world);


141 //* FALLBACK BEHAVIOR, KEEP AT END
    // the last method called occurs if next waypoint is still null
    // if all algorithms fail, hold position at current cell
      next = next?next:this->cell; //hold position

146   int x,y;
      x = next->x; y = next->y;

      Vector2D gc = this->world->local_2_global(std::make_pair(x,y));

151   Waypoint w;
      w.x = gc.x; w.y = gc.y;
      //altitude is controlled independently
      w.z = this->target_z;  //set from current target altitude
```

```
        return w; //return waypoint
156   }
    }
```

Appendix E

FPGA Image Processing Description

```
--
    ----------------------------------------------------------------------------------

-- Company:
-- Engineer:
--
-- Create Date:    21:19:10 02/25/2012
-- Design Name:
-- Module Name:    framememory - Behavioral
-- Project Name:
-- Target Devices:
-- Tool versions:
-- Description:
--
-- Dependencies:
--
-- Revision:
-- Revision 0.01 - File Created
-- Additional Comments:
--
```

```
--
    ----------------------------------------------------------------------------------

library IEEE;
use IEEE.STD_LOGIC_1164.ALL;

use ieee.std_logic_arith.all;
use ieee.std_logic_unsigned.all;

-- Uncomment the following library declaration if using
-- arithmetic functions with Signed or Unsigned values
--use IEEE.NUMERIC_STD.ALL;

-- Uncomment the following library declaration if instantiating
-- any Xilinx primitives in this code.
--library UNISIM;
--use UNISIM.VComponents.all;

entity framememory is
      generic ( pxsize : natural := 8;    --change these values as necessary
          . be careful of extremely small values
             vsize : natural := 640;
             hsize : natural := 480  );

     Port (     vstream : in  STD_LOGIC_VECTOR (pxsize-1 downto 0); --
         continuous video stream.
             enable : in std_logic;      -- '1'
             hsync : in  STD_LOGIC;      --signals at end of horizontal line
             vsync : in  STD_LOGIC;      --signals at end of vertical frame
             clk : in  STD_LOGIC;        --syncronized with video stream
             output : out std_logic_vector(pxsize-1 downto 0); --the value of
                  the next-to-be-overwritten memory location
             outblank : out std_logic    --signals that the output is
                 innacurate and to ignore
         );
end framememory;
```

```
architecture Behavioral of framememory is

constant hbuffer: integer := 8;
constant vbuffer: integer := 3;  --dont think there is one but you never
    know

subtype pixel is std_logic_vector(pxsize-1 downto 0);-- := (others => '0');

type frame_array is array(0 to hsize-1, 0 to vsize-1) of pixel;


--type frame_array is array(0 to hsize-1, 0 to vsize-1) of std_logic_vector(
    pxsize-1 downto 0);


signal frame: frame_array := ((others => (others => (others => '0')))); --
    this is large. may need to put on ext.ram
--signal frame: frame_array;

signal hpos : integer range 0 to (hsize - 1) + hbuffer := 0;
signal vpos : integer range 0 to (vsize - 1) + vbuffer:= 0;

signal out_sig : pixel := (others => '0') ;
signal outblank_sig : std_logic := '0';


begin


next_memory : process(clk)
--output the next memory location before it is written to at next rising
    clock edge
begin
  if rising_edge(clk) then
    if hpos > (hsize - 2) then --in the h buffer
```

```
        out_sig <= "00000000"; -- this is not accurate. we dont know the next
            value
83      outblank_sig <= '1';
      elsif vpos > vsize -1 then --in the v buffer
        out_sig <= "00000000"; --innacurate
        outblank_sig <= '1';
      else
88      out_sig <= frame((hpos + 1), vpos );
        outblank_sig <= '0';
      end if; --what to output
    end if; --clk
    output <= out_sig;
93  outblank <= outblank_sig;
  end process next_memory;


  counters : process(clk, vstream, hsync, vsync)
98 begin
    if enable = '1' then
      if rising_edge(clk) then
          hpos <= hpos + 1;
          vpos <= vpos;
103   end if; --clk hpos+1

      if rising_edge(hsync) then -- you can do this on the falling edge of the
          blank signal if like vga
        hpos <= 0;
        vpos <= vpos + 1;
108   end if; --hsync to 0

      if rising_edge(vsync) then
        hpos <= 0;
        vpos <= 0;
113   end if; --vsync to 0
    end if; --enable

  end process counters;
```

```
118 fillbuffer : process(clk)
    --walk through the buffer array and overwrite. may have synthesis issues on
        "pass" lines
    begin
      if rising_edge(clk) then
        if enable = '1' then
123       if (vpos > (vsize - 1)) then
            --pass
            frame <= frame;
          elsif (hpos > (hsize - 1)) then
            --pass
128         frame <= frame;
          else
            frame(hpos,vpos) <= vstream;
          end if; --in buffer
        end if; --enable
133   end if; --fill buffer

    end process fillbuffer;



138

    end Behavioral;

    --
        ----------------------------------------------------------------------------------


    -- Company:
    -- Engineer:
  4 --
    -- Create Date:    00:28:48 02/28/2012
    -- Design Name:
    -- Module Name:    imagestats - Behavioral
    -- Project Name:
  9 -- Target Devices:
    -- Tool versions:
```

```
-- Description:
--
-- Dependencies:
--
-- Revision:
-- Revision 0.01 - File Created
-- Additional Comments:
--
--
    ----------------------------------------------------------------------------------

library IEEE;
use IEEE.STD_LOGIC_1164.ALL;

-- Uncomment the following library declaration if using
-- arithmetic functions with Signed or Unsigned values
use IEEE.NUMERIC_STD.ALL;

-- Uncomment the following library declaration if instantiating
-- any Xilinx primitives in this code.
--library UNISIM;
--use UNISIM.VComponents.all;

entity imagestats is


    generic ( pxsize : natural := 8;    --change these values as necessary.
        be careful of extremely small values
          vsize : natural := 640;
          hsize : natural := 480  );

    Port (
        clk : in std_logic;
        activate : in std_logic; --this should be a pulse
        sum : in  STD_LOGIC_VECTOR (31 downto 0);
        sumsq : in  STD_LOGIC_VECTOR (31 downto 0);
        count : in  STD_LOGIC_VECTOR (31 downto 0);
```

```
          mean : out  STD_LOGIC_VECTOR (pxsize-1 downto 0);
          variance : out  STD_LOGIC_VECTOR (31 downto 0);
          rdy : out std_logic
        );
end imagestats;

architecture Behavioral of imagestats is


  COMPONENT div32
   PORT(
        rfd : OUT  std_logic;
        rdy : OUT  std_logic;
        --divide_by_zero : OUT  std_logic;
        nd : IN  std_logic;
        clk : IN  std_logic;
        dividend : IN  std_logic_vector(31 downto 0);
       quotient : OUT  std_logic_vector(31 downto 0);
        divisor : IN  std_logic_vector(31 downto 0)
       );
   END COMPONENT;

  component mul32
  port(
    a : in std_logic_vector(31 downto 0);
    b : in std_logic_vector(31 downto 0);
    clk : in std_logic;
    --ce : in std_logic;
    p : out std_logic_vector(31 downto 0)
  );
  end component;



```

```
    --sigs for i/o
84  --signal count_sig : integer range 0 to ((vsize)*(hsize)) := 0;          --
        thoretical maximum
    --signal sum_sig : integer range 0 to ((2*pxsize)-1)*vsize*hsize := 0; --
        thoretical maximum
    --signal sumsq_sig : integer range 0 to (((2*pxsize)-1)**2)*vsize*hsize :=
        0; -- Oo size  -thoretical maximum

    signal count_sig  : std_logic_vector(31 downto 0) := (others => '0');
89  signal sum_sig  : std_logic_vector(31 downto 0) := (others => '0');
    signal sumsq_sig  : std_logic_vector(31 downto 0) := (others => '0');


    --other internal sigs
94  --signal clk_sig : std_logic;

    signal mean_sig : std_logic_vector ((pxsize-1) downto 0) := (others => '0');
    signal variance_sig : std_logic_vector (31 downto 0) := (others => '0');

99  signal variance_mul_rdy :std_logic := '1';
    constant variance_mul_delay : integer := 15;



104 --sigs for mean div32
    signal mean_rfd         : std_logic;
    signal mean_rdy         : std_logic;
    signal mean_divide_by_zero : std_logic;
    signal mean_nd        : std_logic := '0';
109 signal mean_dividend    : std_logic_vector(31 downto 0); --signed?
    signal mean_quotient    : std_logic_vector(31 downto 0); --signed ?
    signal mean_divisor       : std_logic_vector(31 downto 0); --signed ?


114 --sigs for variance mul32
    signal variance_a   : std_logic_vector(31 downto 0); --
```

```
    signal variance_b   : std_logic_vector(31 downto 0); --
    signal variance_p   : std_logic_vector(31 downto 0); --

119

    --sigs for variance div32
    signal variance_rfd       : std_logic;
    signal variance_rdy       : std_logic;
124 signal variance_divide_by_zero : std_logic;
    signal variance_nd      : std_logic := '0';
    signal variance_dividend  : std_logic_vector(31 downto 0); --signed?
    signal variance_quotient  : std_logic_vector(31 downto 0); --signed ?
    signal variance_divisor   : std_logic_vector(31 downto 0); --signed ?
129


    begin

134 --declarations of parts


    meandiv: div32 PORT MAP (
         rfd => mean_rfd,
139      rdy => mean_rdy,
         --divide_by_zero => mean_divide_by_zero,
         nd => mean_nd,
         clk => clk,
         dividend => mean_dividend,
144      quotient => mean_quotient,
         divisor => mean_divisor
        );


149 varmul: mul32 port map(
        clk => clk,
        a => variance_a,
        b => variance_b,
```

```
        p => variance_p
154   );

    vardiv: div32 PORT MAP (
         rfd => variance_rfd,
         rdy => variance_rdy,
159      --divide_by_zero => variance_divide_by_zero,
         nd => variance_nd,
         clk => clk,
         dividend => variance_dividend,
         quotient => variance_quotient,
164      divisor => variance_divisor
        );


    --concurrent statements
169 --sum <= std_logic_vector(to_signed(sum_sig,32));
    --sumsq <= std_logic_vector(to_signed(sumsq_sig,32));

    count_sig <= count;
    sum_sig <= sum;
174 sumsq_sig <= sumsq;
    --clk_sig <= clk;



179   variance_sig <= variance_quotient when variance_rdy = '1' else
          variance_sig;
      variance <= variance_sig;


      mean_sig <= mean_quotient(pxsize-1 downto 0) when mean_rdy = '1' else
          mean_sig; --flipflop
184   mean <= mean_sig;

    --processes
```

```
    load_mean : process (clk)
189 begin
      if rising_edge(clk) then
        case mean_rfd is
          when '1' =>
                    mean_dividend <= sum_sig;
194                 mean_divisor <= count_sig;
                    mean_nd <= activate;

          when others =>
                    mean_dividend <= mean_dividend;
199                 mean_divisor <= mean_divisor;
                    mean_nd <= '0';
        end case; --mean ready for input
      end if; --clk
    end process; --load mean
204

    load_var_mul : process(mean_rdy)
    begin
      if rising_edge(mean_rdy) then
209     variance_a <= mean_sig;
        variance_b <= sum;
      else
        variance_a <= variance_a;
        variance_b <= variance_b;
214   end if; --mean rdy
    end process;


    load_var_div : process(clk)
219 begin
      if rising_edge(clk) then
        if variance_mul_rdy = '1' and variance_rfd = '1' then
          variance_dividend <= std_logic_vector(to_unsigned((to_integer(unsigned
              (sumsq_sig)) - to_integer(unsigned(variance_p))),32));
```

```
        variance_quotient <= std_logic_vector(to_unsigned((to_integer(unsigned
            (count_sig)) - 1),32));
224     else
        variance_dividend <= variance_dividend;
        variance_quotient <= variance_quotient;
      end if; --ready
    end if; --clk
229 end process; --load var div




234


  mul_timer : process (activate)
  variable count : integer range 0 to 127 := 0;
  variable go : std_logic := '0';
239 begin
    if rising_edge(activate) then
      go := '1';
    else
      go := go;
244 end if; --activate

    if go = '1' then
      count := count + 1;
      variance_mul_rdy <= '0';
249 else
      count := 0;
      variance_mul_rdy <= '0';
    end if; --go

254 if count >= variance_mul_delay then
      count := 0;
      go := '0';
      variance_mul_rdy <= '1';
    end if; --maxcount
```

```
259 end process; --mul_timer




264 end Behavioral;

    --
        ----------------------------------------------------------------------------------


    -- Company:
    -- Engineer:
    --
  5 -- Create Date:    02:47:59 02/26/2012
    -- Design Name:
    -- Module Name:    meanandvar - Behavioral
    -- Project Name:
    -- Target Devices:
 10 -- Tool versions:
    -- Description:
    --
    -- Dependencies:
    --
 15 -- Revision:
    -- Revision 0.01 - File Created
    -- Additional Comments:
    --
    --
        ----------------------------------------------------------------------------------


 20 library IEEE;
    use IEEE.STD_LOGIC_1164.ALL;

    --use ieee.std_logic_arith.all;
    --use ieee.std_logic_unsigned.all;
 25 --use ieee.std_logic_signed.all;
```

```
-- Uncomment the following library declaration if using
-- arithmetic functions with Signed or Unsigned values
use IEEE.NUMERIC_STD.ALL;

-- Uncomment the following library declaration if instantiating
-- any Xilinx primitives in this code.
library UNISIM;
use UNISIM.VComponents.all;

entity meanandvar is
    generic ( pxsize : natural := 8;    --change these values as necessary.
        be careful of extremely small values
          vsize : natural := 640;
          hsize : natural := 480  );


    Port ( vstream : in  STD_LOGIC_VECTOR (pxsize-1 downto 0);
           mean : out  STD_LOGIC_VECTOR (pxsize-1 downto 0);
           variance : out  STD_LOGIC_VECTOR (31 downto 0);
        --mean_overflow : out std_logic; --this can never happen
        variance_overflow : out std_logic; --this can however
        calc_done : out std_logic;
           clk : in  STD_LOGIC;
           inblank : in  STD_LOGIC;
        end_of_frame : in std_logic;
           reset : in  STD_LOGIC);

end meanandvar;

architecture Behavioral of meanandvar is

    COMPONENT dsp_div_32b
    PORT(
         rfd : OUT  std_logic;
         rdy : OUT  std_logic;
         divide_by_zero : OUT  std_logic;
         nd : IN  std_logic;
```

```
            clk : IN  std_logic;
            dividend : IN  std_logic_vector(31 downto 0);
            quotient : OUT  std_logic_vector(31 downto 0);
            divisor : IN  std_logic_vector(31 downto 0)
           );
       END COMPONENT;

   --sigs for mean dsp_div_32b
   signal mean_rfd         : std_logic;
   signal mean_rdy         : std_logic;
   signal mean_divide_by_zero : std_logic;
   signal mean_nd        : std_logic := '0';
   signal mean_dividend    : std_logic_vector(31 downto 0); --signed
   signal mean_quotient    : std_logic_vector(31 downto 0); --signed
   signal mean_divisor       : std_logic_vector(31 downto 0); --signed

   --extra mean divider signals
   signal mean_sig : std_logic_vector(pxsize-1 downto 0):= (others => '0') ; --
       unsigned! (output mean is also unsigned)!
   signal flip_mean_nd : std_logic := '0';

   --sigs for variance dsp_div_32b
   signal variance_rfd       : std_logic;
   signal variance_rdy       : std_logic;
   signal variance_divide_by_zero : std_logic;
   signal variance_nd      : std_logic := '0';
   signal variance_dividend  : std_logic_vector(31 downto 0); --signed
   signal variance_quotient  : std_logic_vector(31 downto 0); --signed
   signal variance_divisor   : std_logic_vector(31 downto 0); --signed

   --extra variance divider signals
   signal variance_sig : std_logic_vector(31 downto 0):= (others => '0') ; --
       unsigned! (output variance is also unsigned)!
   signal flip_variance_nd : std_logic := '0';

   signal variance_overflow_temp : std_logic := '0';
   signal variance_overflow_sig : std_logic := '0';
```

```
--loopdeloop accumulators
signal n : integer range 0 to ((vsize)*(hsize)) := 0;
signal sum : integer range 0 to ((2*pxsize)-1)*vsize*hsize := 0; --
    thoretical maximum
signal sumsq : integer range 0 to (((2*pxsize)-1)**2)*vsize*hsize := 0; --
    Oo size  -thoretical maximum

signal blkrst : std_logic_vector(1 downto 0); --state definition used in
    loopdeloop




begin

--calculate mean
--calculate variance based on mean

--filter in another block

--http://en.wikipedia.org/wiki/Algorithms_for_calculating_variance


-- Instantiate the dividers
meandiv: dsp_div_32b PORT MAP (
     rfd => mean_rfd,
     rdy => mean_rdy,
     divide_by_zero => mean_divide_by_zero,
     nd => mean_nd,
     clk => clk,
     dividend => mean_dividend,
     quotient => mean_quotient,
     divisor => mean_divisor
    );
```

```
    vardiv: dsp_div_32b PORT MAP (
         rfd => variance_rfd,
         rdy => variance_rdy,
         divide_by_zero => variance_divide_by_zero,
         nd => variance_nd,
         clk => clk,
         dividend => variance_dividend,
         quotient => variance_quotient,
         divisor => variance_divisor
        );


    --Concurrent signal assignments
      blkrst <= (inblank & reset);
      mean_sig <= mean_quotient(pxsize-1 downto 0) when mean_rdy = '1' else
              mean_sig; --flipflop
      mean <= mean_sig;

      variance_sig <= variance_quotient(((2*pxsize)-1) downto 0) when
          variance_rdy = '1' else --size may change
               variance_sig; --flipflop

      variance_overflow_temp <= '1' when (to_integer(unsigned(variance_quotient
          (31 downto (2*pxsize)))) > 0) else '0';

      variance_overflow_sig <= '1' when variance_overflow_temp = '1' and
          variance_rdy ='1' else
                    '0' when variance_overflow_temp = '0' and variance_rdy = '1'
                         else
                    variance_overflow_sig; -- when variance_rdy = '0';

      variance <= variance_sig;
      variance_overflow <= variance_overflow_sig;

      calc_done <=  variance_rdy ;
```

```
--//concurrent



loopdeloop : process (clk, inblank, reset)
--common to both mean and variance calculations. accumulates n (num inputs),
     sum (sum of inputs), sumsq (sum^2)
--requires concurrent assignment blkrst
begin
  if rising_edge(clk) then --TODO: switch this to video clock rather than
      fast fpga clock
    case blkrst is
      when "00" =>  --not blanked, not reset... update values
                n <= n + 1;
                sum <= sum + to_integer(unsigned(vstream));
                sumsq <= sumsq + (to_integer(unsigned(vstream))**2); --TODO:
                     use better mul than built in
      when "01"|"11" => --reset case... all to zero
                n <= 0;
                sum <= 0;
                sumsq <= 0;
      when others => --aka blanked '10' ... hold values
                n<= n;
                sum <= sum;
                sumsq <= sumsq;
    end case;--blkrst
  end if; --rising edge
end process loopdeloop;


crunch_mean : process(end_of_frame)
--calculate the mean and standard deviation at the end of each frame
--uses n, sum, sumsq accumulated in loopdeloop process

variable mean_var : integer range 0 to ((2*pxsize)-1);
variable variance_var : integer range 0 to ((2*pxsize)-1);
```

```
200 begin
      if rising_edge(end_of_frame) then
        ----these work
        --mean_var := sum / n;
        --variance_var := (sumsq - (sum*mean_var))/(n - 1) ;
205     ----//working :P

        -- load up the dsp div, kick off the operation
        --mean
        mean_dividend <= std_logic_vector(to_unsigned(sum, 32));
210     mean_divisor <= std_logic_vector(to_unsigned(n, 32));
        flip_mean_nd <= not(flip_mean_nd); --kick off the divider "cascade"

        --leftover associations TODO: delete these
        --mean <= std_logic_vector(to_unsigned(mean_var, pxsize));
215     --variance <= std_logic_vector(to_unsigned(variance_var, (2*pxsize)));

      end if; --end of frame
    end process; --crunch mean


220
    crunch_variance : process (mean_rdy)

    variable variance_numerator : integer range 0 to ((((2*pxsize)-1)**2)*vsize*
        hsize) := 0; --as big as sumsq
    begin
225 --variance
      if rising_edge(mean_rdy) then
        --load up dsp div and maybe mul. kick off the operation
        variance_numerator := (sumsq - (sum* to_integer(unsigned(mean_sig))));
        variance_dividend <= std_logic_vector(to_unsigned(variance_numerator,
            32));
230     variance_divisor <= std_logic_vector(to_unsigned((n-1), 32));
        flip_variance_nd <= not(flip_variance_nd); --kick off the divider "
            cascade"
      end if; --mean_rdy
```

```
    end process; --crunch variance

235


    --these probrably should be functions or at very least, components but i'll
        copy-pasta code fornow
240 revert_mean_nd : process(flip_mean_nd, clk)
    variable clk_count : integer range 0 to 3 := 0;
    begin
      if flip_mean_nd'event then
        mean_nd <= '1';
245   end if; --flip_mean_nd

      if rising_edge(clk) then
        if clk_count = 2 then
          mean_nd <= '0';
250       clk_count := 0;
        else
          if mean_nd = '1' then
            mean_nd <= '1';
            clk_count := clk_count + 1;
255       else
            mean_nd <= mean_nd;
            clk_count := 0;
        end if; -- nd = 1
      end if; -- clk_count
260   end if; --clk
    end process; --revert_mean_nd


    revert_variance_nd : process(flip_variance_nd, clk)
265 variable clk_count : integer range 0 to 3 := 0;
    begin
      if flip_variance_nd'event then
        variance_nd <= '1';
```

```
      end if; --flip_mean_nd
270
      if rising_edge(clk) then
        if clk_count = 2 then
          variance_nd <= '0';
          clk_count := 0;
275     else
          if variance_nd = '1' then
            variance_nd <= '1';
            clk_count := clk_count + 1;
          else
280         variance_nd <= variance_nd;
            clk_count := 0;
          end if; -- nd = 1
        end if; -- clk_count
      end if; --clk
285 end process; --revert_variance_nd



    end Behavioral;
```

Appendix F

Simulink Image Processing

```
clc; clear all;
%Import Simulation image Data
field_images_files = dir('field/Test2/*.png');
forest_images_files = dir('forest/Test2/*.png');
rocky_images_files = dir('rocky/Test2/*.png');
snow_images_files = dir('snow/Test2/*.png');


for i = 1:4,
    img = rgb2ycbcr(imread(['snow/Test2/' snow_images_files(i).name]));
    sim Image_processing;
    imwrite(cat(3, R, G, B),['snow/Results/' snow_images_files(i).name],'png
        ');
    centers = centroids;
    file = fopen(['snow/Results/' snow_images_files(i).name '.txt'],'w');
    fprintf(file,'%f %f\n',centers);
    fclose(file);
end

for i = 1:4,
    img = rgb2ycbcr(imread(['field/Test2/' field_images_files(i).name]));
    sim Image_processing;
    imwrite(cat(3, R, G, B),['field/Results/' field_images_files(i).name],'
        png');
```

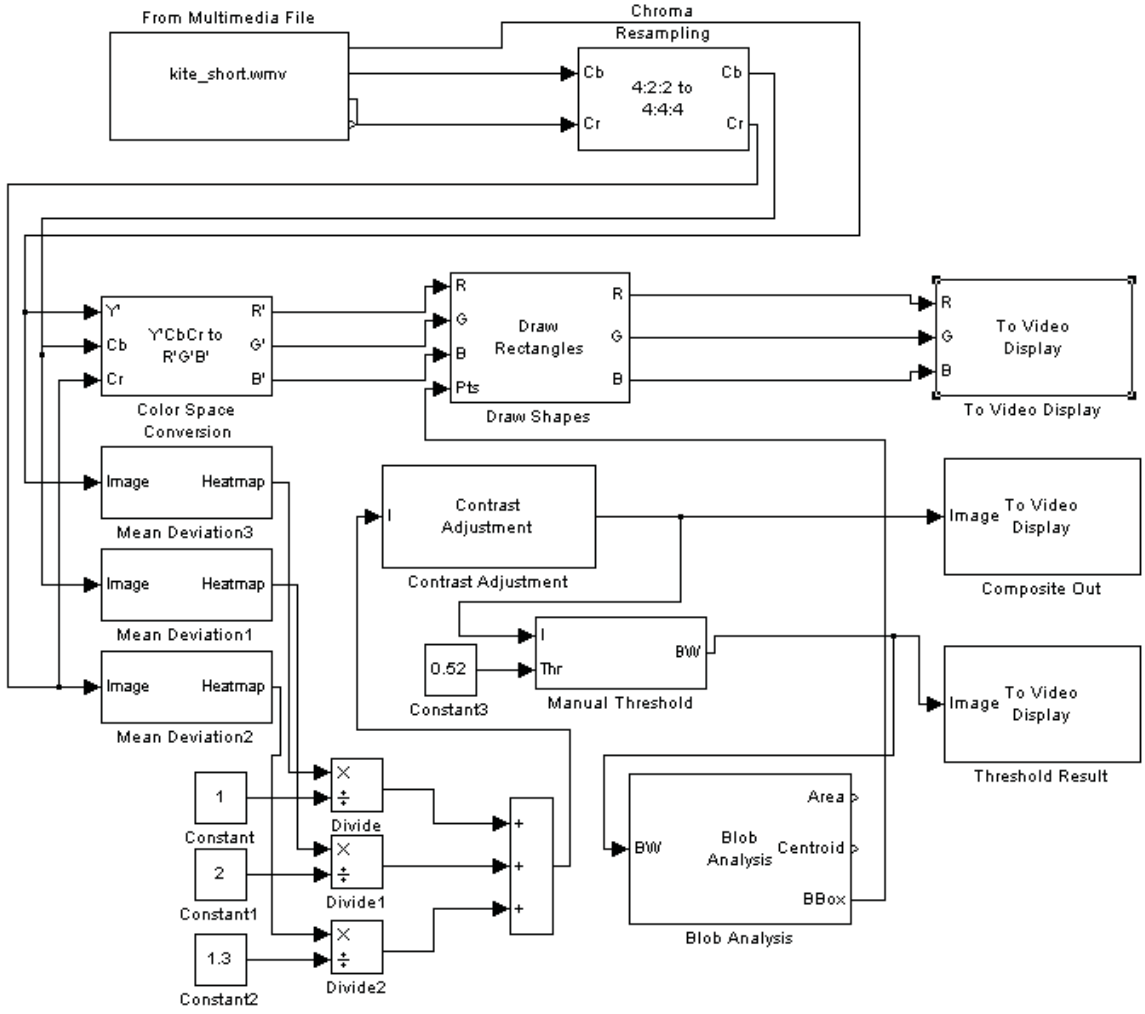

Figure F.1: Simulink implementation of our custom image processing algorithm showing manual adjustments. This easily adjustable model was used to fine-tune the algorithm.

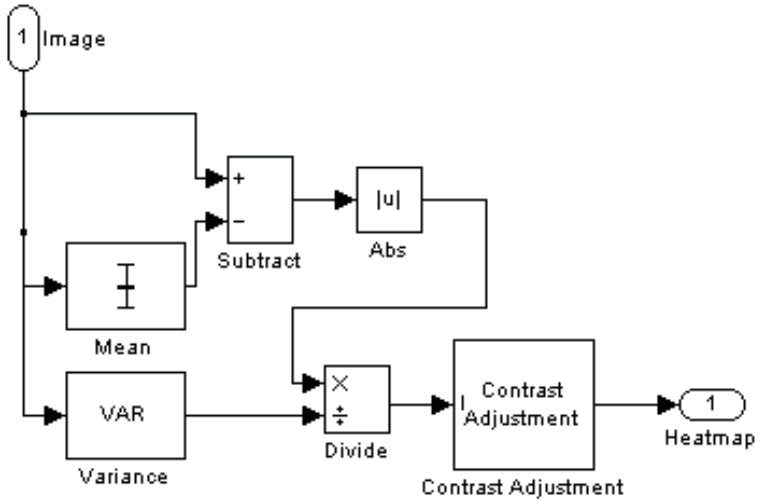

Figure F.2: Simulink implementation of the "Mean Deviation" block showing the algorithm chosen to define usual versus unusual pixels.

```
    centers = centroids;
    file = fopen(['field/Results/' field_images_files(i).name '.txt'],'w');
    fprintf(file,'%f %f\n',centers);
    fclose(file);
end

for i = 1:4,
    img = rgb2ycbcr(imread(['rocky/Test2/' rocky_images_files(i).name]));
    sim Image_processing;
    imwrite(cat(3, R, G, B),['rocky/Results/' rocky_images_files(i).name],'
        png');
    centers = centroids;
    file = fopen(['rocky/Results/' rocky_images_files(i).name '.txt'],'w');
    fprintf(file,'%f %f\n',centers);
    fclose(file);
end

for i = 1:4,
    img = rgb2ycbcr(imread(['forest/Test2/' forest_images_files(i).name]));
```

```
    sim Image_processing;
    imwrite(cat(3, R, G, B),['forest/Results/' forest_images_files(i).name],'
        png');
    centers = centroids;
    file = fopen(['forest/Results/' forest_images_files(i).name '.txt'],'w');
45  fprintf(file,'%f %f\n',centers);
    fclose(file);
end
```

Image Processing Simulink Results

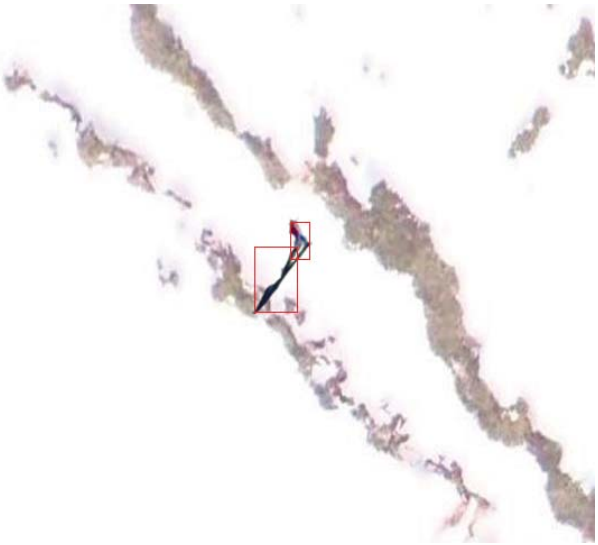

Bibliography

[1] Unknown. (2011, Nov.) Rescue over louisiana. [Online]. Available: http://www.katrinadestruction.com

[2] U. A. F. photo Lt Col Leslie Pratt. (2012) MQ-1 predator unmanned aircraft. [Online]. Available: http://www.af.mil/shared/media/photodb/photos/081131-F-7734Q-001.jpg

[3] (2012) Brigham young university during dry run of WiSAR UAV. [Online]. Available: https://facwiki.cs.byu.edu/WiSAR/

[4] dbenzhuser, "Pathfinding a star," 2006, [Online; accessed 14-Apr-2012]. [Online]. Available: http://upload.wikimedia.org/wikipedia/commons/thumb/f/f4/Pathfinding_A_Star.svg/500px-Pathfinding_A_Star.svg.png

[5] J. Dreo, "The ant colony optimization of the travelling salesman problem," 2004, [Online; accessed 22-Nov-2011]. [Online]. Available: http://en.wikipedia.org/wiki/Travelling_salesman_problem

[6] S. Asano, T. Maruyama, and Y. Yamaguchi, "Performance comparison of FPGA GPU and CPU in image processing," in *Field Programmable Logic and Applications, 2009. FPL 2009. International Conference on*, 31 2009-sept. 2 2009, pp. 126 –131.

[7] J. M. Griggs. (2012) Human figure average measurements. [Online]. Available: http://www.fas.harvard.edu/~loebinfo/loebinfo/Proportions/humanfigure.html

[8] (2012) Sony fcb-ix45c 18x color block camera. [Online]. Available: http://www.goelectronic.com/SONY+FCB-IX45C.html

[9] D. Cooper, J. Frost, and R. Q. Robe, "Compatibility of land SAR procedures with search theory," Potomac Management Group Inc., Tech. Rep., December 2003.

[10] T. W. Heggie and M. E. Amundson, "Dead men walking: Search and rescue in US national parks," *Wilderness and Environmental Medicine*, vol. 20, pp. 244–249, 2009.

[11] D. A. Graham, "A mountain of bills," *Newsweek*, December 2009.

[12] C. Search and R. Board, "Examples of endangered persons refusing SAR help, waiting to call for help or hiding from help because of fear of large bill" *http://www.coloradosarboard.org/csrb-documents/Refusing*, Nov. 2011.

[13] L. Lin, M. Roscheck, M. Goodrich, and B. Morse, "Supporting wilderness search and rescue with integrated intelligence: Autonomy and information at the right time and the right place," 2010. [Online]. Available: https://www.aaai.org/ocs/index.php/AAAI/AAAI10/paper/view/1864

[14] J. R. R. Gaemus E. Collins and P. S. Vegdahl, "A uav routing and sensor control optimization algorithm for target search," *Proceedings of SPIE*, 2007. [Online]. Available: http://link.aip.org/link/PSISDG/v6561/i1/p65610D/s1&Agg=doi

[15] L. H. Nunn, "An introduction to the literature of search theory," CNA Corporation, Tech. Rep., October 2003.

[16] W. Sheng, "Distributed multi-robot coordination in area exploration," *Robotics and Autonomous Systems*, vol. 54, dec. 2006. [Online]. Available: http://dx.doi.org/10.1016/j.robot.2006.06.003

[17] J. Kalomiros and J. Lygouras, "A host co-processor FPGA-based architecture for fast image processing," in *Intelligent Data Acquisition and Advanced Computing Systems: Technology and Applications, 2007. IDAACS 2007. 4th IEEE Workshop on*, sept. 2007, pp. 373 –378.

[18] J.-S. Leu, W.-H. Lin, M.-C. Yu, and H.-J. Tzeng, "Recognition assisted dynamic surveillance system based on OSGi and OpenCV," in *Advanced Communication Technology 13th International Conference on (ICACT'11)*, feb. 2011, pp. 83 –87.

[19] G. Miller and S. Fels, "Developer-centred interface design for computer vision," in *Computer Vision Workshops IEEE International Conference on (ICCV'11)*, nov. 2011, pp. 437 –444.

[20] V. Shehu and A. Dika, "Using real time computer vision algorithms in automatic attendance management systems," in *Information Technology Interfaces 32nd International Conference on(ITI'10)*, june 2010, pp. 397 –402.

[21] "An image search system for uavs," in *NRC Canada's Advanced Innovation and Partnership 2005 Conference((UVS)'05)*.

[22] J. Oh, E.-J. Im, and K. Yoon, "Optical flow computation on a heterogeneous platform," in *Ubiquitous Robots and Ambient Intelligence 8th International Conference (URAI'11)*, nov. 2011, pp. 68 –73.

[23] J. Jung, J. Yun, C.-K. Ryoo, and K. Choi, "Vision based navigation using road-intersection image," in *Control, Automation and Systems 11th International Conference (ICCAS'11)*, oct. 2011, pp. 964 –968.

[24] R. Carnie, R. Walker, and P. Corke, "Image processing algorithms for UAV"sense and avoid"," in *Robotics and Automation, 2006. ICRA 2006. Proceedings 2006 IEEE International Conference on*, may 2006, pp. 2848 –2853.

[25] M. Jasiunas, D. Kearney, J. Hopf, and G. Wigley, "Image fusion for uninhabited airborne vehicles," in *Field-Programmable Technology,Proceedings. 2002 IEEE International Conference (FPT'02)*, dec. 2002, pp. 348 – 351.

[26] P. Andersson, K. Kuchcinski, K. Nordberg, and P. Doherty, "Integrating a computational model and a run time system for image processing on a uav," in *Digital System Design, 2002. Proceedings. Euromicro Symposium on*, 2002, pp. 102 – 109.

[27] B. J. Tippetts, "Real-time implementation of vision algorithms for control, stabilization, and target tracking, for a hovering micro-uav," 2008. [Online]. Available: http://contentdm.lib.byu.edu/ETD/image/etd2374.pdf

[28] D. Jinghong, D. Yaling, and L. Kun, "Development of image processing system based on DSP and FPGA," in *Electronic Measurement and Instruments, 2007. 8th International Conference (ICEMI'07)*, 16 2007-july 18 2007, pp. 2–791 –2–794.

[29] Y. Lei, Z. Gang, R. Si-Heon, L. Choon-Young, L. Sang-Ryong, and K.-M. Bae, "The platform of image acquisition and processing system based on dsp and fpga," in *Smart Manufacturing Application, International Conference (ICSMA'08)*, april 2008, pp. 470 –473.

[30] M. A. Goodrich, B. S. Morse, D. Gerhardt, J. L. Cooper, M. Quigley, J. A. Adams, and C. Humphrey, "Supporting wilderness search and rescue using a camera-equipped mini uav: Research articles," *J. Field Robot.*, vol. 25, no. 1-2, pp. 89–110, Jan. 2008. [Online]. Available: http://dx.doi.org/10.1002/rob.v25:1/2

[31] M. A. Goodrich, T. W. McLain, J. D. Anderson, J. Sun, and J. W. Crandall, "Managing autonomy in robot teams: observations from four experiments," in *Proceedings of the ACM/IEEE international conference on Human-robot interaction*, ser. HRI '07. New York, NY, USA: ACM, 2007, pp. 25–32. [Online]. Available: http://doi.acm.org/10.1145/1228716.1228721

[32] S. Waharte, N. Trigoni, and S. Julier, "Coordinated search with a swarm of uavs," in *Sensor, Mesh and Ad Hoc Communications and Networks Workshops, 2009. . 6th Annual IEEE Communications Society Conference (SECON'09)*, june 2009, pp. 1 –3.

[33] Y. Kuwata, A. Richards, T. Schouwenaars, and J. P. How, "Distributed robust receding horizon control for multivehicle guidance," *IEEE Transactions on Control Systems Technology*, vol. 15, no. 4, pp. 627–641, July 2007.

[34] Paparazzi. (2012) Paparazzi: The free autopilot. [Online]. Available: http://paparazzi.enac.fr/

[35] ENAC. (2012) Enac interactive computing laboratory. [Online]. Available: http://www.lii-enac.fr/en/research.html

[36] Xilinx. (2012) Xtremedsp 48 slice. [Online]. Available: http://www.xilinx.com/technology/dsp/xtremedsp.htm

[37] microsoft. (2012) Lifecam cinema. [Online]. Available: http://www.microsoft.com/hardware/en-us/p/lifecam-cinema/H5D-00001#support

[38] L. Depeche. (2010, May) Pyrnes : mort et prisonnier des glaces. [Online]. Available: http://www.ladepeche.fr/article/2010/05/24/841327-pyrenees-mort-et-prisonnier-des-glaces.html

[39] P. D. Community. (2010, May) Hecto. [Online]. Available: http://paparazzi.enac.fr/wiki/Hecto

[40] T. Instruments. (2012) Pandaboard. [Online]. Available: http://www.pandaboard.org/

[41] ——. (2012) Beagleboard. [Online]. Available: http://beagleboard.org/

[42] R. P. Foundation. (2012) Raspberry pi. [Online]. Available: http://www.raspberrypi.org/

[43] Newegg. (2012) Intel BOXDH61DLB3 LGA 1155 intel H61 USB 3.0 mini ITX intel motherboard. [Online]. Available: http://www.newegg.com/Product/Product.aspx?Item=N82E16813121505

[44] Intel. (2012) Intel desktop boardD525MW. [Online]. Available: http://www.intel.com/content/www/us/en/motherboards/desktop-motherboards/desktop-board-d525mw.html

[45] E-ITX. (2012) Axiomtek PICO820 fanless Pico-ITX embedded mainboard, atom Z530 1.6 ghz. [Online]. Available: http://www.e-itx.com/pico820vga-z530.html

[46] Digilent. (2012) Atlys spartan-6 fpga development board. [Online]. Available: http://www.digilentinc.com/Products/Detail.cfm?NavPath=2,400,836&Prod=ATLYS

[47] Xilinx. (2012) Avnet spartan-6 lx9 microboard. [Online]. Available: http://www.xilinx.com/products/boards-and-kits/AES-S6MB-LX9.htm

[48] A. Devices. (2012) BF506F EZ-KIT lite for the ADSP-BF50X blackfin family. [Online]. Available: http://www.analog.com/en/evaluation/BF506F-EZLITE/eb.html#ppa_print_table

[49] T. Instruments. (2012) C5535 ezdsp usb stick development kit. [Online]. Available: http://www.ti.com/tool/tmdx5535ezdsp

[50] J. Hammes, A. Bohm, C. Ross, M. Chawathe, B. Draper, and W. Najjar, "High performance image processing on fpgas," 2001. [Online]. Available: http://www.cs.colostate.edu/cameron/Publications/hammes_lacsi01.pdf

[51] T. B. Nguyen and S. T. Chung, "An improved real-time blob detection for visual surveillance," in *Image and Signal Processing, 2nd International Congress on (CISP '09)*, oct. 2009, pp. 1 –5.

[52] W. Ahmed, M. Irfan, Muzammil, and Yaseen, "Pointing and target selection of object using color detection algorithm through dsp processor tms320c6711," in *Information and Communication Technologies International Conference on (ICICT'11)*, july 2011, pp. 1 –3.

[53] M.-J. Zhang and W. Gao, "An adaptive skin color detection algorithm with confusing backgrounds elimination," in *Image Processing, IEEE International Conference on (ICIP'05)*, vol. 2, sept. 2005, pp. II – 390–3.

[54] E. Shahinfard, M. Sid-Ahmed, and M. Ahmadi, "A motion adaptive deinterlacing method with hierarchical motion detection algorithm," in *Image Processing, 2008. ICIP 2008. 15th IEEE International Conference on*, pp. 889 –892.

[55] J. Hao and T. Shibata, "A vlsi-implementation-friendly ego-motion detection algorithm based on edge-histogram matching," in *Acoustics, Speech and Signal Processing, 2006. ICASSP 2006 Proceedings. 2006 IEEE International Conference on*, vol. 2, may 2006, p. II.

[56] P. Zhang, T.-Y. Cao, and T. Zhu, "A novel hybrid motion detection algorithm based

on dynamic thresholding segmentation," in *Communication Technology 12th IEEE International Conference on (ICCT'10)*, nov. 2010, pp. 853 –856.

[57] X. Chen and H. Chen, "A novel color edge detection algorithm in RGB color space," in *Signal Processing IEEE 10th International Conference (ICSP'10)*, oct. 2010, pp. 793 –796.

[58] J. Dreo, "Shortest path find by an ant colony," 2004, [Online; accessed 14-Apr-2012]. [Online]. Available: http://en.wikipedia.org/wiki/Ant_colony_optimization_algorithms

[59] L. Li, W. Huang, I. Y.-H. Gu, and Q. Tian, "Statistical modeling of complex backgrounds for foreground object detection," *Image Processing, IEEE Transactions on*, vol. 13, no. 11, pp. 1459 –1472, nov. 2004.

[60] M. Piovoso and P. A. Laplante, "Kalman filter recipes for real-time image processing," *Real-Time Imaging*, vol. 9, pp. 433–439, December 2003. [Online]. Available: http://dl.acm.org/citation.cfm?id=982353.982359

[61] H. L. Alexander, A. J. Azarbayejani, and H. J. Weigl, "Kalman-filter-based machine vision for controlling free-flying unmanned remote vehicles," in *American Control Conference, 1992*, june 1992, pp. 2006 –2011.

[62] S. Russell and P. Norvig, *Artificial Intelligence: A Modern Approach*, 3rd ed. New York: Prentice Hall, 2010.

[63] W. Turri and D. Pointer, "UAV video image stabilization on the SRC map processor," jan 2009. [Online]. Available: http://www.srccomp.com/news/docs/HPEC09_Turri.pdf